องค์ประกอบทางเคมีและฤทธิ์ทางชีวภาพของว่านกีบแรด *Angiopteris evecta* Hoffm.

นางสาวสมจินตนา ทวีพานิชย์

วิทยานิพนธ์นี้เป็นส่วนหนึ่งของการศึกษาตามหลักสูตรปริญญาวิทยาศาสตรมหาบัณฑิต
สาขาวิชาเคมี ภาควิชาเคมี
คณะวิทยาศาสตร์ จุฬาลงกรณ์มหาวิทยาลัย
ปีการศึกษา 2543

ISBN xxx-xxx-xxx-x

CHEMICAL CONSTITUENTS AND BIOLOGICAL ACTIVITY OF *Angiopteris evecta* Hoffm.

Miss. Somjintana Taveepanich

A Thesis Submitted in Partial Fulfillment of the Requirements
for the Degree of Master of Science in Chemistry

Department of Chemistry
Faculty of Science
Chulalongkorn University

Academic Year 2000
ISBN xxx-xxx-xxx-x

Thesis Title	CHEMICAL CONSTITUENTS AND BIOLOGICAL ACTIVITY OF *Angiopteris evecta* Hoffm.
By	Miss. Somjintana Taveepanich
Field of Study	Chemistry
Thesis Advisor	Associate Professor Dr. Sophon Roengsumran

Accepted By the Faculty of Science, Chulalongkorn University in Partial Fulfillment of the Requirement for the Master's Degree

……... Dean of Faculty of Science
(Associate Professor Wanchai Phothiphichitr, Ph.D.)

Thesis Committee

…… …….. Chairman
(Associate Professor Anongrat Karntiang, Ph.D.)

…… Thesis Advisor
(Associate Professor Sophon Roengsumran , Ph.D.)

…… Member
(Associate Professor Amorn Petsom , Ph.D.)

…… Member
(Surachai Pornpakakul, Ph.D.)

…… Member
(Nongnuj Jaiboon, Ph.D.)

สมจินตนา ทวีพานิชย์ : องค์ประกอบทางเคมีและฤทธิ์ทางชีวภาพของว่านกีบแรด *Angiopteris evecta* Hoffm (CHEMICAL CONSTITUENTS AND BIOLOGICAL ACTIVITY OF *Angiopteris evecta* Hoffm).
อาจารย์ที่ปรึกษา : รศ. ดร. โสภณ เริงสำราญ; 106 หน้า. ISBN 974-13-0830-2.

นำเหง้าของว่านกีบแรด *Angiopteris evecta* Hoffm. ที่สดและบดละเอียด มาสกัดด้วยตัวทำละลายสารอินทรีย์ ประกอบด้วย เมทานอล เฮกเซน และเอธิลแอซิเตต ตามลำดับ นำสารสกัดหยาบแต่ละชนิด ไปทำการแยกด้วยเทคนิคทางคอลัมน์โครมาโตกราฟีแยกสารได้ 4 ชนิด ทำการหาสูตรโครงสร้างของสารที่แยกได้ทั้ง 4 ชนิดโดยอาศัยสมบัติทางกายภาพ ทางเคมี ข้อมูลทางสเปกโตรสโคปี และการวิเคราะห์ทางเอ็กซ์เรย์ คริสตอลโลกราฟี สามารถพิสูจน์โครงสร้างได้ คือ Succinic acid (1) Angiopteroside (4-*O*-β-D-Glucopyranosyl-L-*threo*-2-hexen-5-olide) monohydrate (2) D-(+)-glucose (3) และ ของผสมของสเตอร์รอยด์ 2 ชนิด ได้แก่ β-sitosterol และ Stigmasterol (4) จากการวิจัยพบว่าสารประกอบเหล่านี้พบครั้งแรกในเหง้าว่านกีบแรด นำสาร 2 ไปทดสอบฤทธิ์ในการยับยั้งเซลล์มะเร็ง พบว่า สาร 2 มีฤทธิ์น้อย นอกจากนี้ยังพบว่าสาร 2 มีฤทธิ์ในการยับยั้งเอนไซม์เอชไอวี-1 รีเวอร์สทรานสคริปเทสได้

ภาควิชา.....เคมี..... ลายมือชื่อนิสิต.....
สาขาวิชา.....เคมี..... ลายมือชื่ออาจารย์ที่ปรึกษา.....
ปีการศึกษา.....2543..... ลายมือชื่ออาจารย์ที่ปรึกษาร่วม.....

4272413723 : MAJOR CHEMISTRY.
KEY WORD : *Angiopteris evecta* Hoffm./ CHEMICAL CONSTITUENTS/ BIOLOGICAL ACTIVITY/ HIV-1 REVERSE TRANSCRIPTASE.
SOMJINTANA TAVEEPANICH: CHEMICAL CONSTITUENTS AND BIOLOGICAL ACTIVITY OF *Angiopteris evecta* Hoffm. THESIS ADVISOR: ASSOC. PROF. SOPHON ROENGSUMRAN, Ph.D. 106 pp.
ISBN 974-13-0830-2.

The fresh rhizomes of *Angiopteris evecta* Hoffm. were extracted subsequently with organic solvents including methanol, hexane and ethyl acetate, respectively. Each crude extract was isolated and purified using column chromatography to obtain four compounds. The structures of these compounds were characterized using their physical and chemical properties, spectral data and x-ray crystallographic analysis. Four compounds were Succinic acid (1), Angiopteroside (4-*O*-*β*-D-Glucopyranosyl-L-*thero*-2-hexen-5-olide) monohydrate (2), D-(+)-glucose (3) and a mixture of *β*-sitosterol and stigmasterol(4). This research indicated the first report of compound 2 in *Angiopteris evecta* Hoffm. The compound 2 was tested for cytotoxic activity against cancer cell lines. The result indicated that compound 2 showed low activity. Moreover, compound 2 was found to inhibit HIV-1 reverse transcriptase.

Department……CHEMISTRY…..……..Student's signature. ……..

Field of study…… CHEMISTRY...…….Advisor's signature. …….

Academic year……2000……..Co-advisor's signature…….…….

ACKNOWLEDGEMENT

First of all, the author wishes to express the deepest gratitude to her advisor, Assoc. Prof. Dr.Sophon Roengsumran for his invaluable advice, continuous guidance, encouragement, and above all his inspirational comments. Besides, his complete understanding and deep insight into the organic chemistry has not only made work on this study a rewarding experience, but also has given precious experiences which the author wishes to apply in her future research.

Grateful acknowledgements are made to her thesis committee, Assoc. Prof. Dr. Anongrat Karntiang, Assoc. Prof. Dr. Amorn Petsom, Dr. Surachai Pornpakakul and Dr. Nongnuj Jaiboon for their comment, suggestion and correction. Thanks are also extended to Dr. Narongsak Chaichit, Department of Physics, Faculty of Science and Technology, Thammasat University for helping the analysis and determined of X-ray diffraction analysis, Mrs. Songchan Phuthong, Institute of Biotechnology and Genetic Engineering for cytotoxicity test and Dr. Polkit Sangvanich and Miss Pattaraporn Madtikamai, for HIV-1 reverse transcriptase inhibition test.

The author also wishes to extend her profound thanks to all her friends for their cooperation and mental supports during this work. The financial support of the University Development Commission (UDC) scholarship is also gratefully acknowledged. Pursuing the master program at Chulalongkorn University would have been impossible without this financial support.

Last but not least the author would like to dedicate this master thesis with great respect and love to her parents for all things that they have endured and sacrificed for her success. Finally, she never forgets to thank someone special who is a nice person for continuously cheering up.

CONTENTS

Page

LIST OF TABLES

Tables **Page**

LIST OF FIGURES

Figures **Page**

LIST OF SCHEMES

Schemes **Page**

LIST OF ABBREVIATIONS

%	percent
$^{\circ}C$	degree Celsius
ν_{max}	the wavelength at maximum absorption
δ	Chemical shift
µg	microgram (s)
µL	microlitre (s)
br	broad
cm^{-1}	unit of wave number
cont.	continue
$CDCl_3$	chloroform-d
d	doublet (NMR)
dd	double doublet (NMR)
DEPT	Distortionless Enhancement by Polarization Transfer
DMSO	dimethylsulfoxide
Fig.	Figure
g	gram (s)
Hz	Hertz
IR	infrared
J	coupling constant (NMR)
Kg	kilogram
m	medium (for IR)
m	multiplet (for NMR)
M^+	molecular ion
m.p.	melting point
M.W.	molecular weight
m/z	mass to charge ratio
mg	milligram
ml	millilitre (s)

ppm	part per million
q	quartet (for NMR)
R_f	rate of flow in chromatography
s	singlet (for NMR)
s	strong (for IR)
t	triplet (for NMR)
TLC	Thin Layer Chromatography
w	weak (for IR)
wt	weight
wt. by wt.	weight by weight

CHAPTER I

INTRODUCTION

A large number of plants in Thailand have been used as traditional medicine for a long time. Medicinal plants have been the primary treatment in the health care system. Nowadays, they are widely studied by several modern techniques in a more scientific and systematic investigation. There has also been an effort to develop new drugs from medicinal plants in order to make them safe and effective drugs. In addition, there are numerous medicinal plants that were clinically used in Thailand because they are easily available, inexpensive, effective and have less harmful side effects than synthetic drugs[1]. Accordingly, consuming local medicinal plants can reduce the import of synthetic drugs from foreign countries as well.

Natural product chemistry is one of the approaches in searching for chemical constituents from natural plants and involves seeking their activities by bioassay tests and therapeutic applications. The criteria traditionally used to select plant to study might be the history of that plant in treating diseases, preliminary screening bioactivity tests, or literature surveys about chemical constituents that may have the potential as drugs. This thesis is focused on searching for chemical constituents and their bioactivities from the tropical Thai plant, botanically named *Angiopteris evecta* Hoffm.

Angiopteris evecta Hoffm.,belonging to family Marattiaceae, is broadly distributed in the tropical regions all over the world[2]. In Thailand, this plant is distributed in many areas such as central, western, north eastern and southern parts. There have been several common names called in Thailand, *Waan Keepraet* and *Waan Keepma* (Central), *Keepmalom* (Northern), *Keepraet* (Phrae) and *Dugu* (Southern)[3,4].

Angiopteris evecta Hoffm. is an interesting Thai medicinal plant because of indigenous medicinal herb pharmacopoeia. Some parts of the plant can be used as drugs. For instance, the leaves are used as an antibechic, the roots can be used for stopping bleeding and the rhizomes are used as an antipyretic, a diuretic, a tonic, an analgesic, an anti-emetic and an antidiarrheal[5-8].

1.1 GENERAL CHARACTERISTIC OF *Angiopteris evecta* Hoffm.

Angiopteris evecta Hoffm. is a member of the fern family Marattiaceae, which contains seven genera and a total of approximately 200 species distributed worldwide but mainly in the topics. It is a large arborescent fern with leaves tufted near ground level or with the erect rhizome forming a massive. The stipes (leaf stalks) are green, smooth and swollen at the base where a pair of ear-like stipules enclose the stipe base. The leaves contain no strengthening tissue- each frond is supported entirely by the turgor pressure of the sap within the cells. The bi-pinnate fronds are massive, up to eight metres in length. The pinnae and pinnules are attached by swollen bases and the lower pinnules have an ear-like lobe at their base. Pinnae are up to 4 metres long and 40 centimetres wide. The pinnules are 10 to 20 centimetres long and 1 to 4 centimetres wide, with serrulate margins and free veins. The spore producing sori form a submarginal band around the pinnules and are made up of oblong groups of 4 to 6 pairs of sporangia. Each sporangium is round and splits along a central line[9-11].

The picture of pinnae and rhizomes of *Angiopteris evecta* Hoffm.[12] is shown in **Fig. 1.**

a. leaves

b. rhizomes

c. leaves

d. leaves

Figure 1 The picture of *Angiopteris evecta* Hoffm.

Due to very little chemical information, the lack of information of their biological activities and the interesting screening results for inhibiting of HIV-1 reverse transcriptase. The research about *Angiopteris evecta* Hoffm. should be continued.

1.2 THE SCOPE OF THIS RESEARCH

The research began by extracting specimens of the plant with suitable solvents, then isolating compounds from those crude extracts by chromatographic techniques. Structural elucidation of the isolated compounds was deduced from spectroscopic evidences. Finally, biological tests of the isolated compounds were conducted for cytotoxic activity against cancer cell lines and the inhibition of HIV-1 reverse transcriptase.

1.3 THE OBJECTIVES OF THIS RESEARCH

1. To extract, isolate and purify the chemical constituents of *Angiopteris evecta* Hoffm.
2. To identify the structure of the isolated compounds which were obtained from *Angiopteris evecta* Hoffm.
3. To determine the biological activities of isolated compounds which were obtained from *Angiopteris evecta* Hoffm.

CHAPTER II

Literature Review

2.1 CHEMICAL CONSTITUENTS FOUND IN *Angiopteris* – GENUS PLANTS

Literature surveys of chemical constituents of the plants belonging to *Angiopteris* revealed that there have been the flavanoid glycosides isolated from leaves of these plant which were summarized in **Table 1.** The structures of some isolated compounds are shown in **Fig. 2.**

Table 1. Chemical Constituents of plants in *Angiopteris* - genus

Scientific name	Plant parts	Substances	References
Angiopteris evecta	leaves	Violanthin Isoviolanthin Vicenin-1 Vicenin-2 Vicenin-3 Schaftoside	13 13,14
Angiopteris lygodiifolia	leaves	Vicenin-2 Schaftoside Isoschaftoside 6,8 di-C-arabinopyranosyl-apigenin	14

Table 1. Chemical Constituents of plants in *Angiopteris* - genus (continue)

Scientific name	Plant parts	Substances	References
Angiopteris hypoleuca	leaves	Violanthin Schaftoside 6,8 di-C-arabinopyranosyl-apigenin A mixture of vicenin-2, vicenin-3 and schaftoside	14

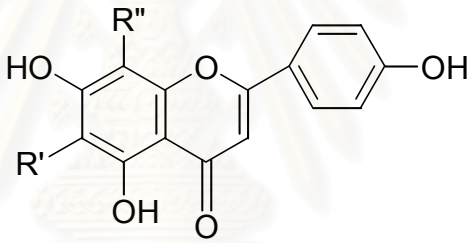

	R′	R″
Violanthin	glucosyl	rhamnosyl
Isoviolanthin	rhamnosyl	glucosyl
Vicenin 1	xylosyl	glucosyl
Vicenin 2	glucosyl	glucosyl
Vicenin 3	glucosyl	xylosyl
Schaftoside	glucosyl	arabinosyl
Isoschaftoside	arabinosyl	glucosyl
6,8-di-C-arabinopyranosyl apiginin	arabinopyranosyl	arabinopyranosyl

Figure 2. The chemical constituents of some plants in *Angiopteris* Genus.

In 1981, Hseu reported the discovery of a fern glycoside, *Angiopteroside* (4-*O*-*β*-D-Glucopyranosyl-L-*threo*-2-hexen-5-olide) monohydrate which was isolated from the dried rhizome of *Angiopteris lygodiifolia* Ros. (Marattiaceae)[15]. The structure is shown in **Fig. 3.**

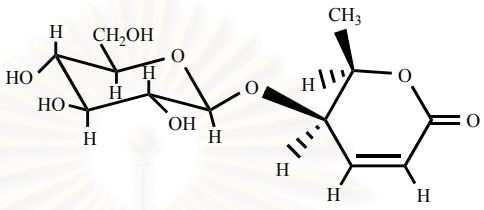

Figure 3 The structure of *Angiopteroside* from *Angiopteris lygodiifolia* Ros.

2.2 Human Immunodeficiency Virus (HIV)

HIV-1, the causative of the acquired immunodeficiency syndrome (AIDS), is the prototypical member of lentivirinae subfamily of retroviruses affecting humans [16]. This virus composes three sets of viral proteins, i.e., the structural proteins (gag, pol, and env), the regulatory proteins (tat, rev, and nef), and the maturation proteins (vif, vpu, and vpr)[17]. The genomic structure of HIV-1 is shown in **Fig. 4.**

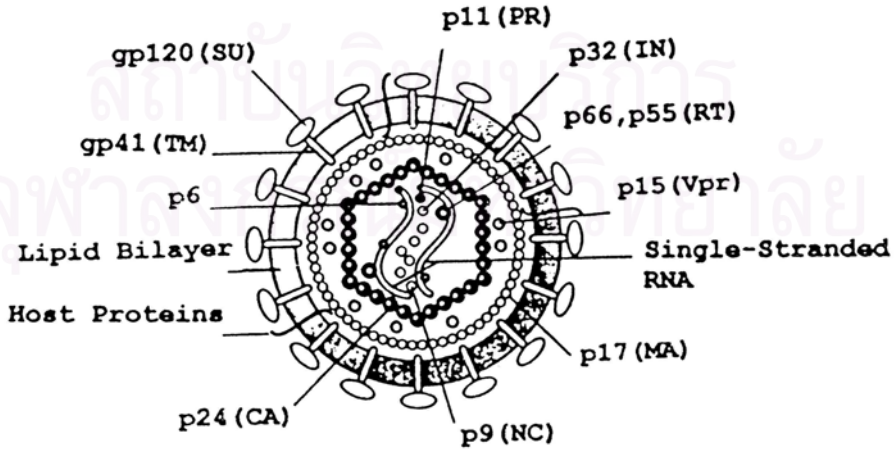

Figure 4. Schematic diagram of HIV-1 virion.

The structure of HIV-1 virion is revealed as an icosahedral structure containing 72 external spikes. These spikes are formed by the two major viral-envelop glycoproteins, gp120 and gp41. The core of HIV-1 contains four nucleocapsid proteins, p24, p17, p9, and p7. This retroviral core also contains two copies of the single stranded HIV-1 genomic RNA associated with the various preformed viral enzymes, including the reverse transcriptase, integrase, and protease [17].

2.2.1 The life cycle of HIV-1 virus and molecular targets for HIV-1.

The life cycle of HIV-1 (as shown in **Fig. 5.**) begins with the interaction of gp120 with the CD4 membrane receptor, and gp41-mediated membrane fusion leading to the entry of HIV-1 into the cell [18-19]. After uncoating, reverse transcription of viral RNA takes place, resulting in the production of the RNA-DNA hybrid. The proviral DNA is separated by the action of ribonuclease H. After transportation to nucleus, the proviral DNA is incorporated into the host DNA through enzyme integrase [20]. The expression of the HIV-1 gene leads to the production of various viral mRNAs. The viral mRNA is transported out of the nucleus and is translated into viral proteins. Posttranslational processing includes myristylation and glycosylation. Viral structural proteins, replicative enzymes and genomic RNA are assembled, associated with envelope glycoproteins. This process is facilitated by a protease specific to HIV. The last stage in the life cycle, HIV-1 virion particles are released by a process of viral budding from the plasma membrane where viral glycoprotein has congregated [21].

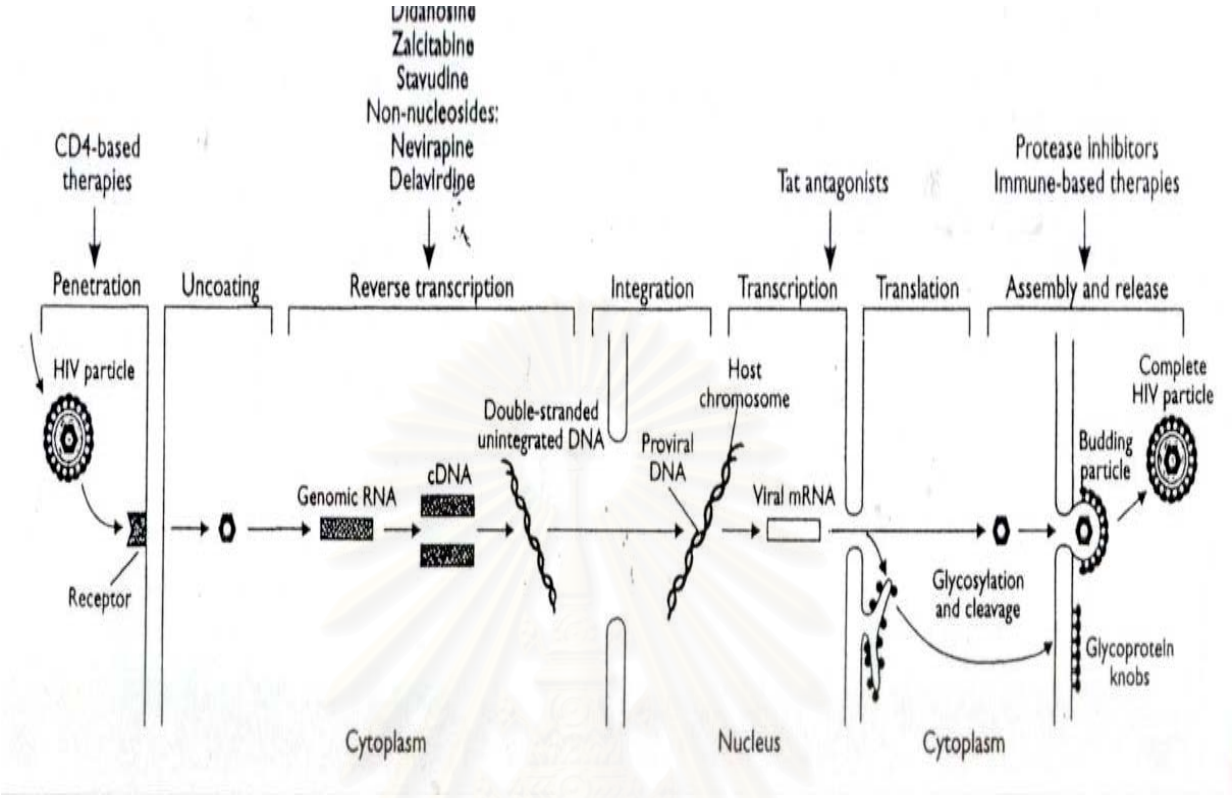

Figure 5. Schematic representation of the HIV-1 life cycle.

2.2.2 Reverse transcriptase (RT) enzyme and binding sites of inhibitors.

RT is a multifunctional enzyme having RNA-directed DNA polymerase and DNA-directed DNA polymerase activities as well as RNase H activity [22]. **Figure 6.** shows the function of RT in viral replication. HIV-RT is a heterodimer containing one 66-kD subunit (p66) and one 51-kD subunit (p51) as shown in **Fig. 7.** The p66 subunit comprises 560 residues and all enzymatic activity of the heterodimer is associated with residues in this subunit. The p51 subunit comprises the initial 440 residues of the p66 subunit. This enzyme is composed of nine domains, named fingers, palm, thumb, connection, and Rnase H in the p66 subunit. The p51 subunit contains only the first four of above mentioned domains. The domains of the p66 subunit form a binding groove for the polynucleotide substrate, at the bottom of which lie the aspartyl residues implicated in polymerase activity [23]. Nucleoside reverse transcriptase inhibitors (NIs) act as competitive inhibitors of the

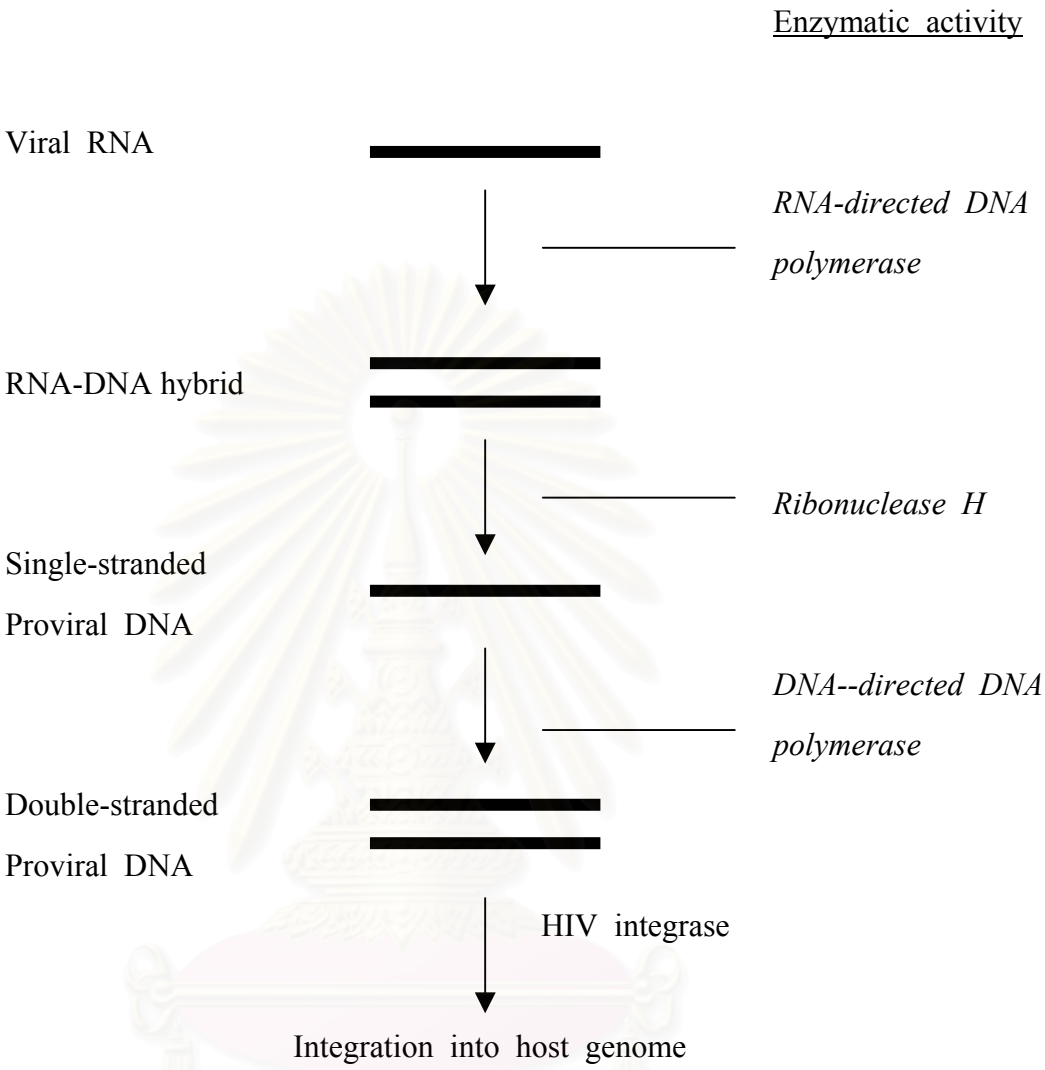

Figure 6. The function of RT in viral replication.

HIV-RT. They interact at the substrate-binding site of the enzyme, where the deoxynucleoside triphosphates normally bind [24]. Inhibition of RT by nonnucleoside reverse transcriptase inhibitors (NNIs) appears to be primarily due to distortion of the polymerase active site. On binding, the NNI creates and occupies a pocket near to the polymerase active site. This process results in a switch to a stable but inactive conformation for the polymerase site [23]. It appears that NNIs binding to their hydrophobic pocket of the HIV-RT does not interfere with the binding of

the natural substrates (deoxynucleoside triphosphate) but slows down the rate of incorporation of the natural substrates into the DNA product [25].

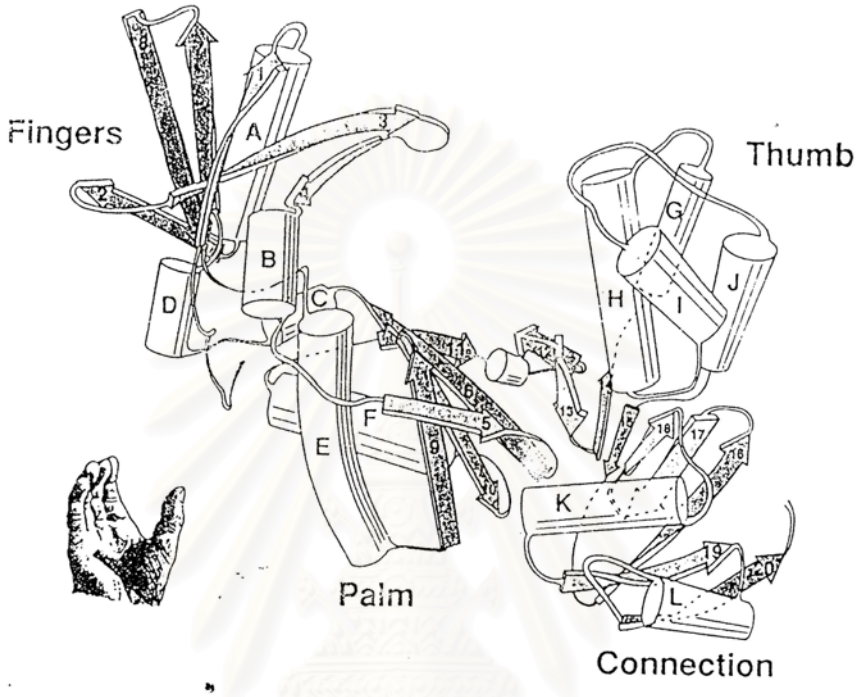

Figure 7. The folding structure of the p66 subunit of HIV-1 reverse transcriptase.

2.2.3 HIV-1 reverse transcriptase inhibitor agents.

There is a relatively large number of agents from several major drug classes that are currently marketed for treating HIV infection. The largest number of these drugs target is the viral RT. RT inhibitors fall into two general classes, i.e., nucleoside and non-nucleoside analogues. The nucleoside analogues that are currently approved for the treatment of HIV infection include 3′-azido-3′-deoxythymidine (AZT, zidovudine, Retrovir®) **1**, 2′,3′-dideoxyinosine (ddI, didanosine, Videx®) **2**, 2′,3′-dideoxycytidine (ddC, zalcitabine, Hivid®) **3**, 2′,3′-didehydro-3′-deoxythymidine (d4T, stavudine, Zerit®) **4**, 2′,3′-dideoxy-3′-thiacytidine (3TC, lamivudine, Epivir®) **5** and abacavir (Ziagen®) **6**. Nevirapine (Viramune®) **7**, delavirdine (Rescriptor®) **8** and efavirenz (Sustiva®) **9** are currently the only NNRTIs

approved for HIV therapy. Structures of approved nucleoside and non-nucleoside HIV-1 reverse transcriptase inhibitors are shown in **Figure 8** and **Figure 9.**

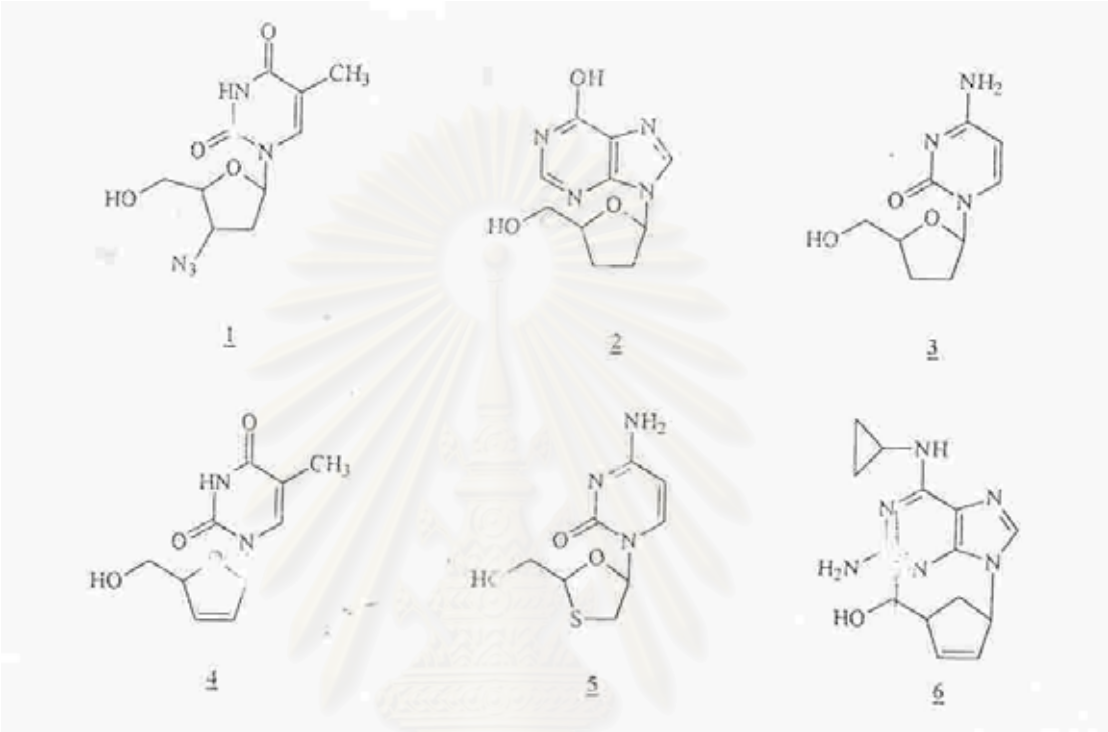

Figure 8. Structures of approved nucleoside HIV-1 reverse transcriptase inhibitors.

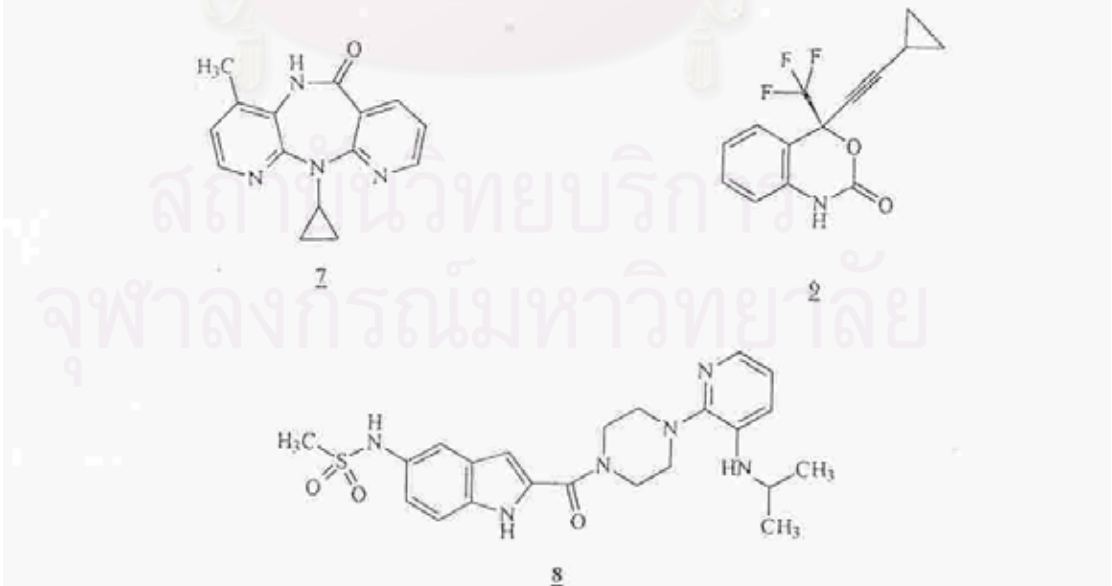

Figure 9. Structures of approved non-nucleoside HIV-1 reverse transcriptase inhibitors.

1. Nucleoside HIV-1 reverse transcriptase inhibitors.

All the nucleoside compounds that have so far been approved for the treatment of HIV infection belong to the class of the 2′,3′-dideoxynucleoside (ddN) analogues i.e., AZT, 3TC, ddT, ddC, d4T and abacavir. Nucleoside HIV-1 reverse transcriptase inhibitors (NRTIs) mimic a naturally occurring building block of DNA. They slow down the progression of HIV replication by they are incorporated into the growing DNA chain by RT. Therefore, these drugs require sequential phosphorylation to the 5′-triphosphate level before they become substrates or competitive inhibitors of RT. Since these compounds do not contain the C-3 hydroxyl group necessary for further chain synthesis, their incorporation into the DNA chain results in chain termination [26]. The illustration of this mechanism of action in shown in **Fig. 10.**

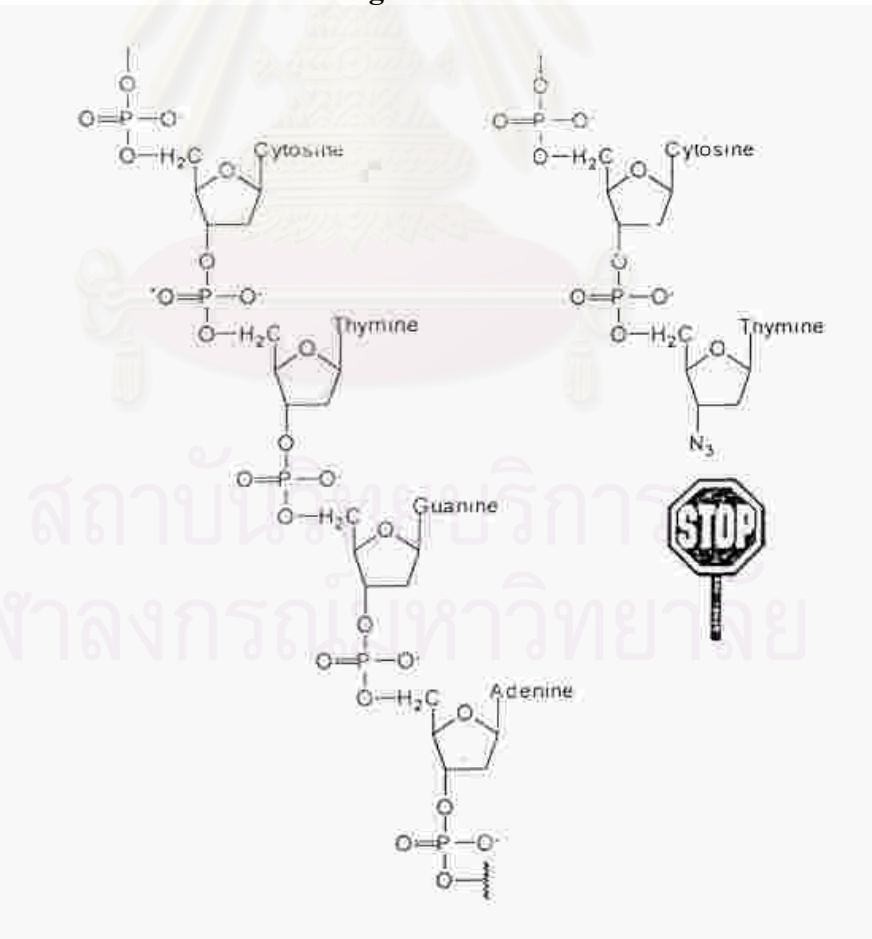

Figure 10. DNA chain termination by AZT-TP.

2. Non-nucleoside HIV-1 reverse transcriptase inhibitors.

Due to the serious side effects and the emergence of resistant viral strains which result from treatment with nucleoside drugs, many researchers have attempted to identify NNRTIs usually via strategies involving broad screening of chemical inventories. As a consequence of these efforts, several NNRTIs of disparate structures have been discovered [27]. These NNRTIs, which act as non-competitive inhibitors with respect to deoxynucleoside triphosphate (dNTPs) at an allosteric site on enzyme, share many common properties. For examples, phosphorylation is not required for RT inhibitoy activity, they are highly specific for HIV-1 relative to HIV-2 or other cellular polymerases, and they are effective against HIV strains resistant to AZT. In fact, a number of competition experiments suggest that the NNRTIs bind to the same or overlapping sites on HIV-1 RT. A crystal structure of RT complexed with the non-nucleoside nevirapine suggested that it was bound in a hydrophobic pocket close to the polymerase active site. Several amino acids residues critical for conferring resistance to other NNRTIs are also located in or near this pocket, supporting the suggestion thaat these inhibitors are binding at similar sites [28]. Many NNRTIs (whose structure as shown in **Fig. 11.**) have been designed and synthesized such as tetrahydroimidazobenzodiazepinone (TIBO) derivative **10** [29], hydroxyethoxy methylphenylthiothymine (HEPT) derivative **11** [30], dipyridodiazepinone **12** [31].

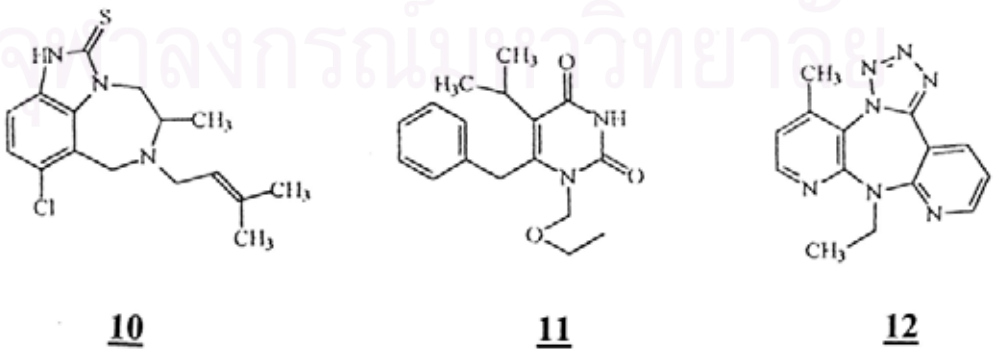

10 **11** **12**

Figure 11. Structures of non-nucleoside reverse transcriptase inhibitors.

CHAPTER III

EXPERIMENTS

3.1 PLANT MATERIALS

The plant materials of *Angiopteris evecta* Hoffm. used in this study were collected from Kanchanaburi Province, Thailand in June 2000. Botanical identification was achieved through comparison with the herbarium specimen plants in the Royal Forest Department of Thailand.

3.2 CHEMICAL REAGENTS

3.2.1 Solvents

All commercial grade solvents, used in this research such as hexane, chloroform, ethyl acetate and methanol, were purified by distillation prior to use. The reagent grade solvents were used for recrystallization.

3.2.2 Other chemicals

1. Merck's silica gel 60 G Art. 7734 (70-230 mesh ASTM) and 9385 (230-400 mesh ASTM) were used as adsorbents for normal column chromatography and flash column chromatography.
2. Merck's TLC aluminum sheets, silica gel $^{60}F_{254}$ precoated 25 sheets, 20x20 cm^2, layer thickness 0.2 mm were used for TLC analysis.
3. TLC spots were visualized with a UV lamp (254 and 365 nm) and with I_2

3.2.3 For Revere Transcriptase Assay.

1. **HIV-1 reverse transcriptase**, recombinant HIV-1-RT, lyophilizate, from potassium phosphate buffer, pH 7.4, containing 0.2% bovine serum albumin (BSA, special quality for molecular biology).

2. **Incubation buffer,** pH 7.8 (50 mM Tris-buffer, containing 319 mM potassium chloride, 33 mM magnesium chloride, 11mM DTT).

3. **Nucleotides,** Tris-HCl (50 mM, pH 7.8) with DIG-dUTP, biotin-dUTP and dTTP.

4. **Template,** template/primer hybrid poly (A) • oligo $(dT)_{15}$ (9 $A_{260\ nm}$/ml), lyophilizate.

5. **Lysis buffer,** ready-to-use, Tris-buffer (50 mM Tris, 80 mM potassium chloride, 2.5 mM DTT, 0.75 mM EDTA and 0.5 % Triton® X-100, pH 7.8).

6. **Anti-dioxigenin-peroxidase** (Anti-DIG-POD), polyclonal anti-body from sheep, lyophilizate.

7. **Washing buffer**.

8. **Conjugate dilution buffer,** sodium phosphate buffer. pH 7.4, containing a blocking reagent.

9. **Substrate buffer,** ABTS® substrate buffer (sodium perborate and citric acid/phosphate buffer).

10. **ABTS® substrate,** powder.

11. **Substrate enhancer,** powder. Use the substrate enhancer only if RT activity is low.

12. **Microtiter plate (MTP) modules** (8-wells), precoated with streptavidin and postcoated with blocking reagent, shrink wrapped, with a desiccant capsule.

13. **Strip frame**, holding a maximum of 12 MTP modules (total of 96 wells), ensures the correct fitting and a tight support of the MTP modules.

14. **Cover foil,** to avoid evaporation. We recommend covering the MTP modules with the self-adhesive cover foils during each incubation step.

3.3 INSTRUMENTS AND EQUIPMENTS

3.3.1 Melting point recorder

The melting points were recorded on a Fisher-John melting point apparatus.

3.3.2 Rotary Evaporator

The eyela rotary evaporator model N-1 was used for the rapid removal of large amounts of volatile solvents.

3.3.3 Optical Rotation

The optical rotation values were measured by a Perkin-Elmer 341 polarimeter.

3.3.4 Elemental Analysis (EA)

The EA values were measured by a Perkin Elmer PE 2400 Series II (CHN/O Analyzer).

3.3.5 Ultraviolet-visible Spectrophotometer (UV-VIS)

The UV-VIS spectra were recorded on a Hewlett Packard 8452A diode array spectrophotometer in chloroform and methanol.

3.3.6 Fourier Transform-Infrared Spectrophotometer (FT-IR)

The FT-IR spectra were recorded on a Nicolet Impact 410 Spectrophotometer. Spectra of solid samples were recorded as KBr pellets.

3.3.7 Nuclear Magnetic Resonance Spectrometer (NMR)

The ^{1}H and ^{13}C Nuclear Magnetic Resonance Spectra were recorded at 200.13 and 50.32 MHz, respectively, on a Bruker Model AC-F200 Spectrometer, and at 500.00 and 125.65 MHz on a JEOL JNM-A500 Spectrometer in deuterated chloroform ($CDCl_3$), dimethylsulfoxide (DMSO), deuterated methanol (CD_3OD) and deuterium oxide (D_2O). Chemical shifts are given in ppm using residual protonated solvent as reference. COSY, NOESY, HMQC and HMBC experiments were performed on the JEOL JNM-A500 Spectrometer.

3.3.8 Mass Spectrometer (MS)

The mass spectra were acquired by a Fison Instruments Mass Spectrometer Model Trio 2000 in EI mode at 70 eV and the LC-MS spectra were obtained in Atmospheric chemical ionization (APcI) mode. The LC-MS condition was measured in MeOH:H_2O (1:1).

3.3.9 X-ray Diffractrometer

The X-ray diffractrometer were obtained on a BRUKER SMART CCD diffractrometer at Department of Physics, Faculty of Science and Technology, Thammasart University.

3.4 EXTRACTION AND ISOLATION

The fresh rhizomes of *A. evecta* Hoffm. (2.70 kg.) were cut into small pieces, pulverized in a blender and then soaked overnight in methanol (2x8L) at room temperature. The methanol solution was filtered and evaporated under reduced pressure to dryness, yielding the crude methanolic extract. Then the crude methanolic extract was extracted with hexane (2L) until the solution was colorless. The filtered hexane solution was evaporated to afford the hexane extract as a greenish-brown oil (2.01 g.). The residue of this step was extracted with ethyl acetate (4L) repeatedly until the solution was clear. The combined ethyl acetate solution was concentrated on a rotary evaporator under reduced pressure to give the ethyl acetate extract as a viscous dark-brown residue (11.74 g.) and the final insoluble residue as a dark-brown oil (112.83 g.).

The crude extracts of the rhizomes of *A. evecta* Hoffm. with various solvents are shown in **Table 2.**

Table 2. The various extracts of the rhizomes of *A. evecta* Hoffm.

Solvent extract	Appearance	Weight (g)	% wt.by wt. of the fresh rhizomes
Hexane	Greenish -brown oil	2.01	0.0744
Ethyl acetate	Dark-brown oil	11.74	0.4348
Methanol	Dark-brown oil	112.83	4.1789

The procedure and results of the extraction are shown in Scheme 1

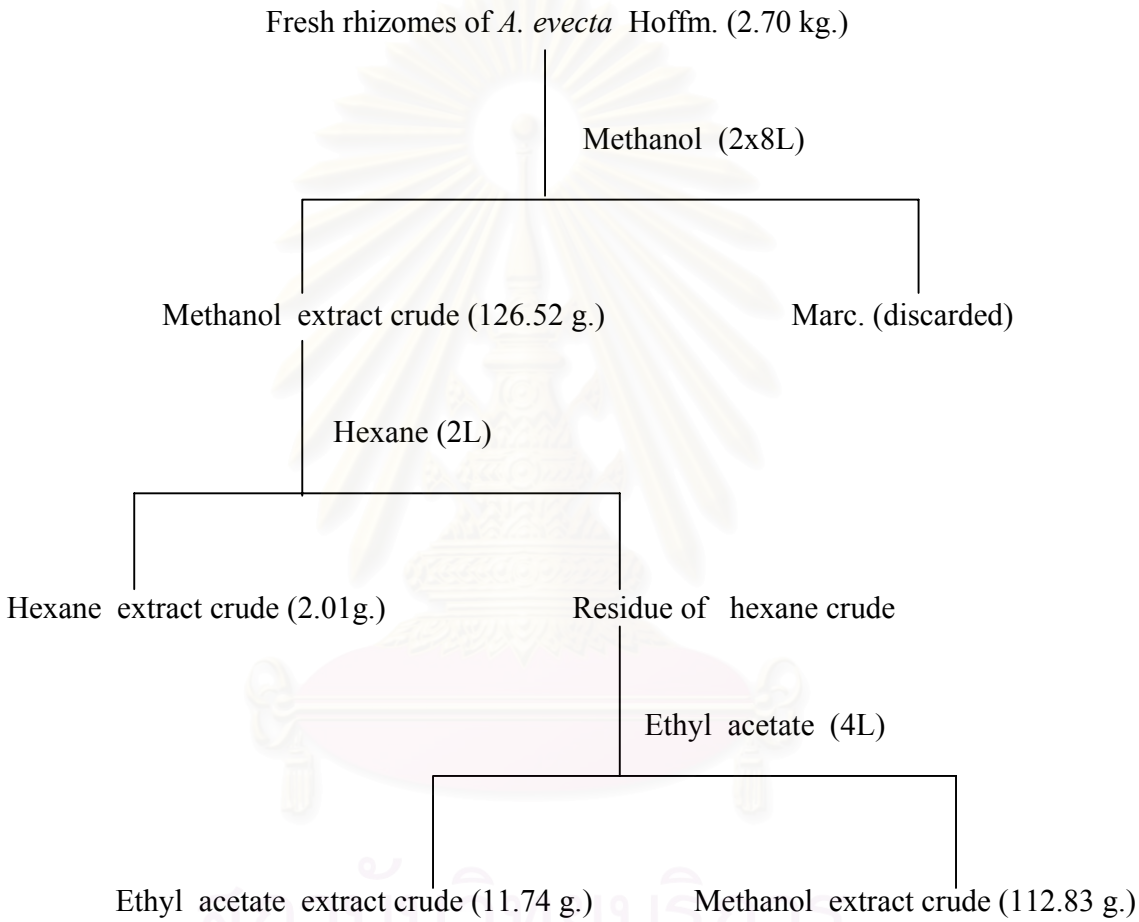

Scheme 1. The procedure of extraction of the fresh rhizomes of *A. evecta* Hoffm.

3.5 ISOLATION OF CRUDE EXTRACT FROM *A. evecta* Hoffm.

3.5.1 Separation of crude ethyl acetate extract .

The crude ethyl acetate extract (11.02 g.) was preadsorbed on silica gel 70-230 mesh ASTM (2 g.) prior to application to the top of the column. The column was eluted with hexane, hexane-ethyl acetate, ethyl acetate and ethyl acetate-methanol respectively. The similar fractions were combined and the solvent was removed by rotary evaporator to give compound 1 and 2 respectively. The isolation of compounds from the crude ethyl acetate extract is briefly summarized in **Scheme 2.**

Scheme 2. Isolation procedures of the crude ethyl acetate extract of the fresh rhizomes of *A. evecta* Hoffm.

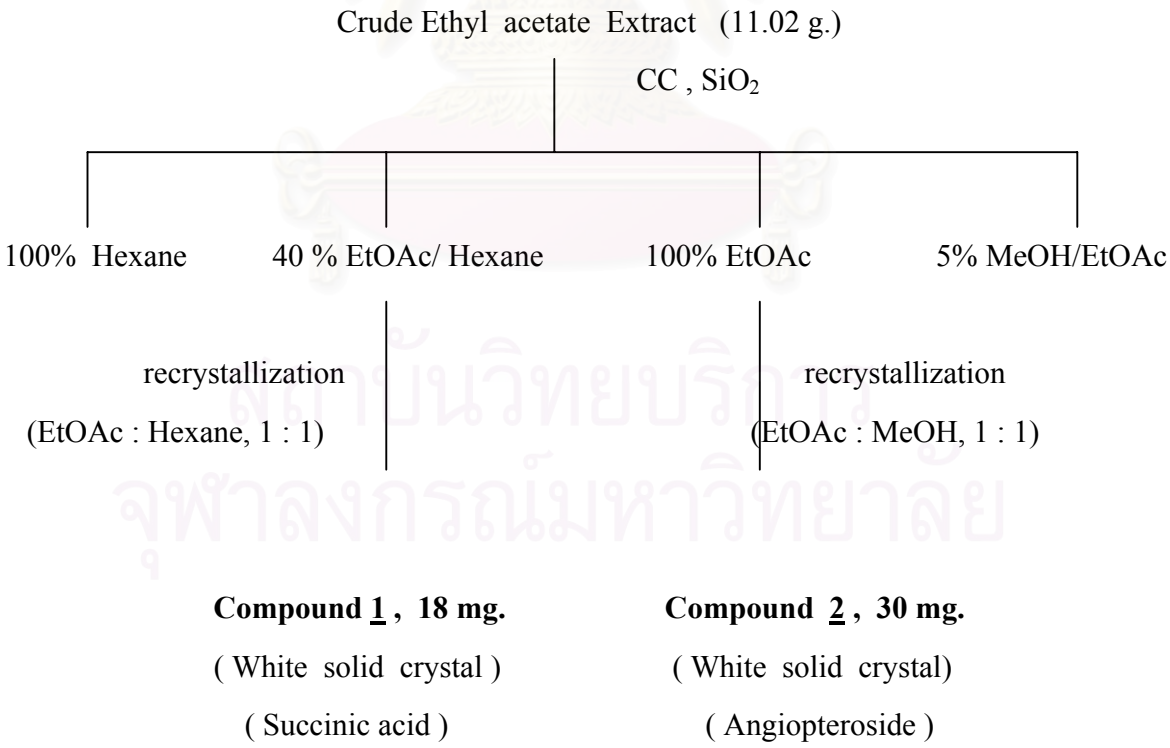

3.5.2 Separation of crude methanol extract .

The crude methanol extract was obtained as a dark-brown oil (112.83 g.). The crude methanol extract (10.12 g.) was mixed with silica gel (2 g.) and applied to a silica gel column. The column was eluted with ethyl acetate and ethyl acetate-methanol gradient in a stepwise fashion until the elutent was ethyl acetate-methanol (50:50). The similar fractions were combined and the solvent was removed by rotary evaporator to give compound 3. Furthermore, fraction with similar composition in crude ethyl acetate provided compound 2. The isolation of compounds from the methanol extract crude is briefly summarized in **Scheme 3.**

Scheme 3. Isolation procedures of the crude methanol extract of the fresh rhizomes of *A. evecta* Hoffm.

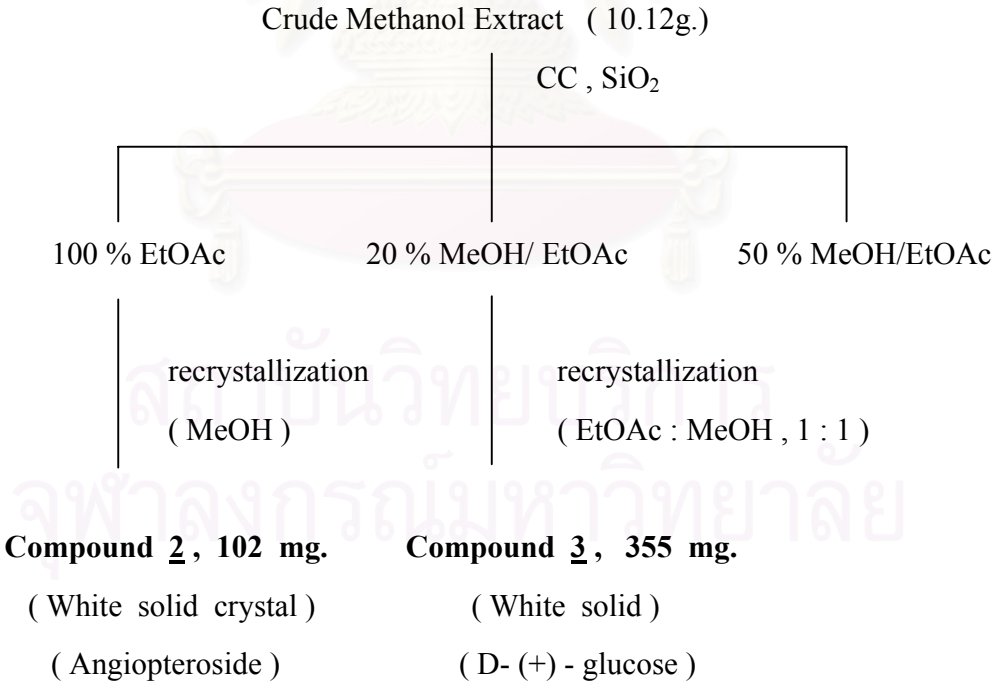

3.5.3 Separation of crude hexane extract.

The crude hexane extract was obtained as a greenish-brown oil (2.01g.) after evaporation. The crude hexane extract (2.00g.) was fractionated by open column chromatography using Merck's silica gel Art. 1.07734.1000 (70-230 mesh ASTM) as an adsorbent. The column was eluted with hexane-ethyl acetate gradient in a stepwise fashion. The similar fractions were combined and the solvent was removed by rotary evaporator to give mixture 4. The isolation of compound from the crude hexane extract is briefly summarized in **Scheme 4.**

Scheme 4. Isolation procedures of the crude hexane extract of the fresh rhizomes of *A. evecta* Hoffm.

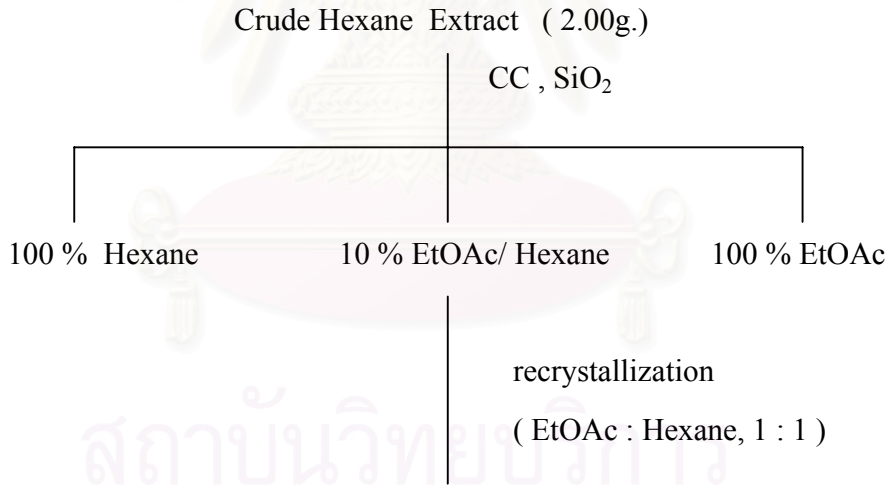

Mixture 4 , 120 mg.

(Needle – white crystal)

(Mixture of stigmasterol and β-sitosterol)

3.6 PURIFICATION AND PHYSICAL PROPERTIES OF ISOLATED COMPOUNDS.

3.6.1 Purification and properties of Compound 1

Compound 1 was obtained from the elution of silica gel column chromatography with 40% ethyl acetate in hexane and was purified by re-crystallization with ethyl acetate and hexane to obtain a white solid crystal (18 mg, 6.67 x 10^{-4} % wt. by wt. of the fresh rhizomes). Compound 1 had m.p. 184-185 °C and showed a single spot at the R_f value 0.38 on TLC plate using 80% ethyl acetate in hexane as the mobile phase. TLC spots were visualized with UV lamp (254 and 365 nm) and with I_2. Compound 1 is soluble in methanol.

Compound 1 is a white solid crystal (18 mg.), UV λ_{max} (nm), MeOH (log ε) : 270sh (0.07).

FT-IR spectrum, (KBr), $\nu_{max}(cm^{-1})$: 3500-2500 (br), 2925 (s), 1693 (s), 1415 (s), 1311 (s), 1203 (s), 1087 (w) and 894 (m) **(Fig. 30 , Table 5)**

^{1}H-NMR spectrum (D_2O, 200 MHz.) δ (ppm) : revealed the significant signal at chemical shift 2.45 (s) ppm. **(Fig. 31)**

^{13}C-NMR spectrum (D_2O, 200 MHz.) δ (ppm) : showed two significant signal at chemical shift 27.6 and 175.9 (q) ppm. **(Fig. 32)**

EI-MS spectrum (*m/z*) 70 eV: 119 (8)[M^++1], 102 (15), 101 (28), 100 (100), 75 (18), 74 (35), 73 (38), 72 (80), 57 (20), 56 (25), 55 (78), 45 (22). **(Fig. 33)**

2.6.2 Purification and properties of Compound 2

Compound 2 was obtained from the elution of silica gel column chromatography with 100% ethyl acetate and was purified by re-crystallization with methanol to obtain a white solid crystal (30 mg, 1.11 x 10^{-3} % wt. by wt. of the fresh rhizomes from crude ethyl acetate extract and 102 mg, 3.78 x 10^{-3} % wt. by wt. of the fresh rhizomes from crude methanol extract). Compound 2 had m.p. 102-103 °C and showed a single spot at the R_f value 0.32 on TLC plate using 50% methanol in ethyl acetate as the mobile phase. TLC spots were visualized with UV lamp (254 and 365 nm) and with I_2. Compound 2 is soluble in organic solvent such as ethyl acetate, methanol and insoluble in hexane and chloroform.

Compound 2 is a white solid crystal (132 mg.), UV λ_{max} (nm), MeOH (log ε) : 270sh (0.13). $[\alpha]_D^{25}$ -233° (EtOH; c 1.0).

FT-IR spectrum, (KBr), $\nu_{max}(cm^{-1})$: 3550-3200 (br), 3135 (m), 2925 and 2896 (w), 1724 (w), 1357 (m), 1265 (m), 1087 and 1056 (s), 829 (m) and 609 (m) **(Fig. 34, Table 12)**

^{1}H-NMR spectrum (CD_3OD, 500 MHz.) δ (ppm) : revealed the significant signals at chemical shift 1.45 (3H, d, *J*=6.4 Hz), 3.17 (1H, dd, *J*=7.6, 8.5 Hz), 3.25 (1H, t, *J*=8.5 Hz), 3.29 (1H, m), 3.33 (1H, t, *J*=8.5 Hz), 3.65 (1H, dd, *J*=5.8, 11.6 Hz), 3.88 (1H, d, *J*=11.6 Hz), 4.41 (1H, d, *J*=7.6 Hz*),* 4.47 (1H, dd, *J*=3.4, 4.9 Hz) , 4.70 (1H, dd, *J*=3.4, 6.4 Hz), 6.12 (1H, d, *J*=9.8 Hz), 7.16 (1H, dd, *J*=4.9, 9.8 Hz) **(Fig. 35, Table 13)**

^{13}C-NMR spectrum (CD_3OD, 500 MHz.) δ (ppm) : 16.2 (t), 62.9 (d), 68.7 (s), 71.7 (s), 74.9 (s), 78.0 (s), 78.2 (s), 78.3 (s), 102.5 (s), 123.6 (s), 145.3 (s), 165.9 (q) **(Fig. 36, Table 13)**

LC-MS spectrum (*m/z*) (APcI, MeOH:H_2O, 1:1): 291 (50) [M^++1], 323 (41) [M^++32], 355 (30) [M^++64] **(Fig. 42).**

EI-MS spectrum (*m/z*) 70 eV: 112 (32), 111 (100), 97 (18), 84 (34), 73 (31), 60(29), 57 (28), 55 (23) **(Fig. 43)**.

2.6.3 Purification and properties of Compound 3

Compound 3 was obtained from the elution of silica gel column chromatography with 20% methanol in ethyl acetate and was purified by re-crystallization with methanol to obtain a white solid (355 mg, 0.0132 % wt. by wt. of the fresh rhizomes). Compound 3 had m.p. 156-158 °C and showed a single spot at the R_f value 0. 25 on TLC plate using 50% methanol in ethyl acetate as the mobile phase. TLC spots were visualized with UV lamp (254 and 365 nm) and with I_2. Compound 3 is soluble in water.

Compound 3 is a white solid (355 mg.), UV λ_{max} (nm), H_2O (log ε) : 266 sh (0.11), $[\alpha]_D^{25}$ +62° (H_2O; c 1.0).

FT-IR spectrum, (KBr), $\nu_{max}(cm^{-1})$: 3550-3100 (br), 2942 (m), 1458 (m), 1342 (m), 1223 (m), 1149 (s), 1110 (s), 1025 (s), 768 (w) and 615 (s) **(Fig. 44, Table 22)**

^{1}H-NMR spectrum (D_2O, 200 MHz.) δ(ppm) : revealed the significant signals at chemical shift 3.06 (t,1H, *J*= 8.0 Hz), 3.13-3.34 (br), 3.44-3.70 (br), 4.42 (d,1H, *J*= 7.8 Hz) and 5.01 (d,1H, *J* = 3.5 Hz) **(Fig. 45)**

^{13}C-NMR spectrum (D_2O, 200 MHz.) δ (ppm) : 59.5, 59.7 (d), 68.6 (s), 70.4 (s), 71.7 (s), 73.1 (s), 74.7 (s), 74.9 (s), 91.0 (s) and 94.6 (s) **(Fig. 46 , Table 23)**

LC-MS spectrum (*m/z*) (APcI, MeOH:H_2O, 1:1): 181 (20) [M^++1], 163 (93)[M^++H_2O] **(Fig. 48).**

EI-MS spectrum (*m/z*) 70 eV: 181 (5) [M^++1], 163 (95), 145 (100), 131 (72), 127(58), 101 (65), 97 (75), 85 (98), 69 (68), 55 (68) **(Fig. 49)**.

2.6.4 Purification and properties of Mixture 4

Mixture of stigmasterol and β- sitosterol was obtained from the elution of silica gel column chromatography with 10% ethyl acetate in hexane and was purified by re-crystallization with ethyl acetate and hexane to give a white needle crystal (120 mg, 0.0044 % wt. by wt. of the fresh rhizomes). The mixture had m.p. 134-135 °C and showed a single spot at the R_f value 0.26 on TLC plate using 30% ethyl acetate in hexane as the mobile phase. TLC spots were visualized with UV lamp (254 and 365 nm) and with I_2. The mixture is soluble in organic solvent such as hexane, ethyl acetate, chloroform and insoluble in methanol.

Mixture 4 is a white needle crystal (120 mg.), UV λ_{max} (nm), $CHCl_3$ (log ε) : 278sh (0.03)

FT-IR spectrum, (KBr), $\nu_{max}(cm^{-1})$: 3690-3150 (br), 2937 (s) and 2867 (s), 1654 (w), 1465 (m) and 1382 (m), 1062 (m), 958 (w) and 804 (w) **(Fig. 50, Table 24)**

^{1}H-NMR spectrum ($CDCl_3$, 200 MHz.) δ (ppm) : revealed the significant signals at chemical shift 0.66-2.26 (br), 3.43-3.56 (br), 4.92-5.23 (1H, br) and 5.30 (1H, d, *J* = 5.0 Hz) **(Fig. 51)**

^{13}C-NMR spectrum ($CDCl_3$, 200 MHz.) δ (ppm) : 11.9-56.9 , 71.8 (s), 121.7 (s), 129.3 (s), 138.3 (s), 140.8 (q) **(Fig. 52, Table 25)**

EI-MS spectrum (m/z) 70 eV: 414[M^+], 412[M^+], 396(12), 381(7), 329(12), 300(17), 271(36), 255(60), 213(45), 159(59), 145(71), 105(63), 95(69), 81(69), 55(100) **(Fig. 54)**

2.7 X-ray Diffraction

Colorless crystal of compound 1 and 2 were recrystallized from ethyl acetate/methanol and methanol respectively and were identified by X-ray diffraction analyses. All data were collected at room temperature using graphite monochromated Mo Kα Radiation (lamda = 0.71069 Å) on BRUKER SAMART CCD diffractrometer. The data were corrected for Lorentz and polarization effects. The crystal data of Compound 1 and 2 were given in **Table 6 and 16** respectively.

The structure were solved by direct methods using SHELXLS-97 and refined by full matrix least-squares on F^2 using SHELXLS-97 with anisotropic thermal parameters for all non-hydrogen atoms. All hydrogen atoms were found from difference Fourier maps and were included in refinement. The fraction coordinates of non-hydrogen atom and selected bond distances and angles of Compound 1 and 2 were listed in **Table 7-Table 11** and **Table 17-Table 21** respectively.

2.8 Biological assay

2.8.1 Cytotoxicity Test [32-33]

Bioassay of cytotoxic activity against 6 tumor cell lines, which were Hs 27 (fibroblast), Kato-3 (gastric), BT 474 (breast), Chago (lung), SW 620 (colon) and HEP-G2 (hepatoma) culture *in vitro* was performed by the MTT (3-(4,5-dimethylthiazol-2-yl)-2,5-diphenyltetrazolium bromide) colorimetric method [32-33]. In principle, the viable cell number / well is directly proportional to the production of formazan, which following solubilization, can be measured spectrophotometrically.

The biological assay of Compound 2 was performed by following the above mentioned procedure and the results of cytotoxicity testing against the 6 cancer cell lines are presented in **Table 26.**

2.8.2 The Principle of Reverse Transcriptase Test. [34-36]

The Reverse Transcriptase Assay, non-radioactive takes advantage of the ability of reverse transcriptase to synthesize DNA, starting from the template/primer hybrid poly (A) • oligo (dT) 15. It avoids the use of [^{3}H]- or [^{32}P]-labeled nucleotides employed for the setup of the classical RT assay. In place of radiolabeled nucleotides, digoxigenin- and biotin-labeled nucleotides in an optimized ratio are incorporated into one and the same DNA molecule, which is freshly synthesized by the RT. Alternatively, the flexibility of the assay allows for the use of a template/primer hybrid of individual choice (e.g., a viral template in place of the template/primer hybrid supplied with the kit). The detection and quantification of synthesized DNA as a parameter for RT activity follows a sandwich ELISA(Enzyme-Linked Immunosorbent-Assay) protocol: Biotin-labeled DNA binds to the surface of microtiter plate (MTP) modules that have been precoated with streptavidin. In the next step, an antibody to digoxigenin, conjugated to peroxidase

(anti-DIG-POD), binds to the digoxigenin-labeled DNA. In the final step, the peroxidase substrate ABTS® is added. The peroxidase enzyme catalyzes the cleavage of the substrate, producing a colored reaction product. The reverse transcriptase test principle is shown in **Fig. 12.** The absorbance of the samples can be determined using a microtiter plate (ELISA) reader and is directly correlated to the level of RT activity in the sample **(Fig. 13)**

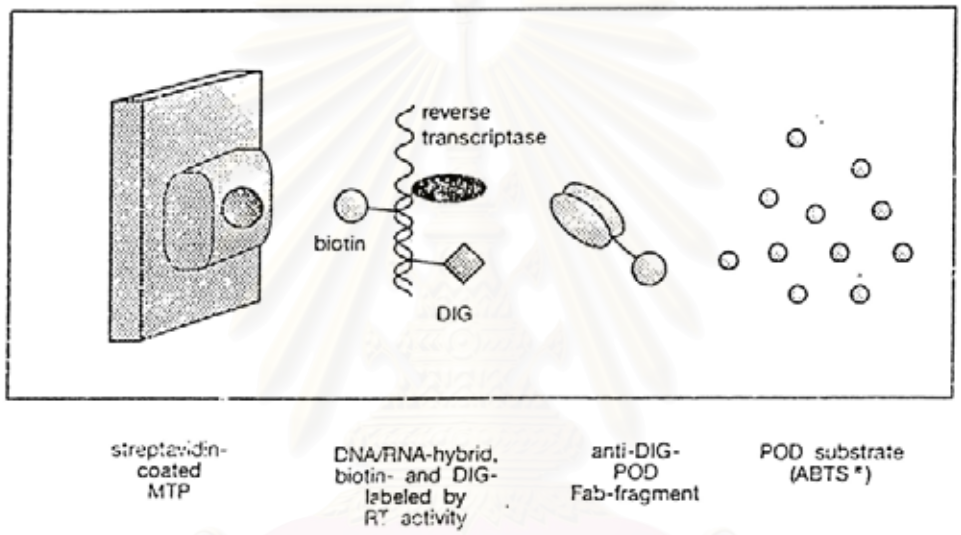

Figure 12. The reverse transcriptase test principle

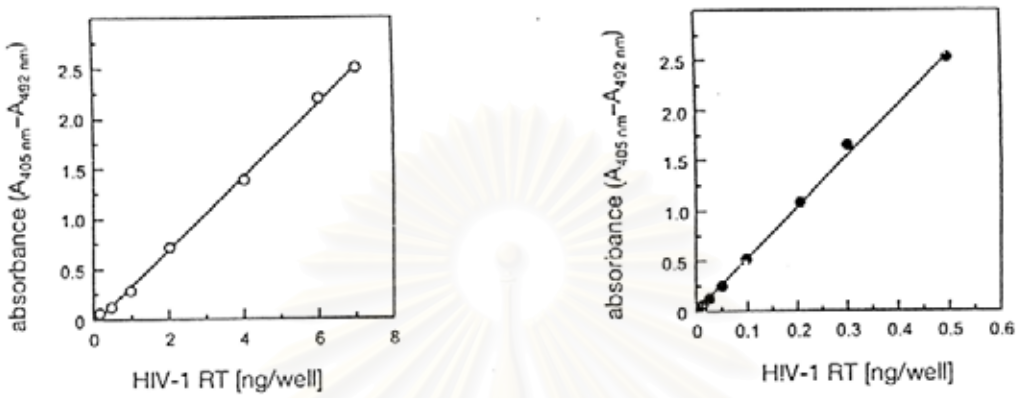

Figure 13. Typical calibration curve, using ABTS® substrate without substrate enhancer. After an enzyme reaction of 1 h (•) or 15 h (o), respectively, absorbance was determined at 405 nm with a reference wavelength at 492 nm.

- **The Reverse Transcriptase Assays.**

The *in vitro* activity of reverse transcriptase was determined with the Boehringer Mannheim ELISA kit [36], and 2′,3′-dideoxyinosine (ddI) was included as a positive control for inhibition of reverse transcriptase.

Assay procedure

In the first step, open enough foil bags for the number of MTP modules to be used. Put them into the frame in the correct orientation. (The correct fitting ensures a tight support of the MTP modules). MTP modules are ready to use and need not be rehydrated prior to addition of the samples. After finishing the reverse transcriptase reaction, add 4-6 ng recombinant HIV-1-RT, diluted in lysis buffer (20 µl/well) per well of the MTP modules. Lysis buffer with no HIV-1-RT added should be used as a negative control. Add 20 µl of RT inhibitors diluted in lysis buffer and 20 µl reaction mixture per

well. Cover the MTP modules with a cover foil and incubate for 1 h at 37 °C. Remove the solution completely. Rinse 5 times with 250 µl of washing buffer per well for 30s each and remove washing buffer carefully. Add 200 µl of anti-DIG-POD working dilution (200 mU/ml) per well, cover the MTP modules with a cover foil and incubate for 1 h at 37 °C. Remove the solution completely. Rinse 5 times with 250 µl of washing buffer per well for 30s each and remove washing buffer carefully again. Add 200 µl of ABTS® substrate solution per well and incubate at room temperature until color development (green color) is sufficient for photometric detection (10-30 min). In the final step, using a microtiter plate (ELISA) reader, measure the absorbance of the samples at 405 nm.

The biological assay of Compound 2 was performed by following the above mentioned procedure and the results of the *in vitro* activity of reverse transcriptase are presented in **Table 27.**

CHAPTER IV

RESULTS AND DISCUSSION

4.1 Preliminary screening results of the crude extracts.

4.1.1 Cytotoxic activity test

In order to study and investigate the biological activity of the rhizomes of *Angiopteris evecta* Hoffm. The three crude extracts were preliminarily screened for cytotoxicity against tumor cell lines, which composed of BT 474 (breast), Chago (lung), Hep-G2 (hepatoma), HS 27 (fibroblast), Kato-3 (gastric) and SW 620 (colon) cancer according to the procedure described in Chapter III. The results were displayed in **Table 3.**

Table 3. Cytotoxic activity against tumor cell lines of crude extract from the rhizomes of *Angiopteris evecta* Hoffm.

Crude (10 μg/ml)	% survival					
	BT 474 (breast)	Chago (lung)	Hep-G2 (hepatoma)	HS 27 (fibroblast)	Kato-3 (gastric)	SW 620(colon)
Hexane crude	102	106	103	70	113	98
Ethyl acetate crude	95	108	98	68	120	99
Methanol crude	61	84	73	44	80	92

From the data in Table 3, it showed that the methanol crude extract of *Angiopteris evecta* Hoffm. showed weak cytotoxicity against all cancer cell lines. The hexane and ethyl acetate crude extracts of *Angiopteris evecta* Hoffm. showed no significant activity on cytotoxicity against 6 tumor cell lines.

4.1.2 The reverse transcriptase test.

In order to study and investigate the biological activity of the rhizomes of *Angiopteris evecta* Hoffm. The three crude extracts were preliminarily screened for HIV-1 reverse transcriptase inhibition activity according to the procedure described in Chapter III. The results were displayed in **Table 4.**

Table 4. The *in vitro* inhibition of HIV-1 RT of crude extracts from the rhizomes of *Angiopteris evecta* Hoffm.

Samples	Final Concentration (mg/ml)	% inhibition
Hexane crude extract	3	41.5
Ethyl acetate crude extract	3	85.7
Ethanol crude extract	3	89.4

From the data in Table 4, it showed that the hexane crude extract of *Angiopteris evecta* Hoffm. did not show inhibitory activity on HIV-1 reverse transcriptase. In spite of that, the ethyl acetate and methanol crude extracts have high inhibitory activities. Therefore, the ethyl acetate and methanol crude extract were selected and then purified before the hexane crude extract by using silica-gel column chromatography with hexane-ethyl acetate and ethyl acetate-methanol gradient solvent system to give three compounds. The hexane crude extract was purified with similar technique and gave one compound.

The rhizome investigation of *A. evecta* Hoffm. from Kanchanaburi Province indicates that compound 1, 2, 3 and mixture 4 have been isolated and purified by solvent extraction and chromatography techniques. The structural characte-rization of these compounds was proposed from spectral data including UV, IR, NMR, MS, and also X-ray crystallographic analysis. The cytotoxicity of these isolated compounds had been observed against cancer cell lines by following the standard procedure and the HIV-1 reverse transcriptase inhibition of these isolated compounds was tested by ELISAS (Enzyme-Linked Immunosorbent-Assays) techniques. The detail of this research will be described as in the following.

4.2 STRUCTURE ELUCIDATION OF THE ISOLATED COMPOUNDS FROM THE FRESH RHIZOMES OF *Angiopteris evecta* Hoffm.

4.2.1 Structure elucidation of Compound 1

Characterization of Compound 1

The IR spectrum of Compound 1 (Fig. 30) revealed the presence of carboxylic acid group according to the broad absorption band between 3500 to 2500 cm^{-1} and the strong absorption band at 2925 cm^{-1} suggested methylene group stretching vibration. In addition, there is the presence of carboxylic acid carbonyl stretching according to the strong absorption band at 1693 cm^{-1}. The IR spectrum showed no unsaturation. The IR spectrum of Compound 1 is summarized in **Table 5.**

Table 5. The IR absorption band assignment of Compound 1.

Wave number (cm^{-1})	Intensity	Vibration
3500-2500	Broad	O-H stretching vibration of acid
2925	Strong	C-H stretching vibration of $-CH_2$
1693	Strong	C=O stretching vibration of acid
1415, 1311, 1203	Strong	C-O stretching vibration and O-H deformation
894	Medium	O-H deformation (out-of-plane)

The ^{1}H-NMR spectrum (Fig.31) of Compound 1 showed one signal at chemical shift 2.45 (s) ppm.

The ^{13}C-NMR spectrum (Fig. 32) showed 2 line. One signal of carboxylic acid group revealed at 175.9 ppm and one signal appeared at 27.6 ppm.

The MS spectrum showed the fragmentation as follow, *m/z* (EIMS) **(Fig. 33)**: 119 (8) [M^{+}+1], 102 (15), 101 (28), 100 (100), 75 (18), 74 (35), 73 (38), 72 (80), 57 (20), 56 (25), 55 (78) and 45 (22). The EI mass spectrum of this compound gave a molecular ion at *m/z* 118, which was corresponding to the molecular formula $C_4H_6O_4$ indicating the DBE of 2.

Moreover, the structure of Compound 1 was also confirmed by X-ray diffraction analysis, which is shown in **Fig. 14.** X-ray diffraction data are presented in **Table 6,7,8,9,10 and 11.**

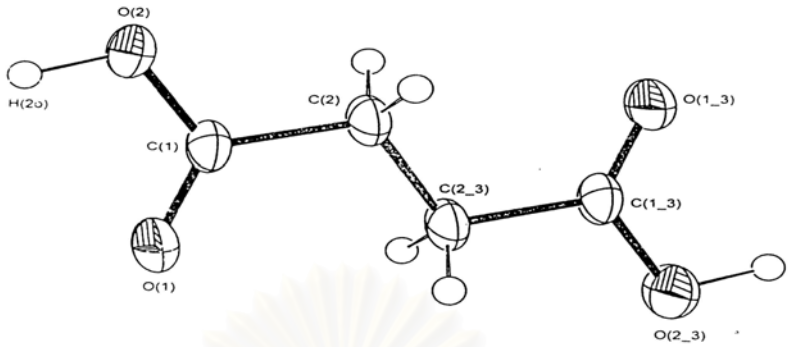

Figure 14. The ORTEP drawing of Compound 1

Table 6. Crystal data and structure refinement for 1.

Empirical formula	$C_4H_6O_4$	
Formula weight	118.09	
Temperature	293(2) K	
Wavelength	0.71073 Å	
Crystal system, space group	monoclinic, $P2_1/a$	
Unit cell dimensions	a = 5.1048(6) Å	alpha = 89.996 (2) deg.
	b = 5.5220(6) Å	beta = 89.993 (2) deg.
	c = 8.8882(10) Å	gamma = 91.568 (2) deg.
Volume	250.45(5) $Å^3$	
Z, Calculated density	1, 1.566 Mg/m^3	
Absorption coefficient	0.14 mm^{-1}	
F(000)	124	
Theta range for data collection	3.69 to 30.43 deg.	
Index ranges	$-7 \le h \le 7, -7 \le k \le 7, -8 \le l \le 12$	
Reflections collected / unique	1805 / 725 [R(int.) = 0.0461]	
Completeness to 2theta = 30.42	94.9%	
Refinement method	Full-matrix least-squares on F^2	
Data / restraints / parameters	725/ 0 / 49	
Goodness-of-fit on F^2	1.060	
Final R indices [I > 2sigma(I)]	R1 = 0.0454, wR2 = 0.1206	
R indices (all data)	R1 = 0.0592, wR2 = 0.1299	
Largest diff. peak and hole	0.203 and -0.343 e. $Å^{-3}$	

Table 7. Atomic coordinates (x 10^4) and equivalent isotropic displacement parameters ($Å^2$ x 10^3) for 1**.**

	x	*y*	*z*	*U*(eq)*
C(1)	2630 (2)	7601 (2)	10335 (1)	29 (1)
C(2)	4723 (3)	5806 (3)	10663 (1)	32 (1)
O(1)	1246 (2)	7527 (2)	9220 (1)	43 (1)
O(2)	2435 (2)	9236 (2)	11401 (1)	47 (1)

*U(eq) is defined as one third of the trace of the orthogonalized Uij tensor.

Table 8. Bond distances (Å) for 1.

Bond Distances	(Å)
C(1) - O(1)	1.2170 (17)
C(1) - O(2)	1.3138 (17)
C(1) - C(2)	1.5062 (16)
C(2) - C(2) #1	1.5090 (3)

Symmetry transformations used to generate equivalent atoms:

#1 = –x+1, -y+1, -z+2

Table 9. Bond angles (deg.) for 1.

Angles	(deg.)
O(1) - C(1) - O(2)	123.74 (11)
O(1) - C(1) - C(2)	123.85 (11)
O(2) - C(1) – C(2)	112.40 (11)
C(1) - C(2) – C(2) #1	112.61 (14)

Symmetry transformations used to generate equivalent atoms :
#1 = –x+1, -y+1, -z+2

Table 10. Anisotropic displacement parameters ($Å^2$ x 10^3). The anisotropic displacement factor exponent takes the form:
$-2\,pi^2\,[\,h^2\,a^{*2}\,U11 + \ldots + 2hka^*b^*U12\,]$

	U11	*U22*	*U33*	*U23*	*U13*	*U12*
C(1)	28 (1)	27 (1)	33 (1)	2 (1)	4 (1)	12 (1)
C(2)	32 (1)	32 (1)	34 (1)	0 (1)	-1 (1)	17 (1)
O(1)	45 (1)	41 (1)	43 (1)	-6 (1)	-11 (1)	25 (1)
O(2)	50 (1)	48 (1)	45 (1)	-14 (1)	-10 (1)	31 (1)

Table 11. Hydrogen bonds for 1 [Å and deg.]

D-H…A	d(D-H)	d(H…A)	d(D…A)	<(DHA)
O(2)-H(2O)…O(1)#2	1.01 (2)	1.68 (2)	2.6863 (13)	173 (2)

Symmetry transformations used to generate equivalent atoms :
#2 = –x, -y+2, -z+2

Considerably, the information obtained from UV, IR, NMR and MS spectra along with physical properties, such as melting point led to the deduction that compound 1 is succinic acid. The structure of compound 1 is shown in **Fig. 15.**

Figure 15. The structure of Compound 1.

4.2.2 Structure elucidation of Compound 2

Characterization of Compound 2

The IR spectrum of Compound 2 **(Fig. 34)** revealed the presence of alcohol group according to the broad absorption band between 3550 to 3200 cm^{-1} and the weak absorption band at 2925 and 2896 cm^{-1} suggest methyl and methylene group stretching vibration. In addition, there is the presence of the lactone unsaturated carbonyl stretching according to the strong absorption band at 1724 cm^{-1} and 1087 and 1056 cm^{-1} which are C-O stretching vibration of hydroxy groups. The IR spectrum of Compound 2 is summarized in **Table 12.**

Table 12. The IR absorption band assignment of Compound 2.

Wave number (cm^{-1})	Intensity	Vibration
3200-3550	Broad	O-H stretching vibration of alcohol
2925,2896	Weak	C-H stretching vibration of $-CH_3$, $-CH_2$
1724	Strong	C=O stretching vibration of lactone
1357, 1265	Medium	C=C stretching vibration of alkene
1087, 1056	Strong	C-O stretching vibration of alcohol
829	Medium	C-H out of plane bending vibration

The ^{1}H-NMR spectrum (Fig. 35, Table 13) of Compound 2 indicated that it showed single-proton absorption at δ7.16 and 6.12 ppm. coupled to each other, $J_{2,3}$ = 9.8 Hz., indicating an cis-olefinic function. An anomeric proton at δ4.41 (1H, d, J = 7.6 Hz) could be the signal of β-anomeric proton of glucose while a group of multiplet signals at δ4.41-3.17 ppm. were signals of sugar moiety and one methyl group at δ1.45 ppm.

The ^{13}C-NMR spectrum (Fig. 36, Table 13) showed 12 lines. One signal of the lactone carbonyl appeared at 165.9 ppm.

DEPT-90 spectrum (Fig. 37), indicated the presence of typical of a glycoside at 102.5, 78.2, 78.0, 74.9, and 71.7 ppm. In addition, it indicated the presence of the unsaturated methines at 123.6 and 145.3 ppm.

DEPT-135 spectrum (Fig. 37), showed one methyl carbon at 16.2 ppm., one methylene carbon at 62.9 ppm. and the carbon signal at 166.7 ppm was quaternary carbon.

The information from 2D-NMR techniques; HMQC correlation **(Table 13)**, HMBC correlation **(Fig. 18, Table 14)**, COSY correlation **(Fig. 19, Table 14)**, and NOESY correlation **(Fig. 20)** were used to assist the interpretation of the structure of compound 2.

Table 13. The HMQC spectral data of Compound 2.

^{13}C-NMR (ppm)	^{1}H-NMR (ppm), coupling constant (Hz)
16.2(t)	1.45d (*J*=6.4)
62.9(d)	3.65dd (*J*=5.8, 11.6), 3.89d (*J*=11.6)
68.7(s)	4.47dd (*J*=3.4, 4.9)
71.7(s)	3.25t (*J*=8.5)
74.9(s)	3.17dd (*J*=7.6, 8.5)
78.0(s)	3.33t (*J*=8.5)
78.2(s)	3.29m
78.3(s)	4.70dd (*J*=3.4, 6.4)
102.5(s)	4.41d (*J*=7.6)
123.6(s)	6.12d (*J*=9.8)
145.3(s)	7.16dd (*J*=4.9, 9.8)
165.9(q)	-

Table 14. The HMQC, HMBC and COSY spectral data of Compound 2.

Position	δ_C	δ_H	HMBC (H to C)	COSY
1	165.9(q)	-	-	-
2	123.6(s)	6.12d (*J*=9.8)	C-1, C-4	H-3(7.16)
3	145.3(s)	7.16dd (*J*=4.9, 9.8)	C-1, C-4, C-5, C-6	H-2(6.12), H-4(4.47)
4	68.7(s)	4.47dd (*J*=3.4, 4.9)	C-2, C-3, C-6, C-1′	H-3(7.16), H-5(4.70)
5	78.3(s)	4.70dd (*J*=3.4, 6.4)	C-4, C-6	H-4(4.47), H-6(1.45)
6	16.2(t)	1.45d (*J*=6.4)	C-2, C-4, C-5	H-5(4.70)
1′	102.5(s)	4.41d (*J*=7.6)	C-4, C-6, C-2′, C-3′	H-2′(3.17)
2′	74.9(s)	3.17dd (*J*=7.6, 8.5)	C-1′, C-3′	H-1′(4.41),H-3′(3.33)
3′	78.0(s)	3.33t (*J*=8.5)	C-2′, C-4′	H-2′(3.17),H-4′(3.25)
4′	71.7(s)	3.25t (*J*=8.5)	C-3′, C-5′, C-6′	H-3′(3.33),H-5′(3.29)
5′	78.2(s)	3.29m	C-2′, C-3′, C-4′, C-6′	H-4′(3.25),H-6′(3.65, 3.88)
6′	62.9(d)	3.65dd (*J*=5.8, 11.6) 3.88d (*J*=11.6)	C-5′	H-5′(3.29)

Compound 2 showed spectral data similar to that of osmundalin from the fern *Osmunda japonica*, which was diastereomer of angiopteroside from the fern *Angiopteris lygodiifolia* Ros.[15], reported previously in the literature [37-38]. From the literature, osmundalin was a colorless powder, m.p. 104-105 ^{o}C and $[\alpha]^{20}_{D}$ -107^{o}(c=1.0,MeOH). The young unopened fronds of this plant are eaten as a vegetable and the dried shoots are sold as the food *akaboshi zenmai.* Moreover, osmundalin had been used as antifeedant. The structure of osmundalin and angiopteroside were shown in **Fig. 16.** The difference of both was the configuration at the position 4 and 5. Osmundalin was 4R,5S while angiopteroside was 4R,5R.

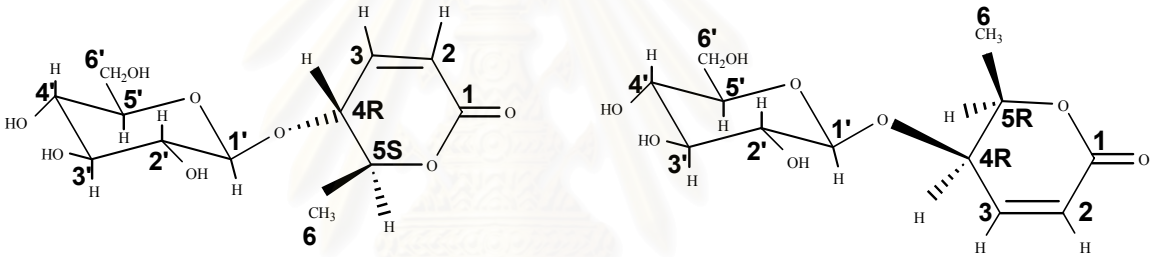

Osmundalin Angiopteroside

Figure 16. The structure of osmundalin and angiopteroside.

The ^{1}H, ^{13}C-NMR signal of compound 2 and osmundalin are presented in the **Table 15** as follows.

Table 15. The ^{1}H, ^{13}C-NMR spectra of Compound 2 with Osmundalin*.

Position	Compound 2		Osmundalin	
	δ_H (ppm)	δ_C (ppm)	δ_H (ppm)	δ_C (ppm)
1	-	165.9	-	165.2
2	6.12	123.6	6.03	121.6
3	7.16	145.3	7.10	147.8
4	4.47	68.7	4.49	73.4
5	4.70	78.3	4.59	79.3
6	1.45	16.2	1.46	18.6
1′	4.41	102.5	4.50	102.9
2′	3.17	74.9	3.21	74.9
3′	3.33	78.0	3.40	78.0
4′	3.25	71.7	3.32	71.6
5′	3.29	78.2	3.38	78.2
6′	3.65	62.9	3.67	62.8
	3.85		3.88	

- Compound 2 and osmundalin were measured in CD_3OD.

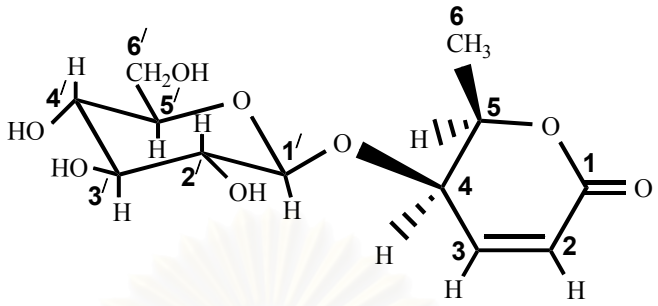

Figure 17. The structure of Compound 2.

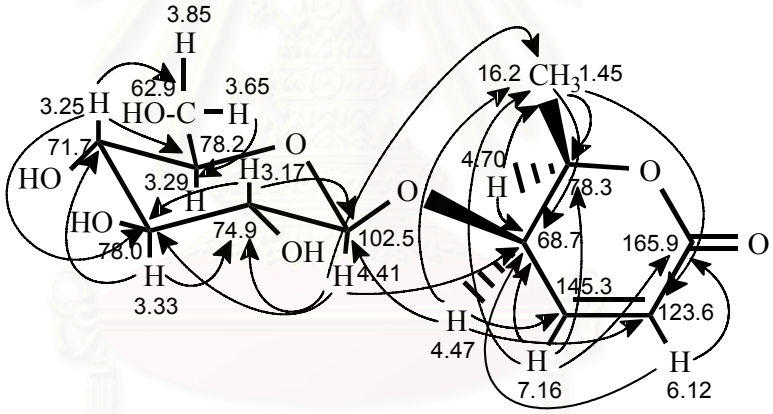

Figure 18. The HMBC correlation of Compound 2.

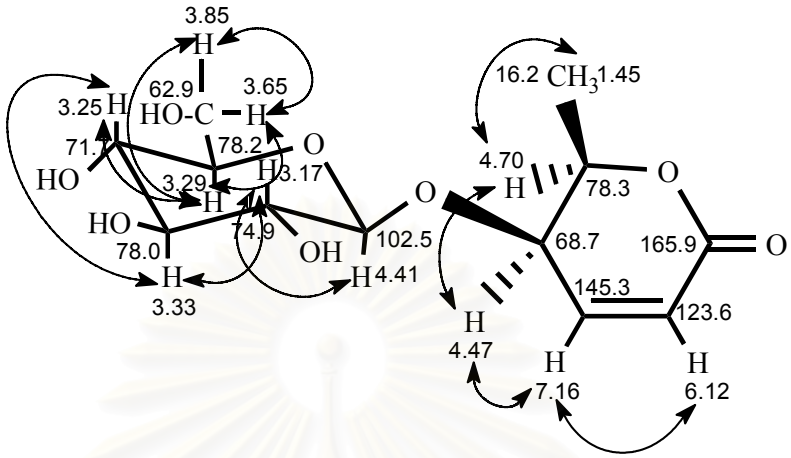

Figure 19. The COSY correlation of Compound 2.

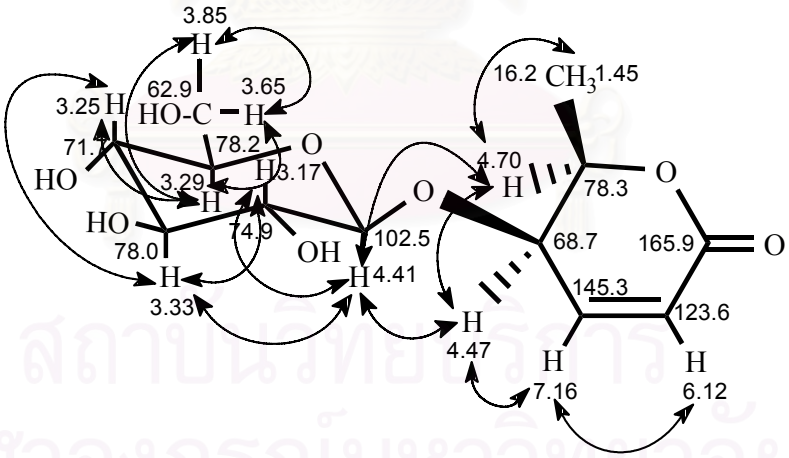

Figure 20. The NOESY correlation of Compound 2.

The LC-MS spectrum (Fig. 42) showed a molecular ion peak corresponding to angiopteroside assigned to be $C_{12}H_{18}O_8$ [M^++1] (*m/z*= 291) which indicated 4 DBE.

The EI-MS spectrum (Fig. 43) showed the fragmentation as follow, *m/z* :112 (32), 111 (100), 97 (18), 84 (34), 73 (31), 60 (29), 57 (28), 55 (23).

The ion fragmentation pattern in the mass spectrum in this compound indicated that it was angiopteroside. The possible mass fragmentation of Compound 2 is shown in **Scheme 5.**

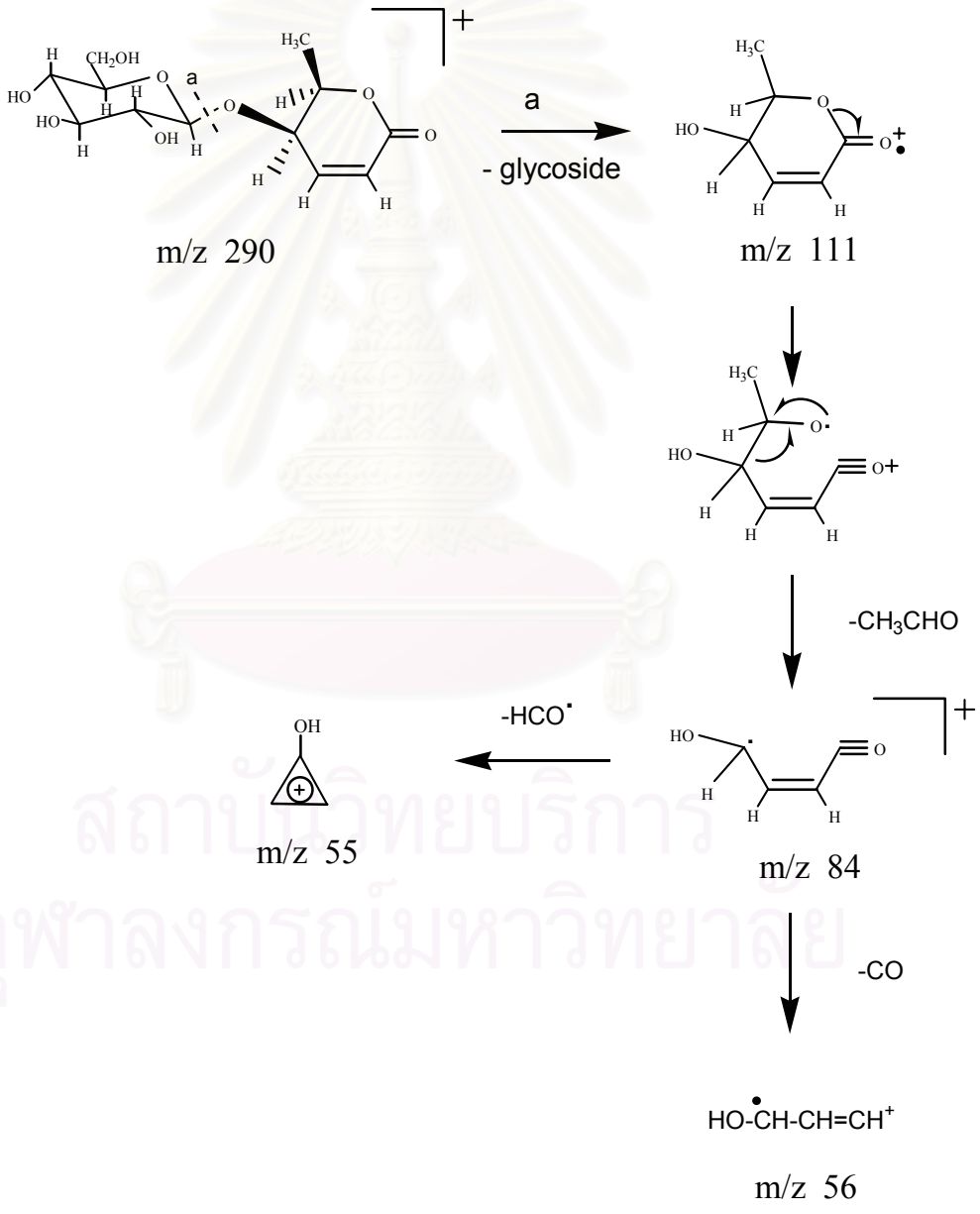

Scheme 5. The possible mass fragmentation pattern of Compound 2.

Moreover, the structure of Compound 2 was also confirmed by X-ray diffraction analysis, which indicated that Compound 2 was identical to angiopteroside which was diastereomer of osmundalin. The ORTEP drawing of Compound 2 is shown in **Fig. 21.**

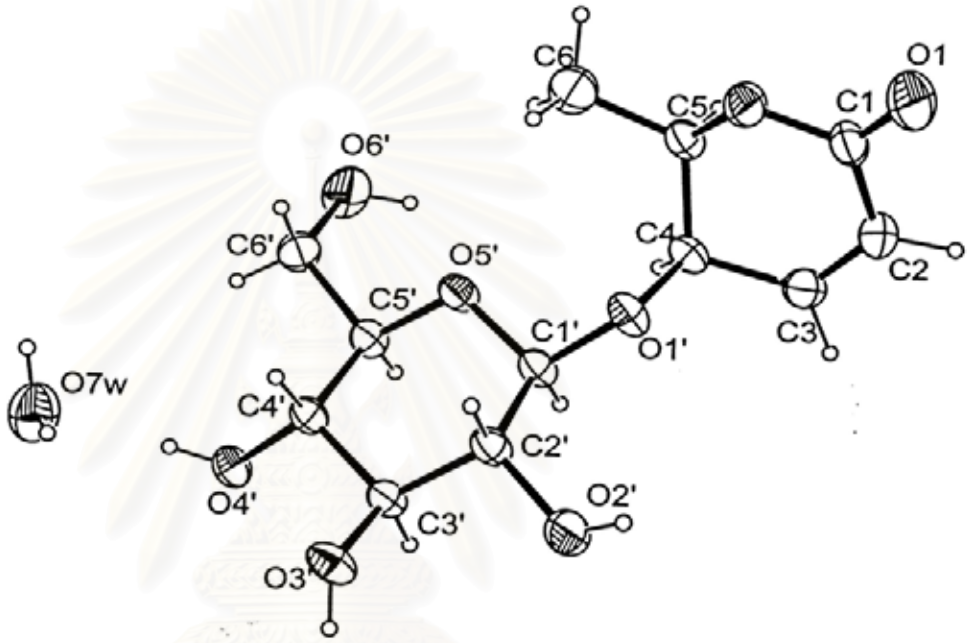

Figure 21. The ORTEP drawing of Compound 2

X-ray diffraction of this compound had been reported by Hseu, T.H. from *Angiopteris lygodiifolia* Ros.[15] but the present data were different from previous data. Colorless crystal of Angiopteroside ($C_{12}H_{18}O_8$. H_2O) from *Angiopteris lygodiifolia* Ros. were grown in chloroform-methanol and crystal system was orthorhombic while colorless crystal of Angiopteroside ($C_{12}H_{18}O_8$. H_2O) from *Angiopteris evecta* Hoffm. were grown in ethyl acetate-methanol and crystal system was monoclinic. The ORTEP drawing of Compound 2 and Angiopteroside from *Angiopteris lygodiifolia* Ros. are shown in **Fig. 22.**

From the above data, they indicated that both Angiopterosides had similar conformation structure but they were grown from different solvent. Therefore they had different crystal system. This phenomenon was psudopolymorph.

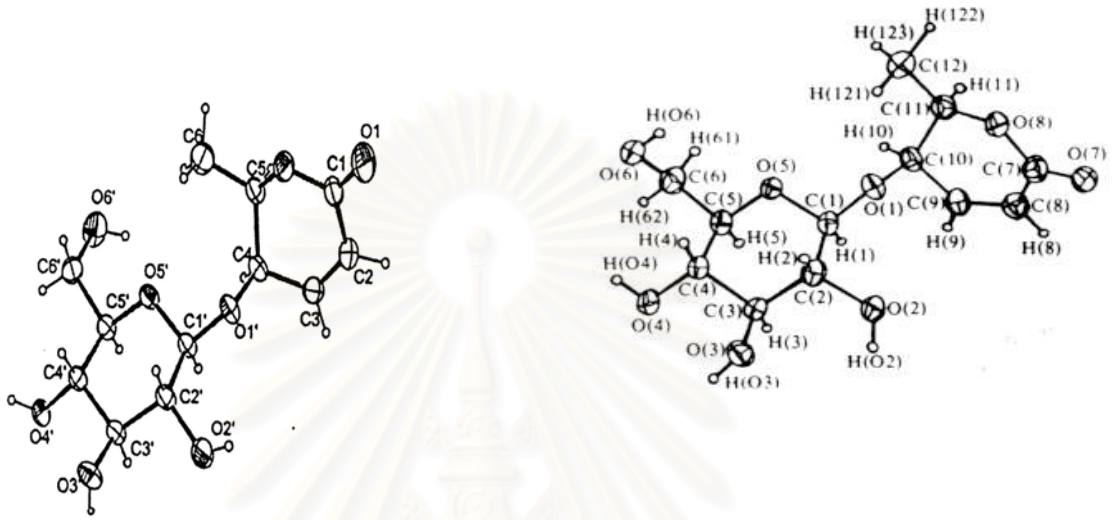

Monoclinic Orthorhombic

Figure 22. The ORTEP drawing of Compound 2 (monoclinic) and Angiopteroside from *Angiopteris lygodiifolia* Ros. (orthorhombic)

X-ray diffraction is presented in **Table 16, 17, 18, 19, 20 and 21** respectively.

From all spectral data (IR, ^{1}H and ^{13}C-NMR spectra including 2D-NMR, mass spectrum and X-ray diffraction analysis), it was concluded that Compound 2 is Angiopteroside(4-*O*-*β*-D-Glucopyranosyl-L-*threo*-2-hexen-5-olide)Monohydrate.

Table 16. Crystal data and structure refinement for 2.

Empirical formula	$C_{12}H_{20}O_9$		
Formula weight	308.28		
Temperature	293(2) K		
Wavelength	0.71073 Å		
Crystal system, space group	monoclinic, $P2_{(1)}$		
Unit cell dimensions	a = 7.83450(10) Å	alpha	= 90 deg.
	b = 6.92330(10) Å	beta	= 91.57 deg.
	c = 12.93220(10) Å	gamma	= 90 deg.
Volume	701.185(15) $Å^3$		
Z, Calculated density	2, 1.460 Mg/m^3		
Absorption coefficient	0.126 mm^{-1}		
F(000)	328		
Theta range for data collection	1.57 to 30.46 deg.		
Index ranges	$-10 \le h \le 9$, $-9 \le k \le 9$, $-17 \le l \le 16$		
Reflections collected / unique	5258 / 3533 [R(int) = 0.0112]		
Completeness to 2theta = 30.46	94.8%		
Refinement method	Full-matrix least-squares on F^2		
Data / restraints / parameters	3533/ 1 / 253		
Goodness-of-fit on F^2	1.067		
Final R indices [I > 2sigma(I)]	R1 = 0.0300, wR2 = 0.0818		
R indices (all data)	R1 = 0.0320, wR2 = 0.0829		
Absolute structure parameter	-0.2(6)		
Largest diff. peak and hole	0.322 and -0.245 e. $Å^{-3}$		

Table 17. Atomic coordinates (x 10^4) and equivalent isotropic displacement parameters ($Å^2$ x 10^3) for 2

	x	*y*	*z*	*U*(eq)*
C(1′)	1592 (2)	7500 (2)	2604 (1)	24 (1)
C(1)	3592 (2)	4663 (2)	-561 (1)	32 (1)
C(2′)	1646 (2)	9700 (2)	2665 (1)	26 (1)
C(2)	4864 (2)	4475 (2)	298 (1)	37 (1)
C(3′)	751 (2)	10404 (2)	3630 (1)	24 (1)
C(3)	4437 (2)	4635 (2)	1277 (1)	35 (1)
C(4′)	-1017 (2)	9495 (2)	3716 (1)	23 (1)
C(4)	2588 (2)	4899 (2)	1549 (1)	26 (1)
C(5′)	-943 (2)	7313 (2)	3550 (1)	24 (1)
C(5)	1478 (2)	3977 (2)	703 (1)	26 (1)
C(6′)	-2722 (2)	6459 (2)	3457 (1)	32 (1)
C(6)	-430 (2)	4277 (2)	753 (1)	35 (1)
O(1′)	2287 (2)	6947 (2)	1657 (1)	27 (1)
O(1)	3965 (2)	4912 (2)	-1456 (1)	50 (1)
O(2′)	3346 (1)	10412 (2)	2733 (1)	45 (1)
O(2)	1940 (1)	4641 (2)	-323 (1)	31 (1)
O(3′)	593 (1)	12465 (1)	3578 (1)	32 (1)
O(4′)	-1626 (1)	9842 (1)	4734 (1)	30 (1)
O(5′)	-124 (1)	6874 (2)	2601 (1)	27 (1)
O(6′)	-2713 (2)	4405 (2)	3424 (1)	49 (1)
O(7W)	-4630 (2)	11681 (2)	4443 (1)	48 (1)

*U(eq) is defined as one third of the trace of the orthogonalized Uij tensor.

Table 18. Bond distances (Å) for 2.

Bond Distances	(Å)
C(1′) - O(1′)	1.4058 (13)
C(1′) - O(5′)	1.4127 (14)
C(1′) - C(2′)	1.5259 (17)
C(1) - O(1)	1.2132 (16)
C(1) - O(2)	1.3384 (14)
C(1) - C(2)	1.4779 (19)
C(2′) - O(2′)	1.4209 (15)
C(2′) - C(3′)	1.5269 (15)
C(2) - C(3)	1.323 (2)
C(3′) - O(3′)	1.4336 (16)
C(3′) - C(4′)	1.5286 (16)
C(3) - C(4)	1.5114 (17)
C(4′) - O(4′)	1.4320 (13)
C(4′) - C(5′)	1.5274 (15)
C(4) - O(1′)	1.4448 (14)
C(4) – C(5)	1.5199 (16)
C(5′) - O(5′)	1.4332 (13)
C(5′) - C(6′)	1.5155 (17)
C(5) - O(2)	1.4585 (14)
C(5) - C(6)	1.5117 (18)
C(6′) - O(6′)	1.4229 (17)

Table 19. Bond angles (deg.) for 2

Angles	(deg.)	Angles	(deg.)
O(1′) - C(1′) - O(5′)	107.78 (9)	C(3′) - C(4′) - C(5′)	111.02 (9)
O(1′) - C(1′) - C(2′)	107.85 (9)	C(3) - C(4) - C(5)	108.33 (11)
O(5′) - C(1′) – C(2′)	109.32 (9)	O(5′) - C(5′) – C(6′)	106.36 (9)
O(2′) - C(2′) – C(1′)	111.96 (11)	O(5′) - C(5′) – C(4′)	110.51 (9)
O(2′) - C(2′) - C(3′)	106.84 (10)	C(6′) - C(5′) - C(4′)	111.03 (10)
C(1′) - C(2′) - C(3′)	110.42 (9)	O(1′) - C(4) – C(5)	112.97 (10)
O(1) - C(1) - O(2)	118.77 (12)	O(1′) - C(4) – C(3)	107.54 (10)
O(1) - C(1) - C(2)	123.63 (12)	C(3) - C(2) - C(1)	121.92 (12)
O(2) - C(1) - C(2)	117.54 (11)	O(6′) - C(6′) – C(5′)	112.77 (11)
O(3′) - C(3′) - C(2′)	108.74 (10)	O(2) - C(5) – C(4)	111.98 (10)
O(3′) - C(3′) - C(4′)	109.60 (10)	O(2) - C(5) – C(6)	105.46 (10)
C(2′) - C(3′) - C(4′)	111.46 (9)	C(6) - C(5) - C(4)	117.23 (10)
C(4) - C(3) - C(2)	120.18 (11)	C(1′) - O(1′) - C(4)	114.79 (9)
O(4′) - C(4′) - C(3′)	108.91 (9)	C(1) - O(2) - C(5)	118.62 (10)
O(4′) - C(4′) - C(5′)	108.08 (9)	C(1′) - O(5′) - C(5′)	112.41 (8)

Table 20. Anisotropic displacement parameters ($Å^2$ x 10^3). The anisotropic displacement factor exponent takes the form:
$-2\ pi^2\ [\ h^2\ a^{*2}\ U11 + \ldots + 2hka^*b^*U12\ ]$

	U11	*U22*	*U33*	*U23*	*U13*	*U12*
C(1′)	29 (1)	23 (1)	21 (1)	-1 (1)	5 (1)	0 (1)
C(1)	32 (1)	34 (1)	32 (1)	-6 (1)	9 (1)	-1 (1)
C(2′)	31 (1)	23 (1)	24 (1)	-4 (1)	9 (1)	-6 (1)
C(2)	26 (1)	38 (1)	46 (1)	-8 (1)	4 (1)	5 (1)
C(3′)	29 (1)	21 (1)	22 (1)	-2 (1)	4 (1)	-2 (1)
C(3)	29 (1)	35 (1)	39 (1)	-9 (1)	-6 (1)	6 (1)
C(4′)	27 (1)	23 (1)	19 (1)	-1 (1)	3 (1)	0 (1)
C(4)	32 (1)	20 (1)	24 (1)	-2 (1)	2 (1)	3 (1)
C(5′)	27 (1)	22 (1)	22 (1)	1 (1)	5 (1)	-2 (1)
C(5)	30 (1)	24 (1)	26 (1)	-2 (1)	6 (1)	-2 (1)
C(6′)	30 (1)	28 (1)	39 (1)	-2 (1)	5 (1)	-5 (1)
O(1′)	37 (1)	21 (1)	24 (1)	-2 (1)	9 (1)	2 (1)
O(1)	46 (1)	70 (1)	35 (1)	-2 (1)	16 (1)	-5 (1)
O(2′)	37 (1)	45 (1)	53 (1)	-20 (1)	13 (1)	-17 (1)
O(2)	29 (1)	41 (1)	24 (1)	0 (1)	4 (1)	-1 (1)
O(3′)	45 (1)	20 (1)	31 (1)	-5 (1)	5 (1)	-3 (1)
O(4′)	32 (1)	36 (1)	22 (1)	-4 (1)	7 (1)	1 (1)
O(5′)	31 (1)	25 (1)	25 (1)	-5 (1)	7 (1)	-4 (1)
O(6′)	38 (1)	28 (1)	81 (1)	1 (1)	8 (1)	-10 (1)
O(7W)	40 (1)	51 (1)	53 (1)	4 (1)	12 (1)	-1 (1)

Table 21. Hydrogen bonds for 2 [Å and deg.]

D-H…A	d(D-H)	d(H…A)	d(D…A)	<(DHA)
O(2′)-H(2′W)…O(1)#1	0.80 (2)	1.97 (2)	2.7340 (15)	158 (2)
O(3′)-H(3′W)…O(4′)#2	0.84 (2)	2.03 (2)	2.8337 (13)	160 (2)
O(4′)-H(4′W)…O(7W)	0.88 (2)	1.82 (2)	2.6930 (16)	173 (2)
O(6′)-H(3′W)…O(3′)#3	0.90 (3)	2.05 (3)	2.9194 (16)	161 (2)
O(7W)-H(7A)…O(6′)#4	0.80 (3)	1.97 (3)	2.7674 (18)	173 (3)
O(7W)-H(7B)…O(2′)#5	0.80 (3)	2.03 (3)	2.8262 (19)	174 (3)

Symmetry transformations used to generate equivalent atoms :
#1 = –x+1, y+1/2, -z, #2 = –x, y+1/2, -z+1, #3 = x, y-1, z, #4 = x, y+1, z, #5 = x-1, y, z

4.2.3 Structure elucidation of Compound 3

Characterization of Compound 3

The IR spectrum of Compound 3 (Fig. 44) revealed a strong broad absorption band at 3550-3100 cm^{-1} which was corresponded to the O-H stretching vibration of hydroxy functional group and at 1223, 1149, 1110 and 1025 cm^{-1} which were C-O stretching vibration of hydroxy group. In addition, the C-H stretching vibration of $-CH_2$ was observed at 2942 cm^{-1}. The IR spectrum of Compound 3 is summarized in **Table 22.**

Table 22. The IR absorption bands assignment of Compound 3.

Wave number (cm^{-1})	Intensity	Vibration
3100-3550	Broad, Strong	O-H stretching vibration of C-OH
2942	Medium	C-H stretching vibration of -CH_2
1452, 1342	Medium	O-H deformation (in plane)
1223, 1149, 1110, 1025	Strong	C-O stretching vibration of C-OH
768, 615	Medium	O-H deformation (out-of plane)

The ^{1}H-NMR spectrum (Fig. 45) of Compound 3 possessed one methine proton (C<u>H</u>-CH_2) at 3.06 ppm. An anomeric proton at δ4.42 (1H,d, *J*=7.8 Hz) could be the signal of β-anomeric proton of glucose while an anomeric proton at δ5.01 (1H,d, *J*=3.5 Hz) could be the signal of α-anomeric proton of glucose. The other signals were multiplet signals at δ3.13-.3.34 and 3.44-3.70 ppm.

The ^{13}C-NMR spectrum (Fig. 46, Table 23) exhibited a total at ten carbon signals at 59.5, 59.7, 68.6, 70.4, 73.1, 74.7, 74.9, 91.0 and 94.6 ppm. The assigned

carbon signals based on the ^{13}C-NMR spectrum were confirmed by the information obtained from the DEPT-90 and DEPT-135 spectra **(Fig. 47)**

DEPT-90 spectrum (Fig. 47) indicated the presence of six saturated methines at 68.6, 70.4, 71.7, 73.1, 74.7 and 74.9 ppm. and two methines of (O-CH-OH) at 91.0 and 94.6 ppm.

DEPT-135 spectrum (Fig. 47) showed two methylene carbons at 59.5 and 59.7 ppm. It did not indicate any methyl and quaternary carbons.

Compound 3 showed spectral data identical to that of D-(+)-glucose which was reported in the literature [39]. The ^{13}C-NMR signal of Compound 3 and D-(+)-glucose are presented in the **Table 23** as follows. The structure is shown in **Fig. 23.** which is α and β form of D-(+)– glucose.

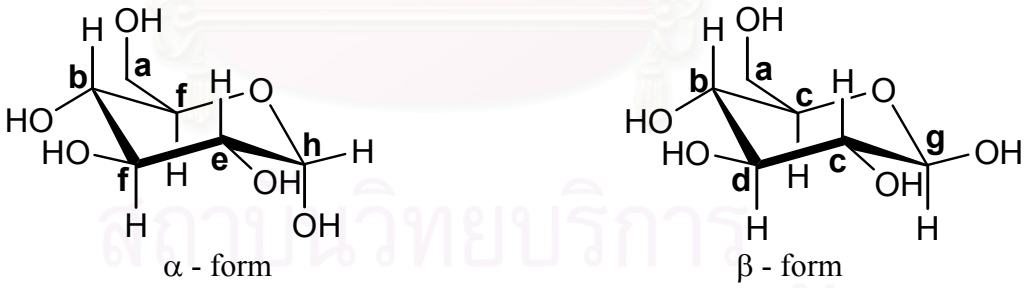

Figure 23 The structure of α and β form of D-(+)– glucose.

Table 23 The ^{13}C-NMR spectra of Compound 3 and D-(+)– glucose*.

Position	δ_C (ppm)	
	Compound 3	D- (+) – glucose
A	59.5, 59.7	61.9
B	68.6	70.7
C	70.4	72.5
D	71.7	73.8
E	73.1	75.2
F	74.7, 74.7	76.8
G	91.0	93.0
H	94.8	96.8

* Compound 3 was measured in D_2O while D-(+)–glucose was measured in dioxane.

Compound 3 showed a molecular ion with m/z = 180 $[M^+]$ ($C_6H_{12}O_6$) **(Fig. 48, 49)**, which indicated a DBE of 1. Other significant fragmentation peak was detected at m/z = 163 $[M^+ - H_2O]^+$

From the literature [40], D-(+)– glucose had m.p. 156-158 ^oC and $[\alpha]_D^{23}$ $+52.7^o$ (c=10, H_2O). In spite of their easy interconversion in solution, α and β forms of carbohydrates are capable of independent existence, and many have been isolated in pure form as crystalline solids. When crystallized from ethanol, D-(+)– glucose yields α-D-glucopyranose, m.p. 146 ^oC and $[\alpha]_D$ $+112.2^o$. Crystallization from a water-ethanol mixture produces β-D-glucopyranose, m.p.148-155^oC and $[\alpha]_D$ $+18.7^o$. In the solid state the two forms do not interconvert and are stable indefinitely. Their structures have been unambiguously confirmed by X-ray crystallography.

Considerably, the information obtained from UV, IR, NMR and MS spectra along with physical properties, such as melting point and optical rotation led to the

deduction that compound 3 is D-(+)- glucose which had both α and β forms of D-(+)– glucose. The ratio between the α and β anomeric forms in compound 3 was calculated from the coupling constant which was determined to be α : β (1:2.3). The structure of compound 3 is shown in **Fig. 24.**

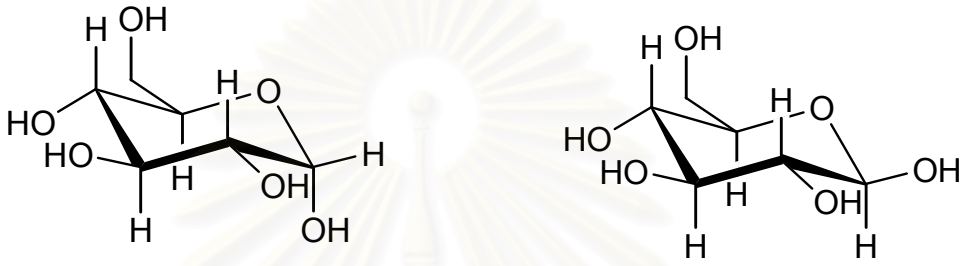

α - form β - form

Figure 24. The structure of Compound 3.

4.2.4 Structure elucidation of Mixture 4

Characterization of Mixture 4

The IR spectrum of Mixture 4 (Fig. 50) showed the presence of a hydroxy group according to the broad absorption band at 3150 to 3690 cm^{-1}. The strong absorption band at 2937 and 2867 cm^{-1} suggested the presence of C-H stretching vibration of methyl and methylene group. The IR spectrum of Mixture 4 is summarized in **Table 24.**

Table 24. The IR absorption band assignment of Mixture 4.

Wave number (cm^{-1})	Intensity	Vibration
3150-3690	Broad	O-H stretching vibration of alcohol
2937, 2867	Strong	C-H stretching vibration of $-CH_3$, $-CH_2$
1654	Weak	C=C stretching vibration of olefin
1465	Medium	O-H bending vibration of alcohol
1382	Medium	C-H bending vibration of$-CH_3$, $-CH_2$
1062	Medium	C-O stretching vibration
958	Weak	C-H out of plane bending vibration of disubstituted vinyl
804	Weak	C-H out of plane bending vibration of disubstituted vinyl

The ^{1}H-NMR spectrum (Fig. 51) showed that the signals of protons at chemical shift 0.66-2.26 ppm. corresponded to those of methyl, methylene and methine groups ($-C\underline{H}_3$, $-C\underline{H}_2$, $-C\underline{H}$ respectively) of the steroids. The proton adjacent to a hydroxyl group ($-C\underline{H}$-OH) was shown as the multiplet signal at 3.43-3.56 ppm. While the multiplet signals at 4.92-5.23 (1H) ppm. and the doublet signal at 5.30 (2H, *J*=5.0 Hz) ppm. were assigned to be the signals of vinylic proton ($-C\underline{H}$=C-) and in a cis-vinylic form.

The ^{13}C-NMR, DEPT-90, DEPT-135 spectra (Fig. 52,53) showed the olefinic carbon signals at 121.7, 129.3, 138.3 and 140.8 ppm. The carbon signal at 71.8 ppm. exhibited the $\underline{C}$-OH of the steroid.

According to the information of a mixture 4, it was suggested that mixture 4 could be a mixture of steroid. To confirm the structure, ^{13}C-NMR spectrum of mixture 4 was compared to stigmasterol and β-sitosterol as shown in **Table 25.**[41]

Table 25. The ^{13}C-NMR spectra of mixture 4, stigmasterol and β-sitosterol.

Position	δ_C (ppm)		
	Compound 1	Stigmasterol	β-sitosterol
1	37.2	37.4	37.1
2	31.7	31.7	31.8
3	71.8	71.8	71.9
4	42.3	42.4	42.4
5	140.8	140.0	140.9
6	121.7	121.7	121.8
7	31.9	31.9	32.0
8	31.9	31.9	32.0
9	50.2	50.3	50.3
10	36.5	36.6	36.6
11	21.1	21.1	21.1
12	39.8	39.8	39.9
13	42.3	42.4	42.4
14	56.8	57.0	56.8
15	24.3	24.4	24.3
16	28.9, 28.2	28.9	28.2
17	56.0	56.0	56.2
18	12.2, 11.9	12.2	11.9
19	19.4	19.4	19.4
20	40.5, 36.1	40.5	36.2
21	21.1, 19.1	21.1	19.1
22	138.3, 33.9	138.4	34.0
23	129.3, 29.2	129.4	29.3
24	51.2, 50.1	51.3	50.3
25	31.9, 26.1	31.9	26.2
26	19.0, 18.8	19.0	18.8
27	21.1, 19.8	21.1	19.8
28	25.4, 23.1	25.4	23.1
29	12.0, 11.9	12.0	11.9

The MS spectrum showed the fragmentation as follows, *m/z* (EIMS) **(Fig. 54)**: 414[M^+], 412[M^+], 396(12), 381(7), 329(12), 300(17), 271(36), 255(60), 213(45), 159(59), 145(71), 105(63), 95(69), 81(69), 55(100).

The mass spectrum **(Fig. 54)** showed a molecular ion peak corresponding to stigmasterol assigned to be $C_{29}H_{50}O$ and EIMS [M^+] (*m/z* = 414) **(Fig. 54)** which indicated 5 DBE and β-sitosterol assigned to be $C_{29}H_{48}O$ and EIMS [M^+] (*m/z* = 412) **(Fig. 54)** which indicated 6 DBE. The ion fragmentation pattern in the mass spectrum of this mixture indicated that it was a mixture of steroids which is shown in **Scheme 6.**

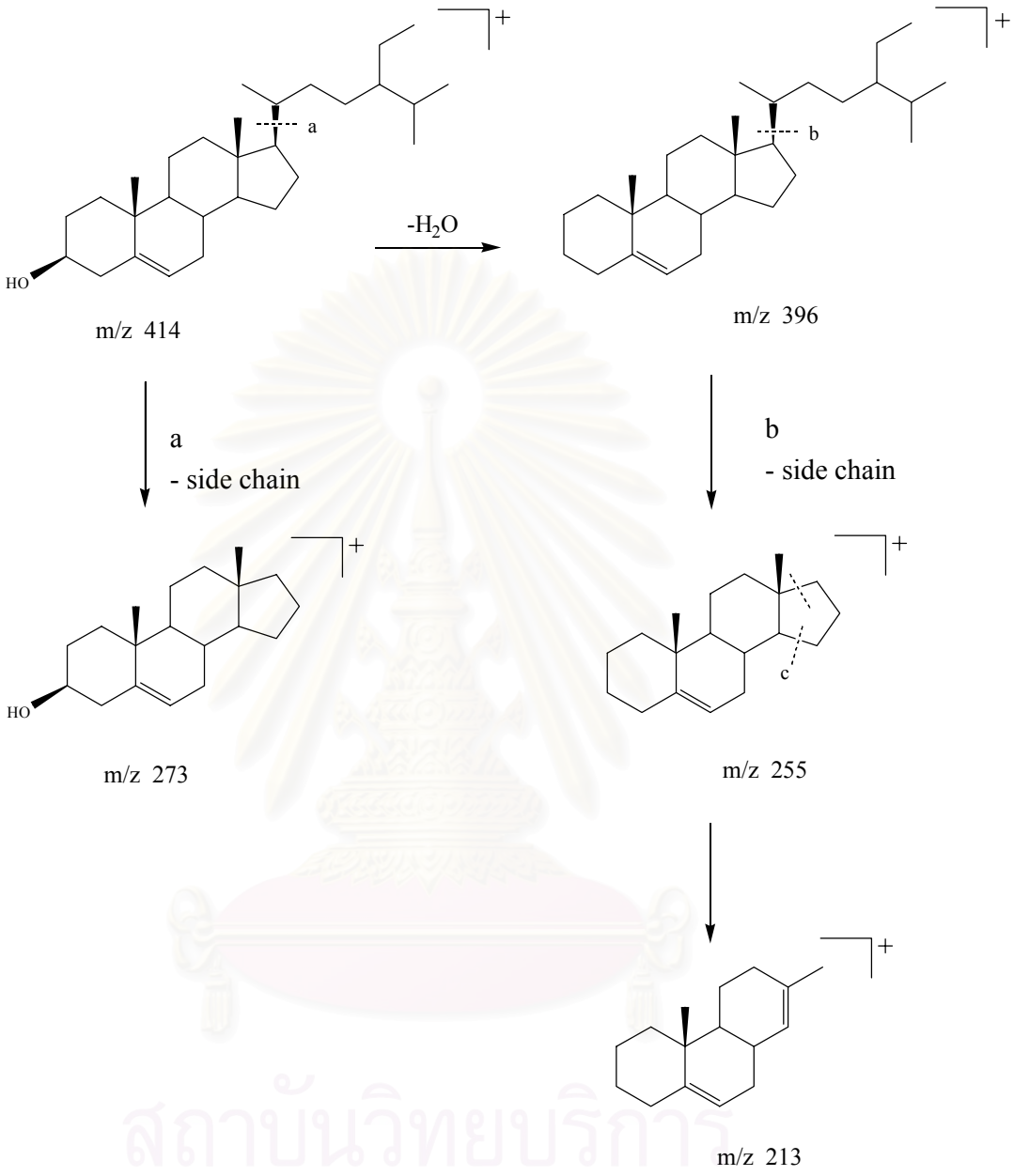

Scheme 6. The possible mass fragmentation pattern of mixture 4 for β-sitosterol

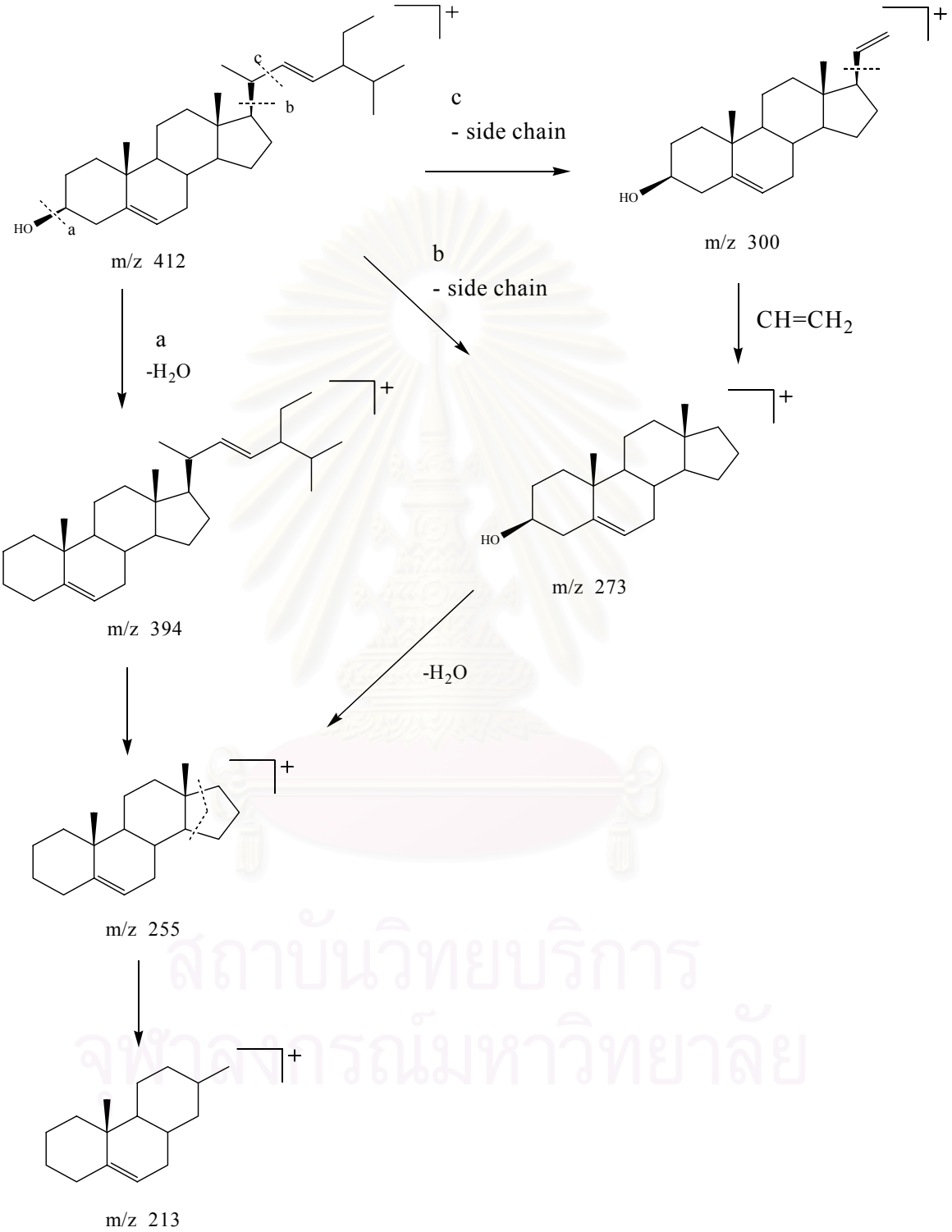

Scheme 6. (cont.) The possible mass fragmentation pattern of mixture 4 for Stigmasterol.

From all of the data, it could be concluded that mixture 4 was a mixture of β-sitosterol and stigmasterol. The structure of this mixture was presented in **Fig. 25.**

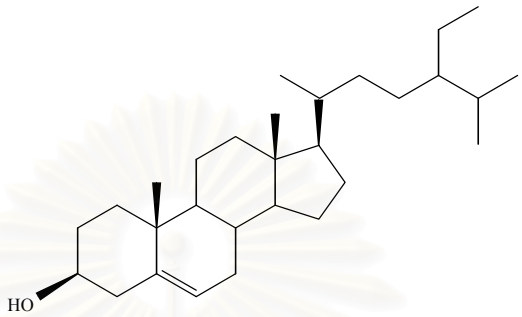

β-sitosterol

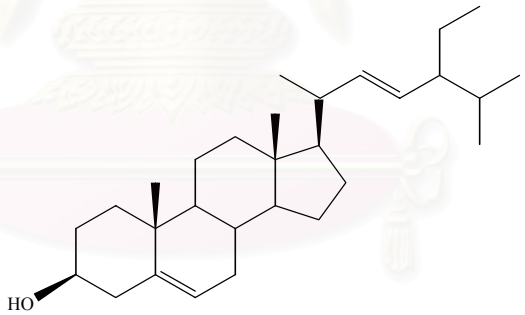

Stigmasterol

Figure 25. The structure of stigmasterol and β-sitosterol

4.3 Result of biological activity test of the isolated compound.

4.3.1 Cytotoxic activity test.

The *in vitro* activity of compound 2 (10 μg/ml) from *Angiopteris evecta* Hoffm. was tested against 6 cell lines, which composed of BT 474 (breast), Chago (lung), Hep-G2 (hepatoma), HS 27 (fibroblast), Kato-3 (gastric) and SW 620 (colon) cancer and the results are shown in **Table 26.**

Table 26. Cytotoxic activity against tumor cell lines of compound 2 from *Angiopteris evecta* Hoffm.

Compound[1] (10 μg/ml)	% survival					
	HS 27 (fibroblast)	Kato-3 (gastric)	BT 474 (breast)	Chago (lung)	SW 620(colon)	Hep-G2 (hepatoma)
2	78	112	113	55	91	105
Doxorubicin [2]	35	54	28	63	20	17

[1] dissolved in ethanol

[2] Doxorubicin: Doxorubocin hydrochloride was used as positive control.

From **Table 26**, there were compared with Doxorubicin, it indicated that compound 2 showed weak cytotoxicity against Chago cell lines This compound contained glycoside and unsaturated lactone.

4.3.2 The reverse transcriptase test.

The *in vitro* inhibition of HIV-1 RT of compound 2 (300 μg/ml) from *Angiopteris evecta* Hoffm. is reported in **Table 27.**

Table 27. The *in vitro* inhibition of HIV-1 RT of compound 2 from *Angiopteris evecta* Hoffm..

Compound (μg/ml)	% inhibition
2	84
ddI [1]	92

[1] ddI : 2′,3′-dideoxyinosine was used as positive control.

From **Table 27**, it indicated that compound 2 showed strong activity *in vitro* as inhibitor for HIV-1 RT for the first time. This compound contained glycoside and unsaturated lactone. Percentage inhibition of each concentration of compound 2 and ddI are showed in **Table 28.**

The IC_{50} values of compound 2 and ddI were determined by graphic plotting between concentration of sample (x-axis) and % inhibition (y-axis). To determine IC_{50} values, a perpendicular line was drawn from the y-axis at the % inhibition value of 50 to the x-axis as shown in **Figure 26 and 27.**

Table 28. Percentage inhibition of each concentration of compound 2 and ddI.

Samples	Concentration (nM)	% inhibition
Compound 2	340	5.3
	680	42.2
	1020	72.4
	1700	85.5
ddI	340	8.1
	680	38.2
	1020	78.7
	1700	92.4

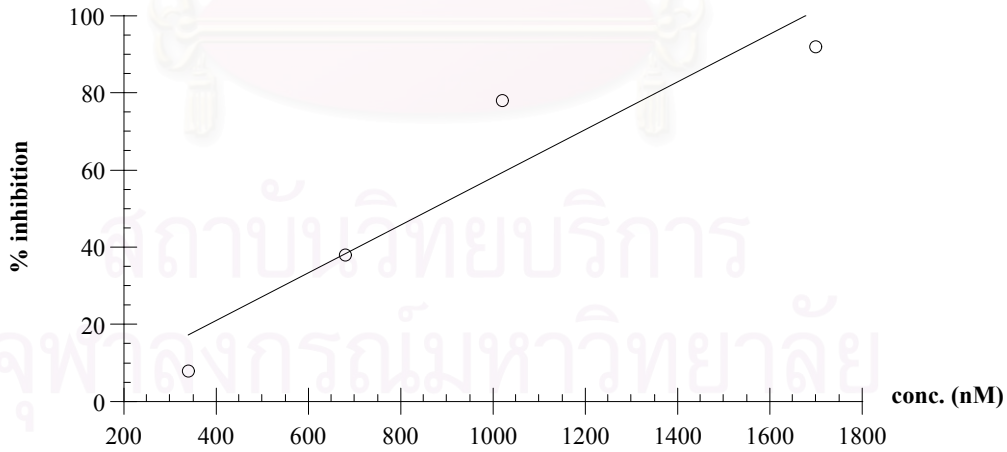

Figure 26 IC_{50} values of compound 2

Equation: y = 0.057x-1.937 (R = 0.928)

y = %inhibition when, y = 50

x = conc. (nM) **x = 914 nM**

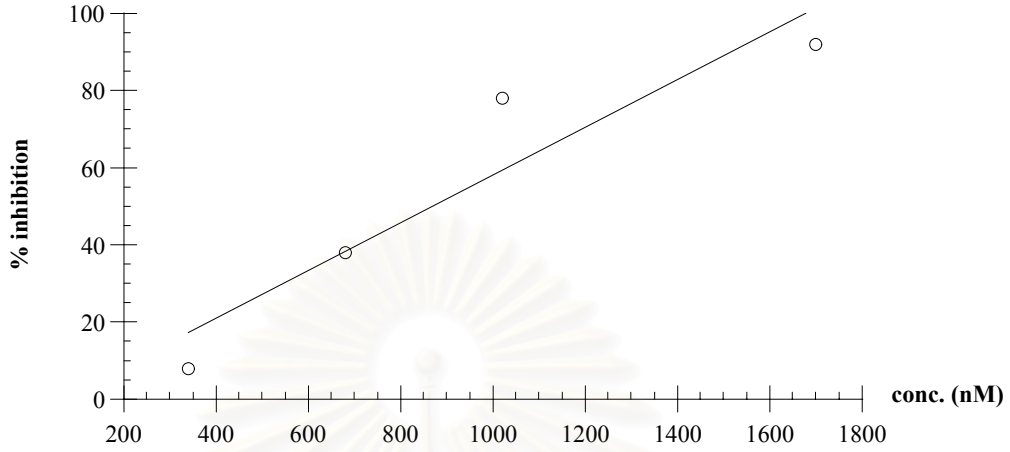

Figure 27. IC_{50} values of ddI

Equation: y = 0.062x-3.714 (R = 0.937)

y = %inhibition when, y = 50

x = conc. (nM) **x = 866 nM**

From Figure 26 and 27. The IC_{50} values of ddI and compound 2 were summarized in **Table 29.**

Table 29 IC_{50} values of ddI and compound 2.

Samples	IC_{50} (nM)
ddI	914
Compound 2	866

IC_{50} is the concentration of compound required to give 50%inhibition of HIV-1 reverse tanscriptase activity.

Table 29 indicated that compound 2 exhibited high inhibitory activity against HIV-1 reverse transcriptase with IC_{50} of 914 nM compare with 866 nM of ddI.

4.4 The proposed mechanism of the inhibition of HIV-1 reverse transcriptase of compound 2.

From the above result, it was found that compound 2 could inhibit HIV-1 reverse transcriptase. In the structural point of view, compound 2 looks similar to 3′-azido-3′-deoxythymidine (AZT) and 2′,3′-dideoxyinosine (ddI), which were nucleoside reverse transcriptase inhibitors. They compose of a heterocyclic ring, with double bond conjugated to a carbonyl group connect to a sugar moiety. The structure of compound 2, AZT and ddI are shown in **Fig. 28.** This led to the proposed mechanism corresponding to the mechanism of nucleoside reverse transcriptase inhibitors that belong to the class of the 2′,3′-dideoxynucleoside (ddN) analogues. The dideoxynucleosides exert anti-HIV activity at the reverse transcriptase level. As triphosphates, they compete with cellular dideoxynucleoside-5′-triphosphates, and they act as chain terminators in the synthesis of proviral DNA, thereby interfering with elongation of the viral DNA chain and prevent correct folding of DNA chain. The proposed mechanism of DNA chain termination of compound 2 is shown in **Fig. 29.**

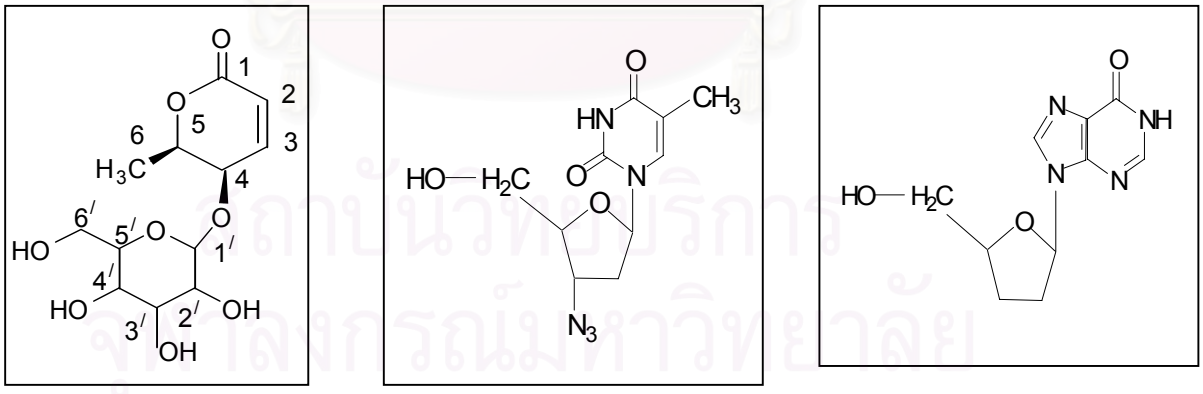

Figure 28. The structure of compound 2, AZT and ddI.

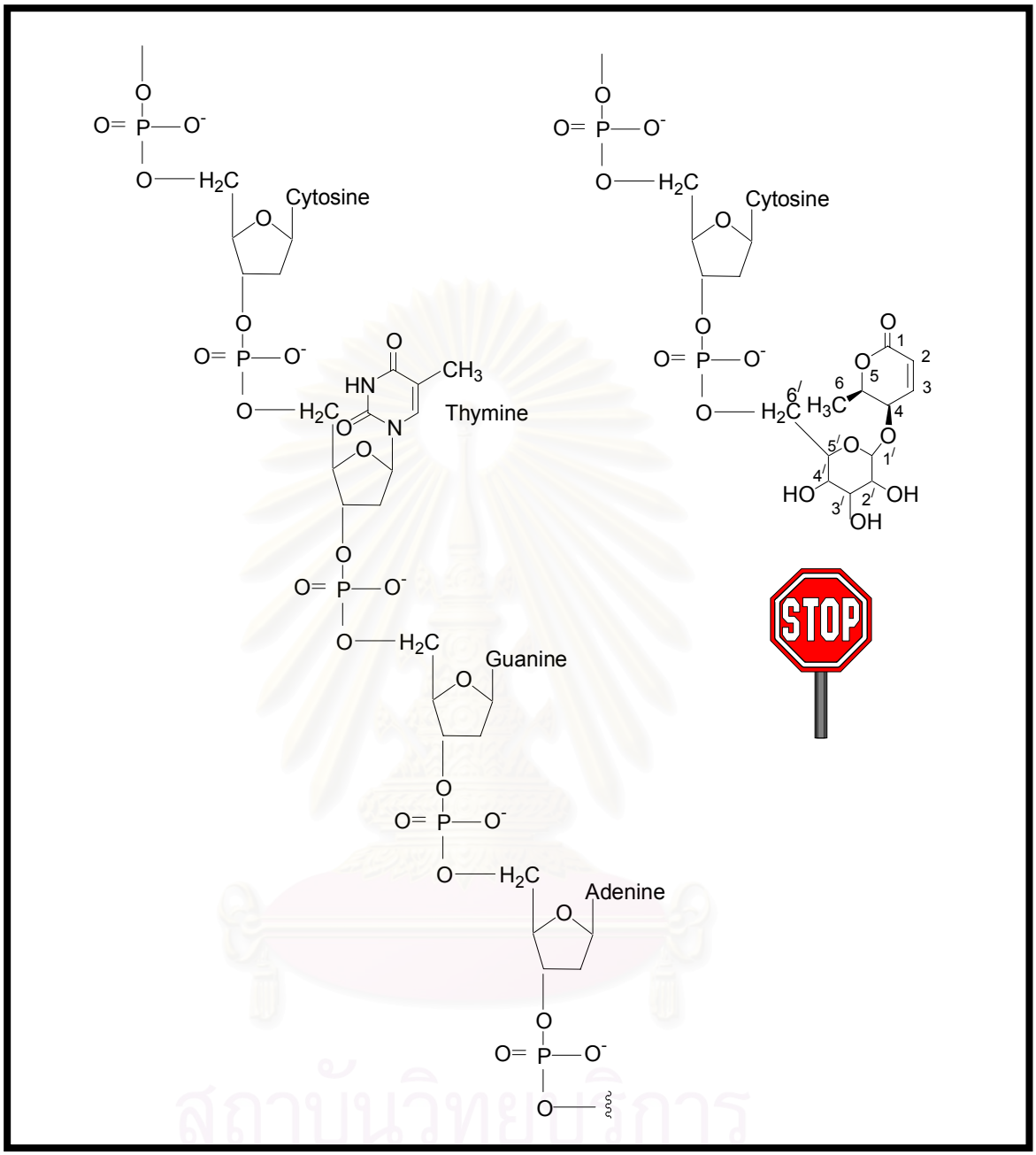

Figure 29. The proposed mechanism of DNA chain termination of compound 2

CHAPTER IV

Conclusion

In this research, the fresh rhizomes (2.70 kg) of *Angiopteris evecta* Hoffm. were extracted with methanol. The crude methanol extract was extrated with hexane and ethyl acetate, respectively, to obtaine three different crude extracts; crude hexane extract (2.01 g, 0.0744 % wt.by wt. of the fresh rhizome), crude ethyl acetate extract (11.74 g, 0.4348 % wt.by wt. of the fresh rhizome) and crude methanol extract (112.83 g, 4.1789 % wt.by wt. of the fresh rhizome). Four substances were isolated from the rhizome using traditional chromatoghaphic techniques. The structures were determined from physical, chemical properties, various spectroscopic methods and also by comparison with the spectral data which previously reported. Their structures were established as: Succinic acid (1), Angiopteroside (2), D-(+)–glucose (3), Mixture of stigmasterol and β-sitosterol (4). The crystal structures of Succinic acid (1) and Angiopteroside (2) were determined by using X-ray diffraction analysis and their ORTEP drawing were shown in Figure 14 and 21, respectively. All isolated compounds from the rhizomes of *Angiopteris evecta* Hoffm. could be summarized as shown in **Table 30.**

Table 30 Isolated compounds from the rhizomes of *A. evecta* Hoffm.

Compound	Name of compound	Weight (g)	%wt.by wt.of the starting material
1	Succinic acid	18	$6.67*10^{-3}$
2	Angiopteroside	132	$4.89*10^{-3}$
3	D-(+)–glucose	355	$13.2*10^{-3}$
4	Stigmasterol and β-sitosterol	120	$1.11*10^{-3}$

In the aspect of biological activities, Compound 2 was tested for cytotoxicity against 6 tumor cell lines and inhibition of HIV-1 reverse transcriptase. Compound 2 showed weak cytotoxic activity against Chago cell lines. Moreover, Compound 2 was found to inhibit HIV-1 reverse transcriptase and exhibited IC_{50} value of 914 nM.

5.1 Proposal for the future work

The discovery of chemical constituents belonging to *A. evecta* Hoffm. firstly reported in this research would be interesting for future investigation. It could be clearly seen that various biologically active compounds could be isolated from the active fraction of the rhizomes of *A. evecta* Hoffm.

The study of the relationship between the structure of isolated compounds including their derivatives and inhibitory activity against HIV-1 reverse transcriptase or Structure-Activity Relationship (SAR) should be covered. Moreover, the chemical constituents and biological activity study of other parts of *A. evecta* Hoffm. should also be investigated. The results from that study would reveal the similarity or difference and might lead to understanding of biosynthesis pathway of some major components.

REFERENCES

1. National Identity Board. *Medicinal Plants of Thailand Past and Present.* Bangkok: Amarin Printing Group, **1991.**
2. Wallace, J. W.; Story, D. T. **Flavonoids and their phylogenetic implication in representative species of the Marattiales.** *J. Nat. Prod.* **1978**; 41, 651.
3. นันทวัน บุณยะประภัศร และ อรนุช โชคชัยเจริญพร. สมุนไพรพื้นบ้าน(เล่ม4). พิมพ์ครั้งที่ 1: กรุงเทพมหานคร: **2543**, 313-314.
4. จินดาพร ภูริพัฒนาวงศ์. เภสัชเวทกับตำรายาแผนโบราณ. กรุงเทพมหานคร: สมาคมแพทย์แผนไทย กรมการแพทย์ กระทรวงสาธารณสุข. โรงพิมพ์องค์การการสงเคราะห์ทหารผ่านศึก, **2539,** 346-347.
5. เชาวน์ กสิพันธุ์. ตำราเภสัชศึกษา. กรุงเทพมหานคร: สมาคมแพทย์เภสัชกรรมไทยโบราณ, **2522**, 327.
6. เทพนม เมืองแมน, ภรณี หวังธำรงวงค์, อรยา สุตเธียรกุล, วรัญญา แสงเพชรส่อง และ ร่มไทร กล้าสุนทร. คู่มือสมุนไพรรักษาโรคตามกลุ่มอาการ. กรุงเทพมหานคร: คณะสาธารณสุขศาสตร์ มหาวิทยาลัยมหิดล, **2533**, 178-179.
7. สายสนม กิตติขจร. ตำราสรรพคุณสมุนไพรยาไทยแผนโบราณ. กรุงเทพมหานคร: โรงพิมพ์อักษรไทย, **2526**, 227-228.
8. Pongboonrod, S. *Mai Thad Thailand.* Bangkok: Kasem Press, **1976**, 486.
9. Saralamp, P.; Chuakul, W.; Temsiririrkkul, R.; Clayton, T.; *Medicinal plant in Thailand.* Bangkok: Amarin Printing and Publishing Public, **1996**, 1.
10. Smitinand, T.; Larsen K. *Flora of Thailand.* Bangkok, The TISTR Press, **1989**, 3, 640-641.
11. Benwell, A.; Horton, S. *National Parks and Wildlife Service.* New South Wales, **1998**, 1-5.
12. Saralamp, P.; Temsirirkkul, R.; Chuakul, W.; Riewpaiboon, A.; Prathanturarug, S.; Suthisisang, C.; Pongcharoensuk, P. *Medicinal Plants in Siri Ruckhachati Garden.* Bangkok: Siambooks and Publications, **1996**, 50-51.
13. Wallace, J. W.; Story, D. T.; Besson, E.; Chopin, J. **Violanthin and isoviolanthin from the Marattiaceous fern *Angiopteris evecta.*** *Phytochemistry*. **1979**; 18, 1077.

14. Wallace, J. W.; Yopp, D. L.; Besson, E.; Chopin, J. **Apigenin di-C-glycosylflavones of *Angiopteris* (Marattiales).** *Phytochemistry*. **1981**; 20, 2701-2703.
15. Hseu, T.H. **Structure of Angiopteroside (4-*O*-*β*-D-Glucopyranosyl-L-*threo*-2-hexen-5-olide) Monohydrate, a fern glycoside from *Angiopteris lygodiifolia* Ros.** *Acta Cryst.* **1981**; B37, 2095-2098.
16. Morrison, J.M. *Virus induced enzyme*. London: John Wiley & Sons, **1991.**
17. Bunnell, B.A.; Morgan, R.A. *Drug of Today.* **1996**; 32, 209-224.
18. O'Brien, W.A.; Pomerantz, R.J. **HIV infection and associated diseases.** *Viral pathogenesis.* Philadephia: Lippincott-Raven Publishers, **1997**.
19. Broder, S.; Merigan, T.C.; Bologonesi, D. *Textbook of AIDS medicine*. New York: Williams & Wilkins, **1994**.
20. Ritter, J.M.; *Textbook of clinical pharmacology.* U.K.: The Bath, **1995**.
21. Ho, D.D.; Pomerantz, R.J.; Kaplan, J.C. **Pathogenesis of infection with human immunodeficiency virus.** *N Eng J Med.* **1987**; 317, 278-279.
22. Tan, C.K.; Zhang, J.; Li, Z.Y.; Tarpley, W.G.; Downey, K.M.; So, A.G. **Functional characterization of RNA-dependent DNA polymerase and Rnase H activities of a recombinant HIV reverse transcriptase.** *Biochemistry.* **1991**; 30, 2651-2655.
23. Esnouf, R.M.; Ren, J.; Hopkins, A.L.; Ross, C.K.; Jones, E.Y.; Stammers, D.K.; Stuart, D.I. **Unique features in the structure of the complex between HIV-1 reverse transcriptase and the bis(heteroaryl)piperazine(BHAP) U-90152 explain resistance mutations for this non-nucleoside inhibitor.** *Proc. Natl. Acad. Sci. USA.* **1997**; 94, 3984-3989.
24. Clercq, E.D. **Toward improved anti-HIV chemotherapy: Therapeutic strategies for intervention with HIV infections.** *J. Med. Chem.* **1995**; 38(14), 2491-2517.
25. Spence R.A.; Kati, W.M.; Anderson, K.S.; Johnson, K.A. **Mechanism of inhibition of HIV-1 reverse transcriptase by nonnucleoside inhibitors.** *Science* **1995**; 267, 988-993.
26. Mitsuya, H.; Yarchoan, R. **Development of antiretroviral therapy for AIDS and related disorders.** In: Broder, S.; Merigan, T.C.; Bologonesi, D. editors. *Textbook of AIDS medicine.* Baltimore: Williams & Wilkins. **1994**; 721-742.

27. Romero, D.L.; Busco, M.; Tan, C.K.; Reusser, F.; Palmer, J.R.; Poppe, S.M.; et.al. **Nonnucleside reverse transcriptase inhibitors that potently and specifically block human immunodeficiency virus type 1 replication.** *Proc. Natl. Acad. Sci. USA*. **1991**; 88, 8806-8810.
28. Kohlstaedt, L.A.; Wang, J.; Friedman, J.M.; Rice, P.A.; Steitz, T.A. **Crystal structure of 3.5 Å resolution of HIV-1 reverse transcriptase complexed with an inhibitor.** *Science.* **1992**; 256, 1783-1789.
29. Breslin, H.J.; Kukla, M.J.; Ludovici, D.W.; **Synthesis and anti-HIV-1 activity of 4,5,6,7-tetrahydro-5-methylimidazo[4,5,1-*jk*][1,4]benzo-diazepin-2(1*H*)-one(TIBO) derivatives. 3.** *J. Med. Chem.* **1995**; 38, 771-793.
30. Furman, P.A.; Moxham, C. **MKC-442: Non-nucleoside reverse trans-criptase inhibitor.** *Drugs Fut.* **1998**; 23(7), 718-724.
31. Terrett, N.K.; Bojanic, D.; Merson, J.R.; Stephenson, P.T. **Imidazo[2′,3′:6,5]dipyrido[3,2-b:2′,3′-e]-1,4-diazepines:Non-nucleoside HIV-1 reverse transcriptase inhibitors with greater enzyme affinity than nevirapine.** *Bioorg Med. Chem. Lett.* **1992**; 2, 1745-1750.
32. Twentyman, P.R.; Luscombe, M. **A study of some variables in a tetra-zonium dye (MTT) based assay for cell growth and chemo-sensitivity.** *Br. J. Cancer*. **1987**; 56, 279.
33. Alley, M.C.; Scudiero, D.A.; Monks, A.; Hursey, M.L.; Czerwinski, M.J.; Fine, D.L.; Abott, B.J.; Mayo, J.G.; Shoemaker, R.H.; Boyd, M.R. **Feasibility of Drug Screening with Panels of Human Tumor Cell Lines Using a Microculture Tetrazonium Assay.** *Cancer Res.* **1998**; 48, 589.
34. Boehringer Mannheirn Gmbh, *Reverse Transcriptase Assay*, Mannheirn, Germany, **2000.**
35. Eberie, J.; Seibl, R. *J. Virol. Methods*. **1992**; 40, 347.
36. Rice, W.G.; Schaeffer, C.A.; Graham, L.; Bu, M.; Mcdougal, J.S.; Orloff, S. L.; Villinger, F.; Young M.; Oroszlan, S.; Fesen, M.R.; Pommier, Y.; Mendeleyev, J.; Kun, E. *Proc. Nat. Acad. Sci*. **1993**; 90, 9721.
37. Hollenbeak, K.H.; Kuehne, M.E. **The isolation and structure determi-nation of the fern glycoside osmundalin and the synthesis of its aglycone osmundalactone.** *Tetrahedron*. **1974;** 30, 2307-2316.

38. Numata, A.; Takahashi, C.; Fujiki, R.; Kitono, E.; Kitajima, A.; Takemura, T. **Plant Constituents Biologically Active to Insects.VI. Antifeedants for Larvae of the Yellow Butterfly, *Eurema hecabe mandarina*, in Osmunda japonica.(2).** *Chem. Pharm. Bull.* **1990**; 38(10), 2862-2865.
39. Breitmaier, E.; Voelter, W. *Carbon-13 NMR Spectroscopy.* New York: VCH Publishers, **1987**, 822C.
40. Budavari, S.; O'Neil, M.J.; Smith, A.; Heckelman, P.E.; Kinneary, J.F. *The Merck Index.* New Jersey: Merck, **1996,** 576.
41. Kornkanok, S. **Phytochemical Studies of *Bidens biternata* Merr & Sherff.** M.Sc's Thesis, Department of Phamaconosy, Graduate school, Chulalongkhon University. **1994.**

APPENDIX

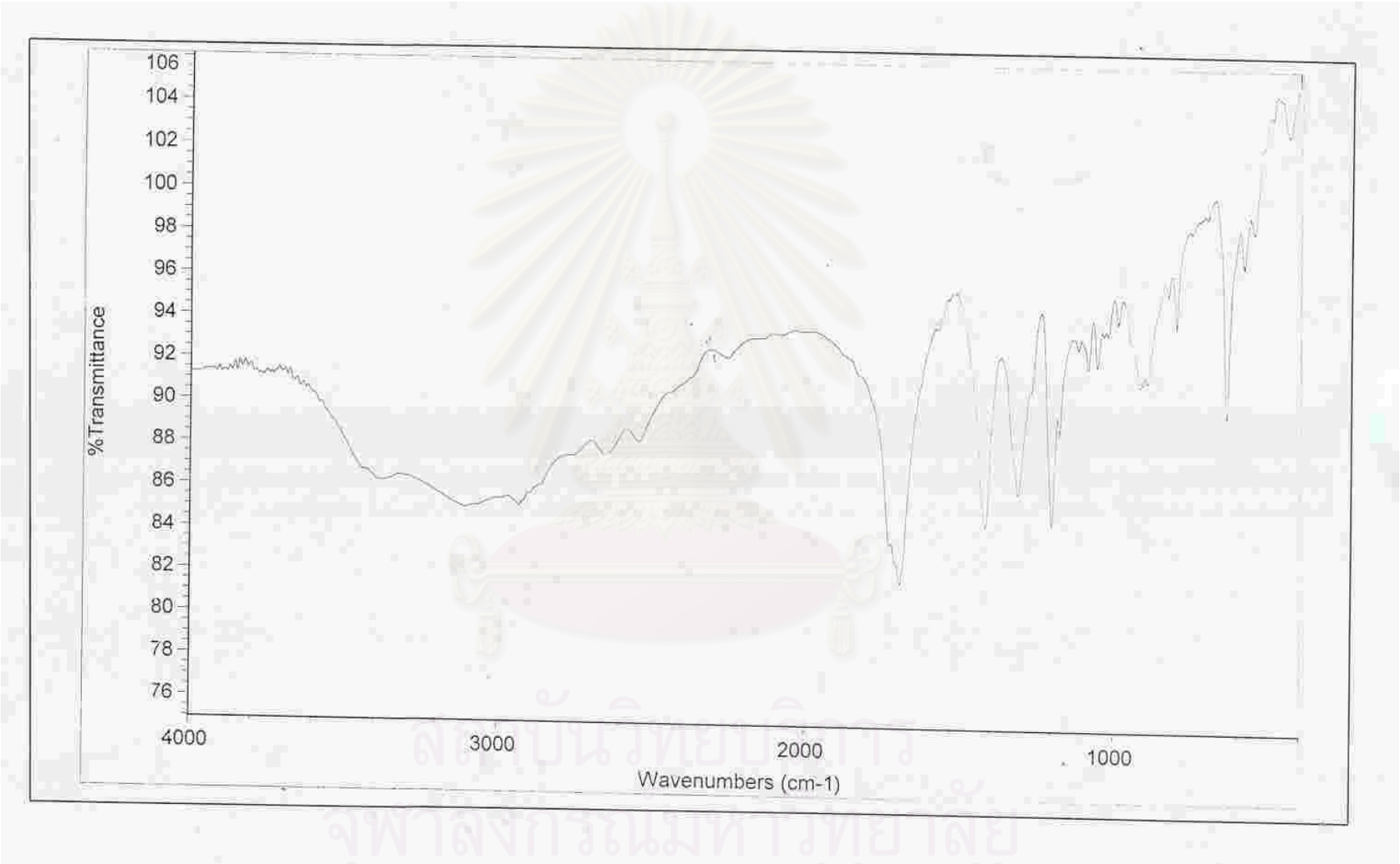

Figure 30. The IR spectrum of Compound 1. (Succinic acid

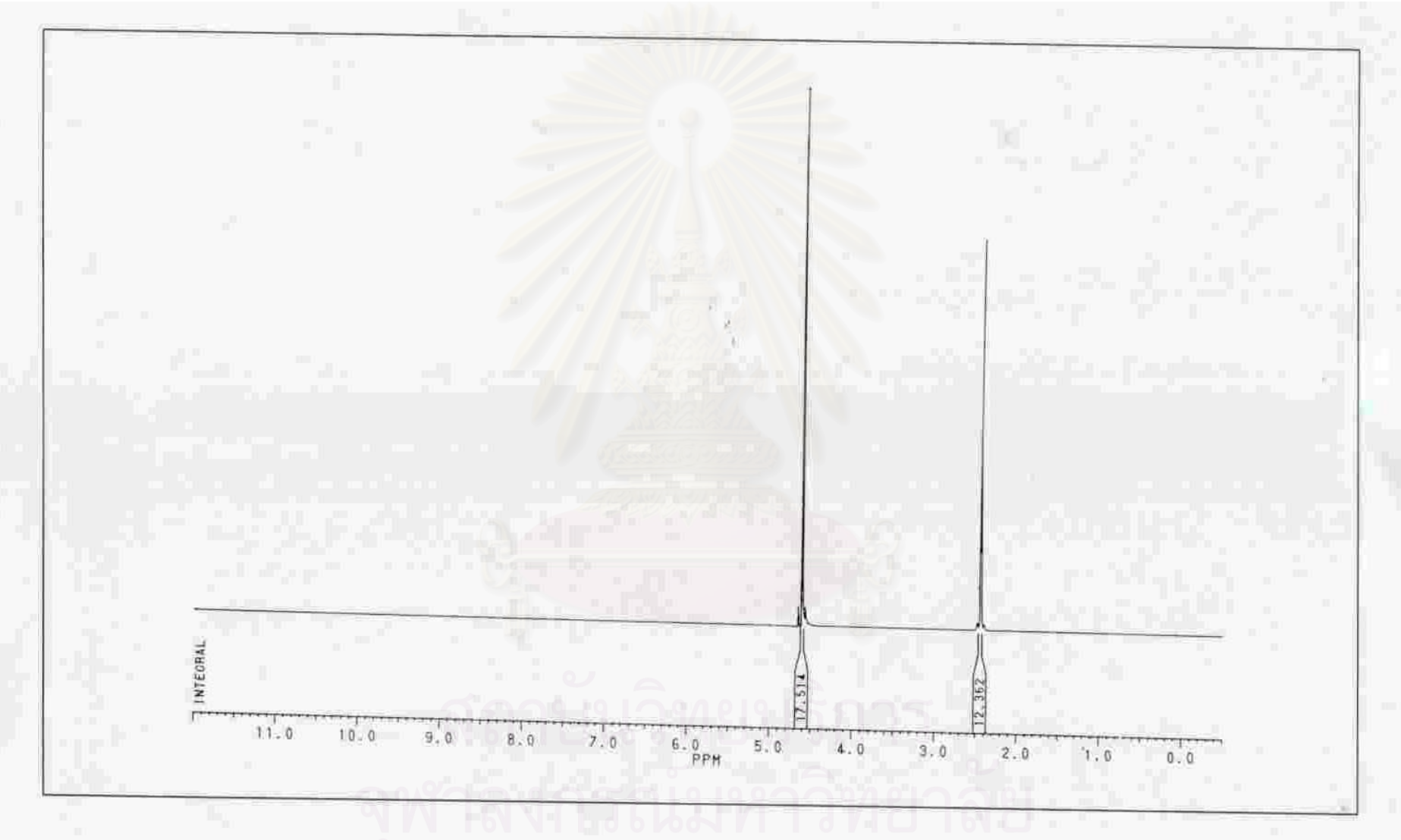

Figure 31. The 1H-NMR spectrum of Compound 1. (Sucinic acid)

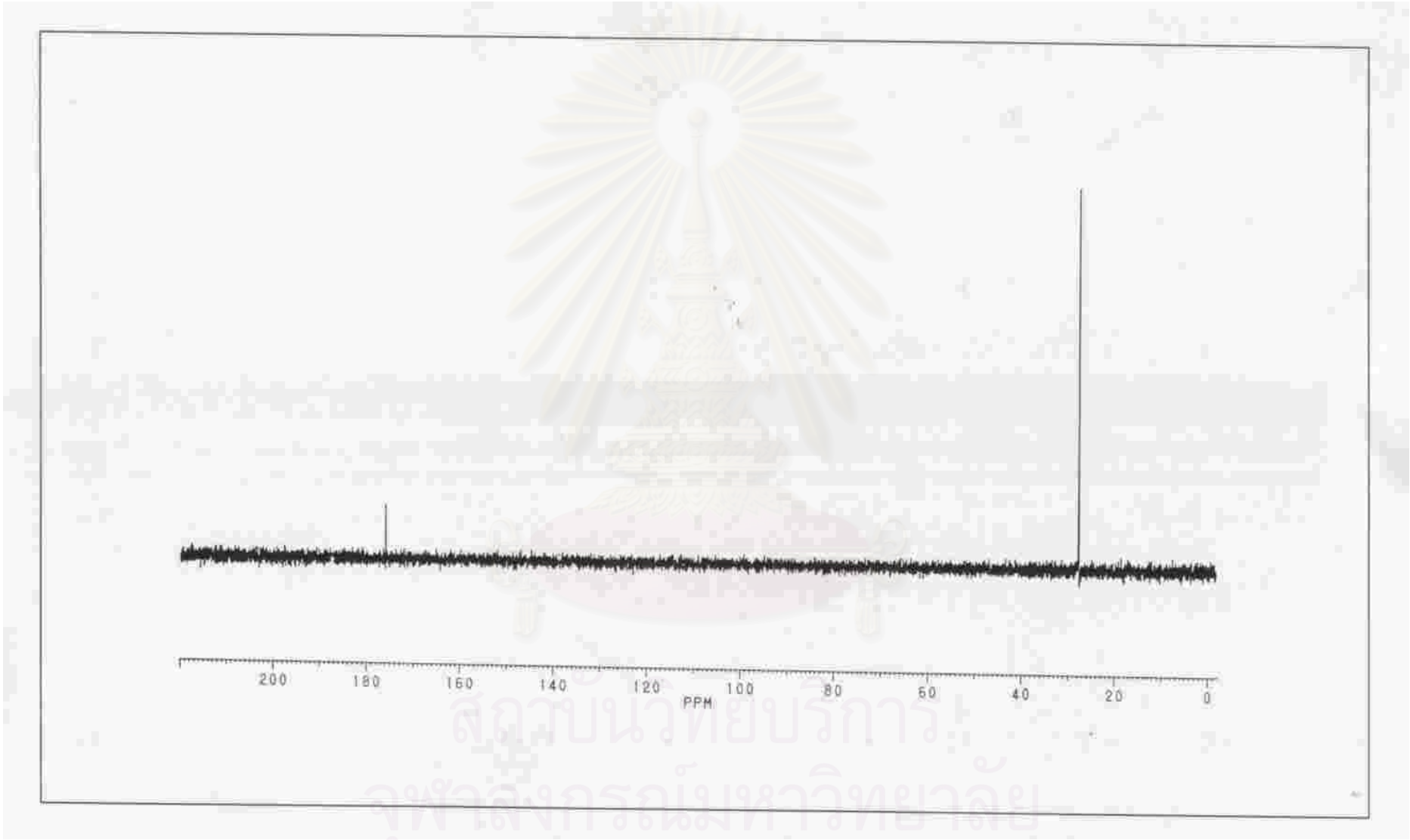

Figure 32. The 13C-NMR spectrum of Compound 1 (Succinic acid)

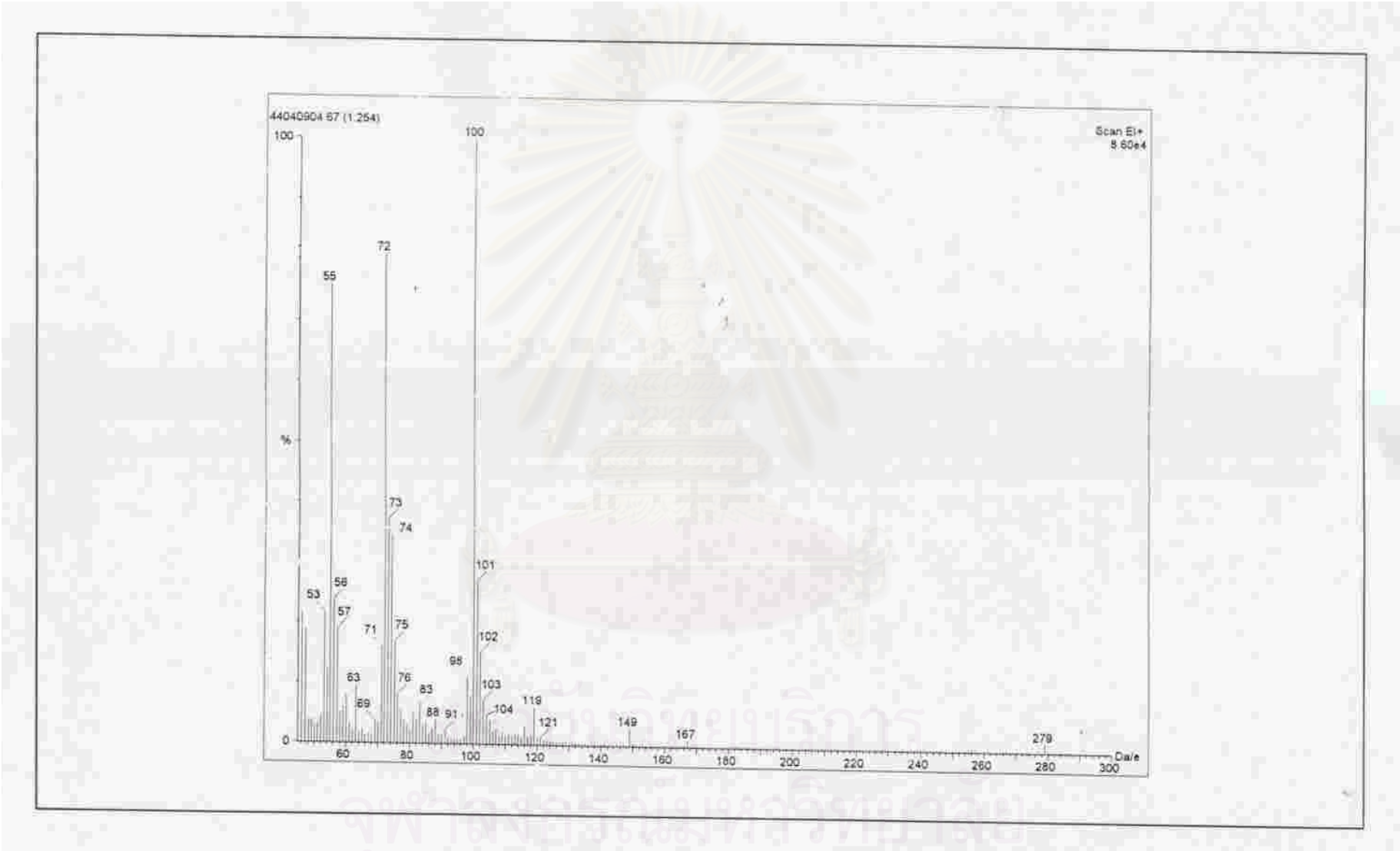

Figure 33. The EI MS spectrum of Compound 1 (Succinic acid)

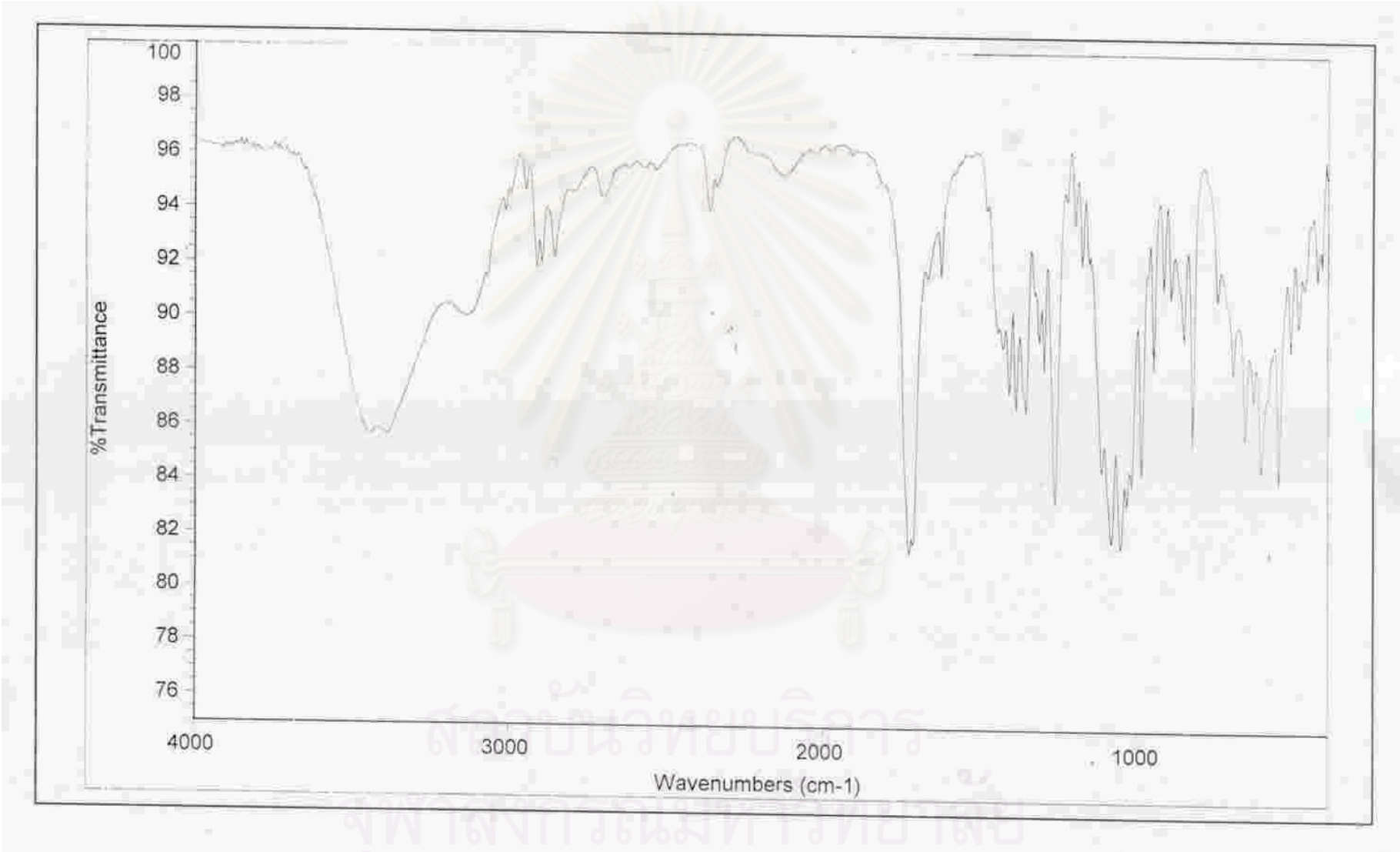

Figure 34. The IR spectrum of Compound 2 (Angiopteroside)

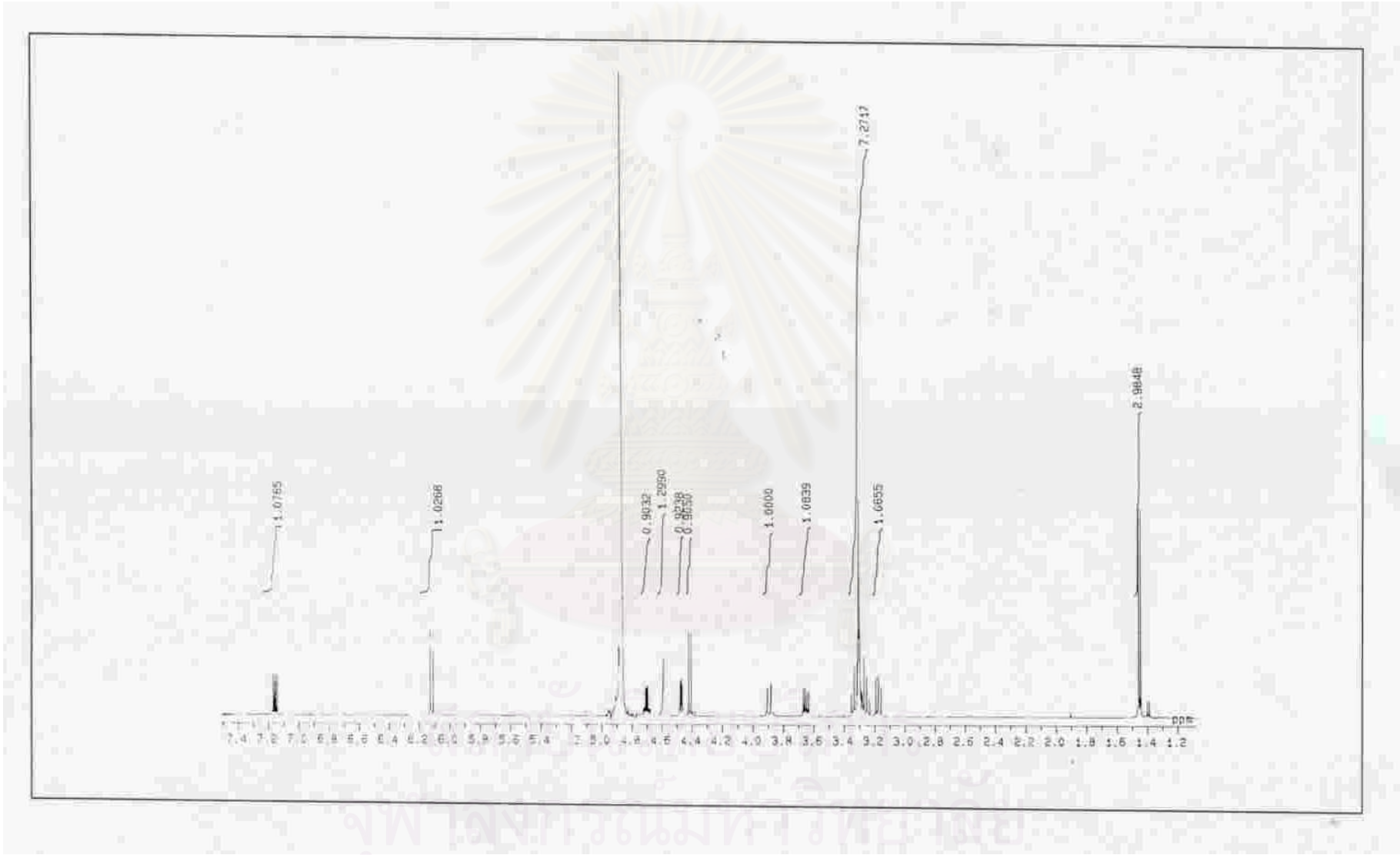

Figure 35. The 1H-NMR spectrum of Compound 2 (Angiopteroside)

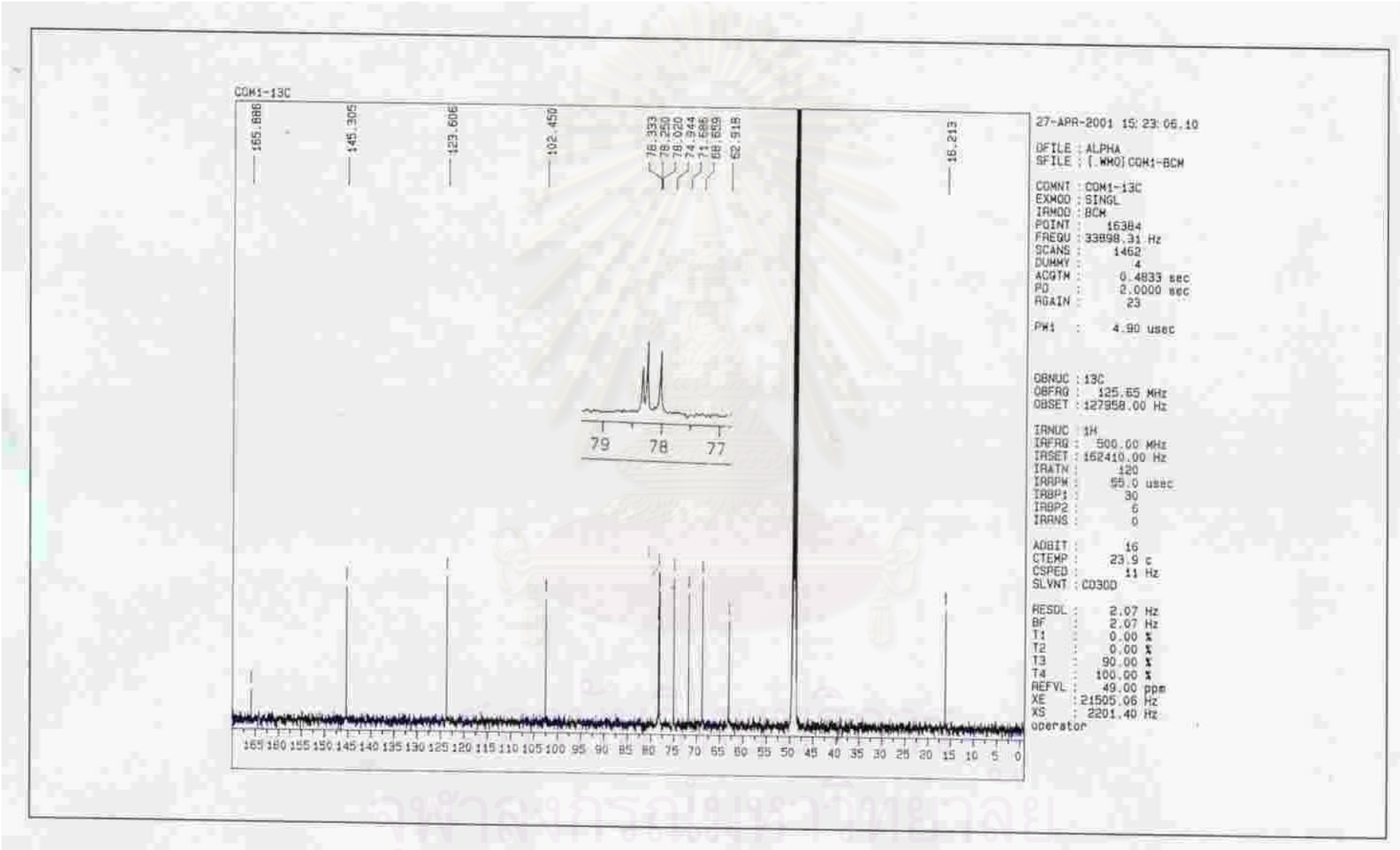

Figure 36. The 13C-NMR spectrum of Compound 2 (Angiopteroside)

Figure 37. DEPT 90, 135 and 13C-NMR spectrum of Compound 2 □
(Angiopteroside)

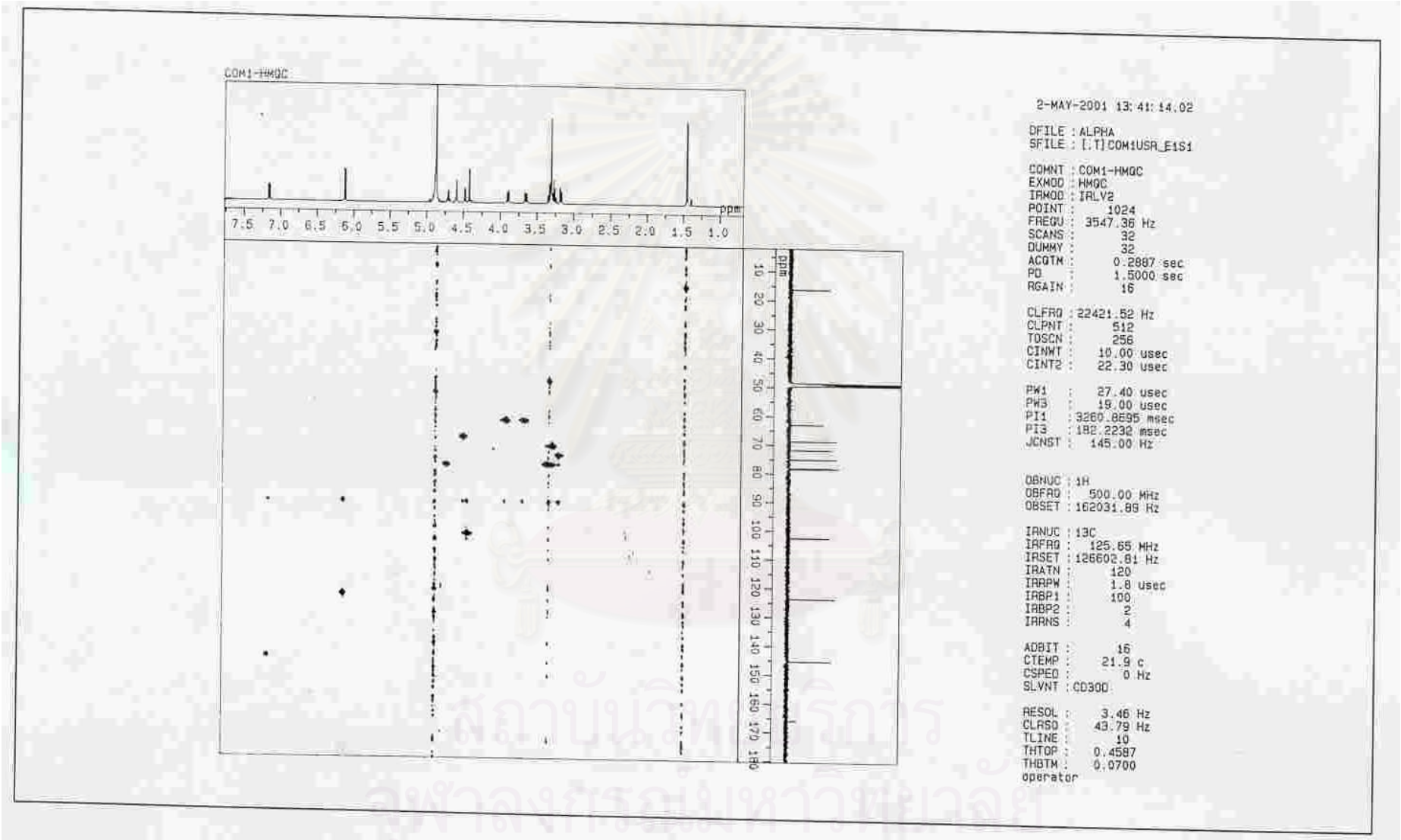

Figure 38.The HMQC-NMR spectrum of Compound 2(Angiopteroside)

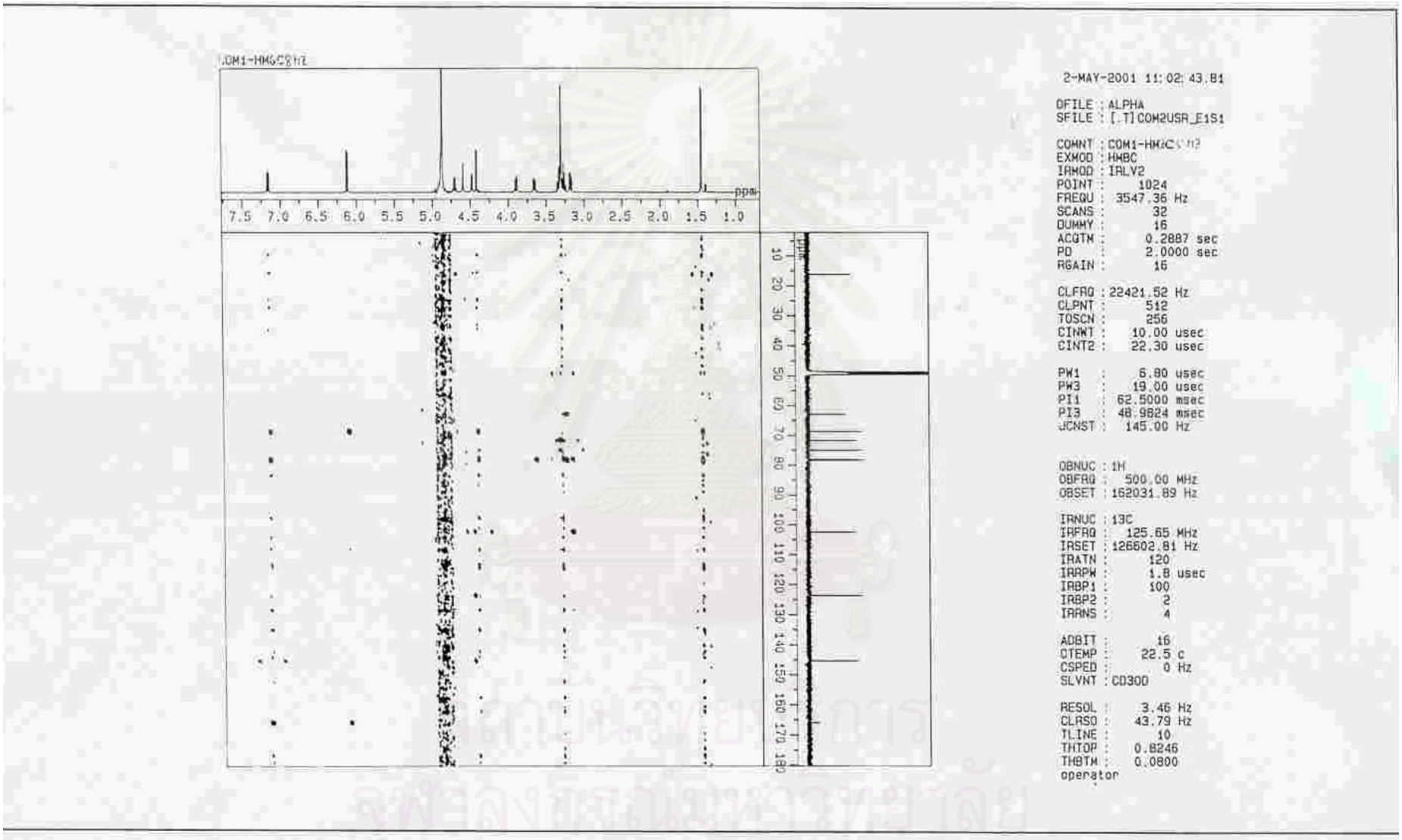

Figure 39. The HMBC-NMR spectrum of Compound 2 (Agiopteroside)

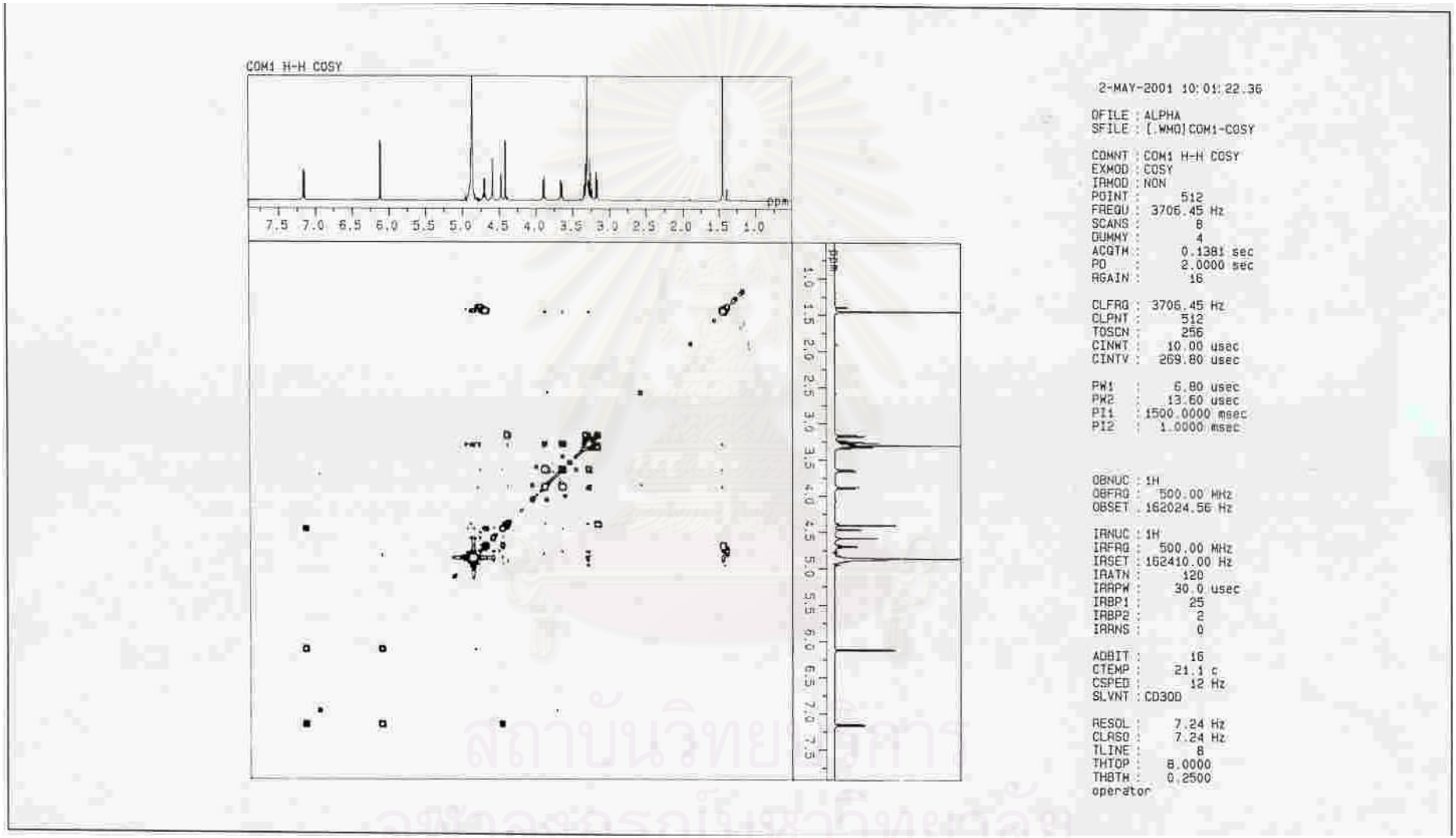

Figure 40. The COSY-NMR spectrum of Compound 2 (Agiopteroside)

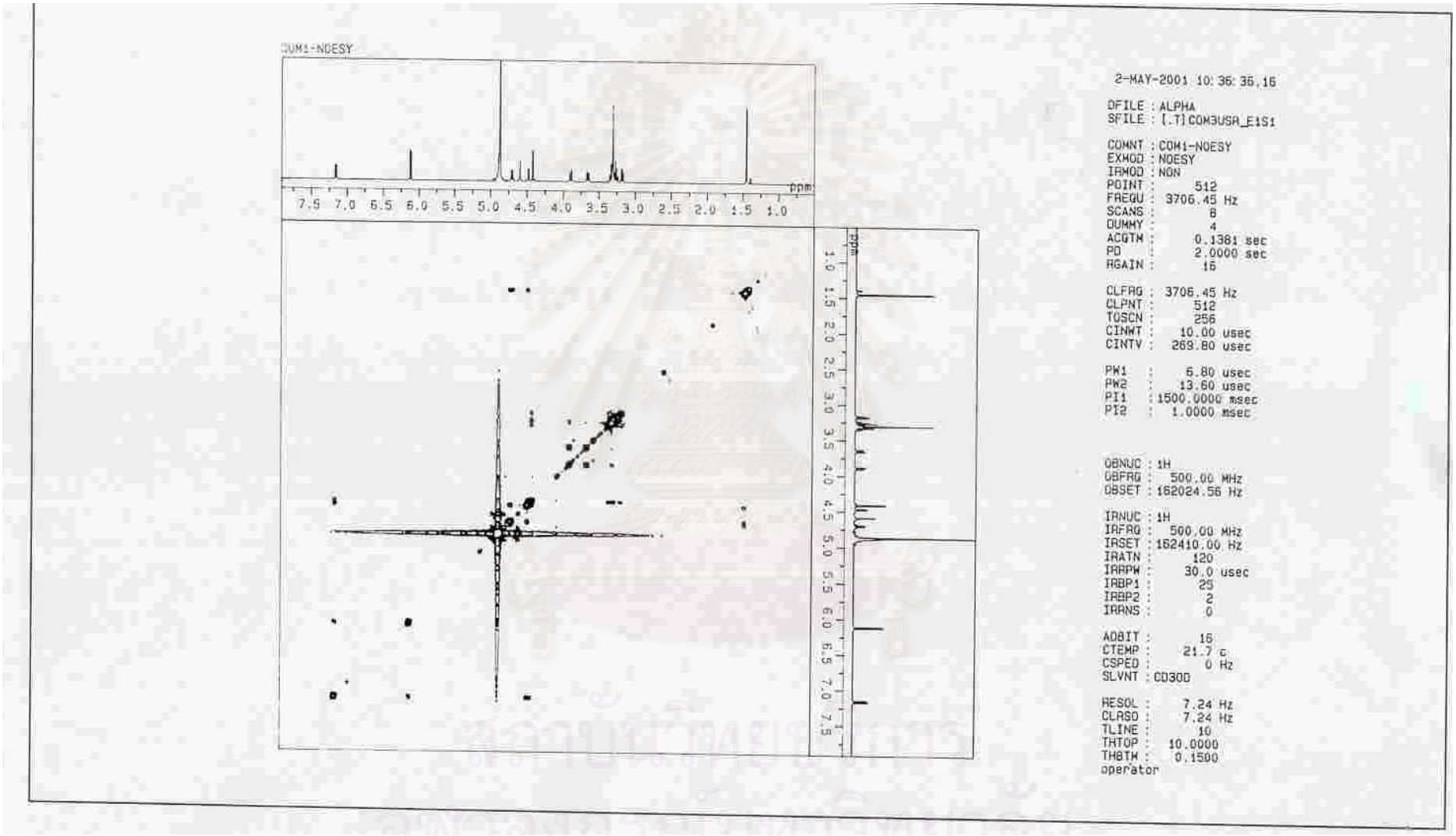

Figure 41. The NOESY-NMR spectrum of Compound 2 (Agiopteroside)

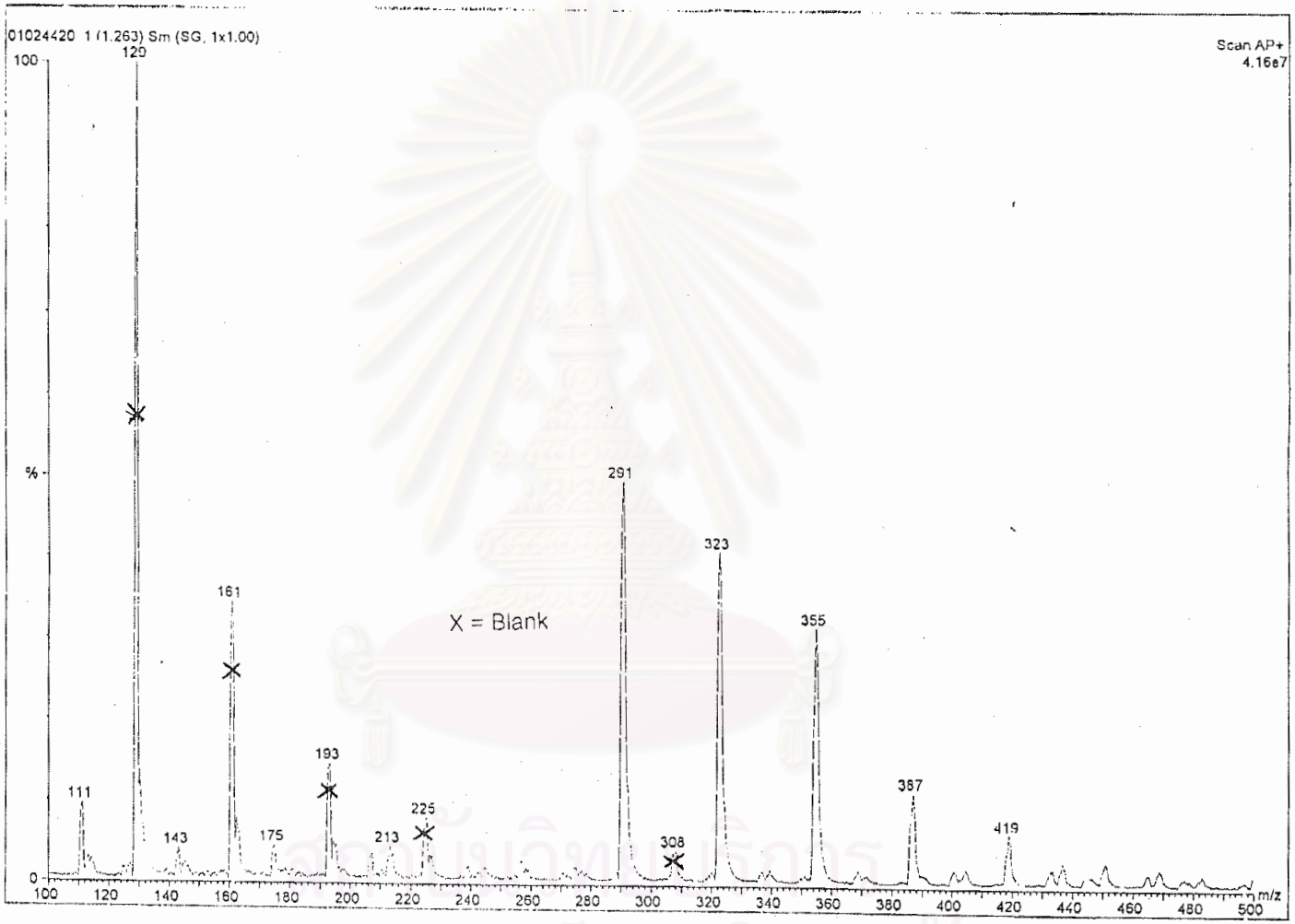

Figure 42. The LC mass spectrum of Compound 2. (Angiopteroside)

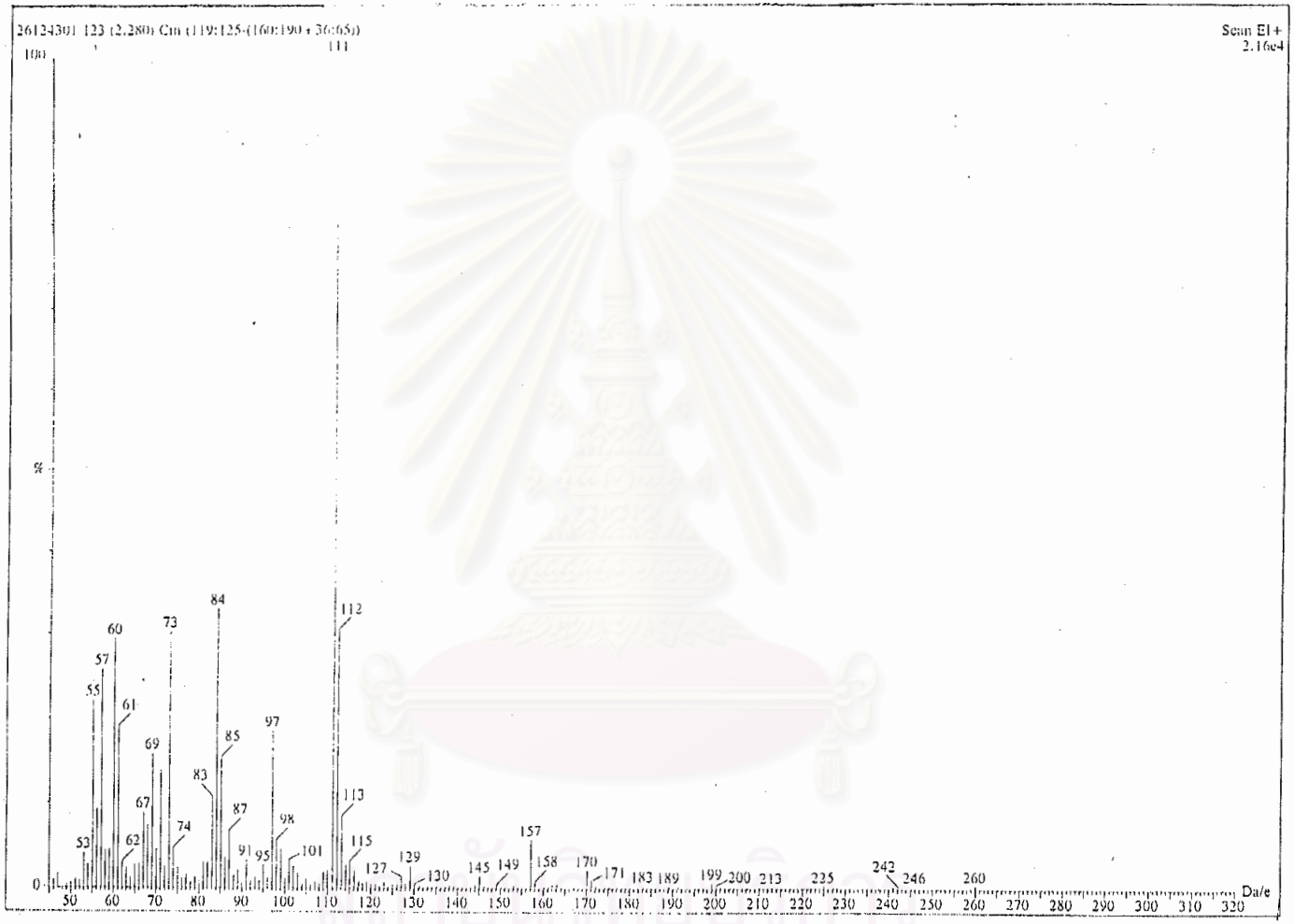

Figure 43. The EI mass spectrum of Compound 2. (Angiopteroside)

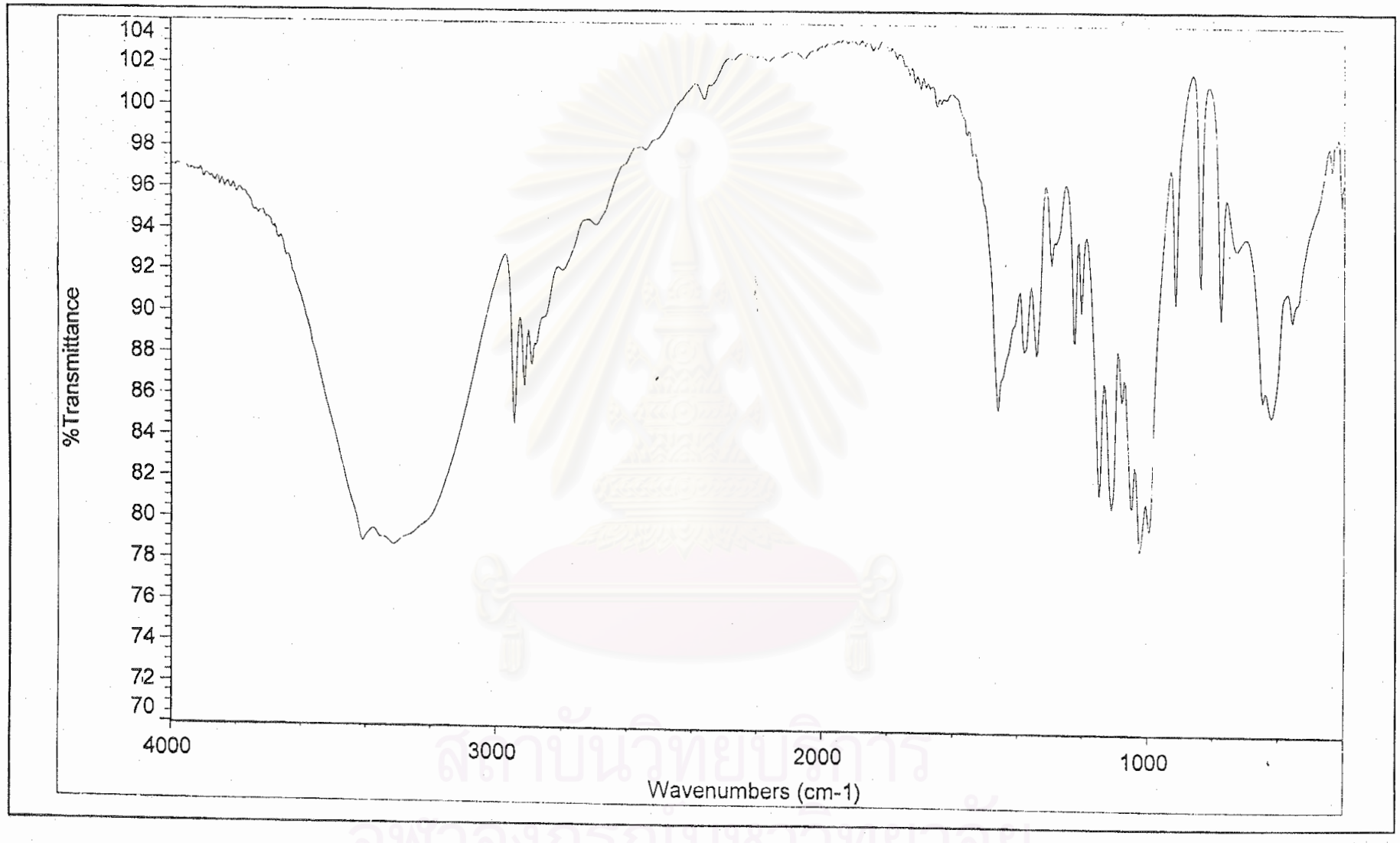

Figure 44. The IR spectrum of Compound 3. (D-(+)-glucose)

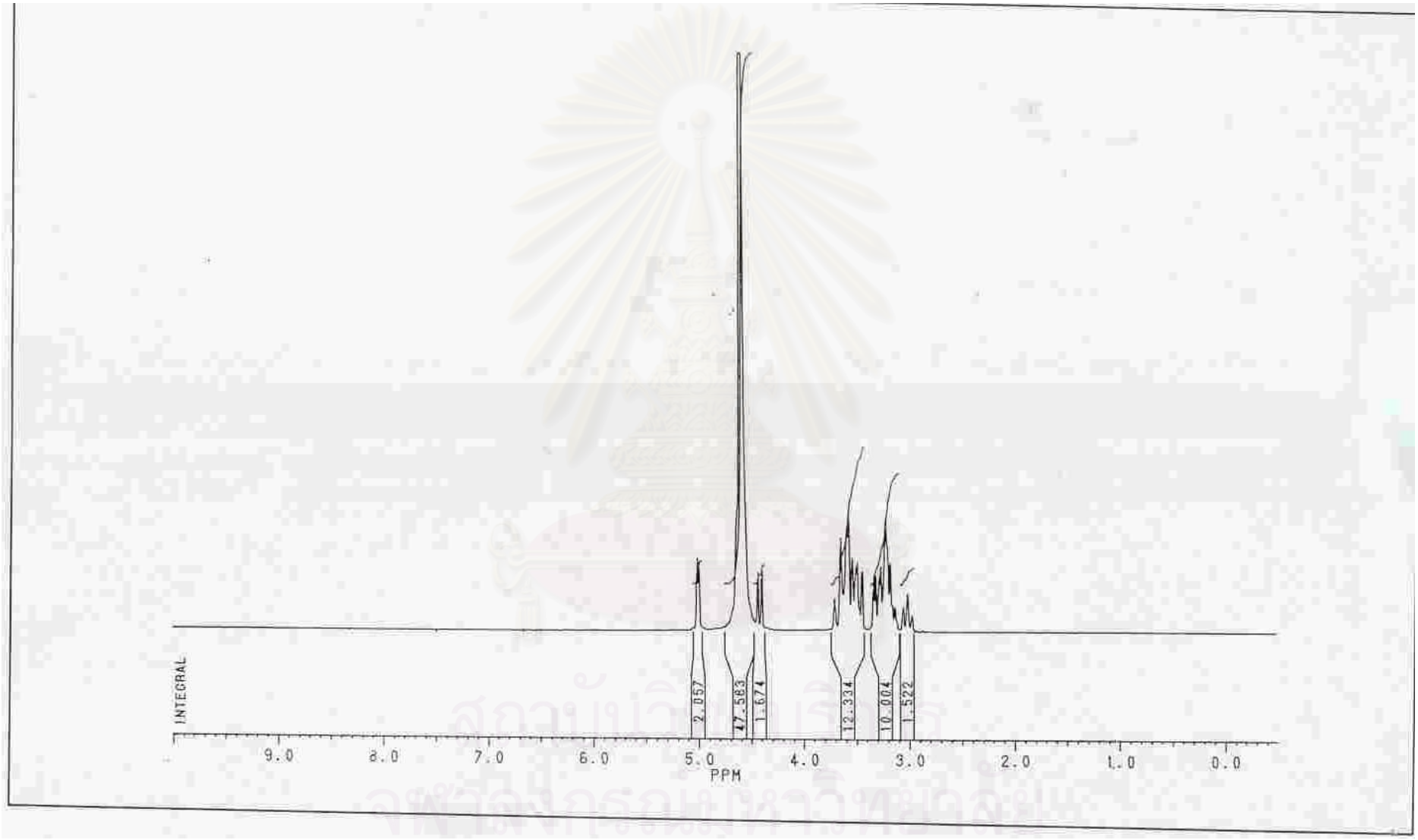

Figure 45. The 1H-NMR spectrum of Compound 3. (D -(+)- glucose)

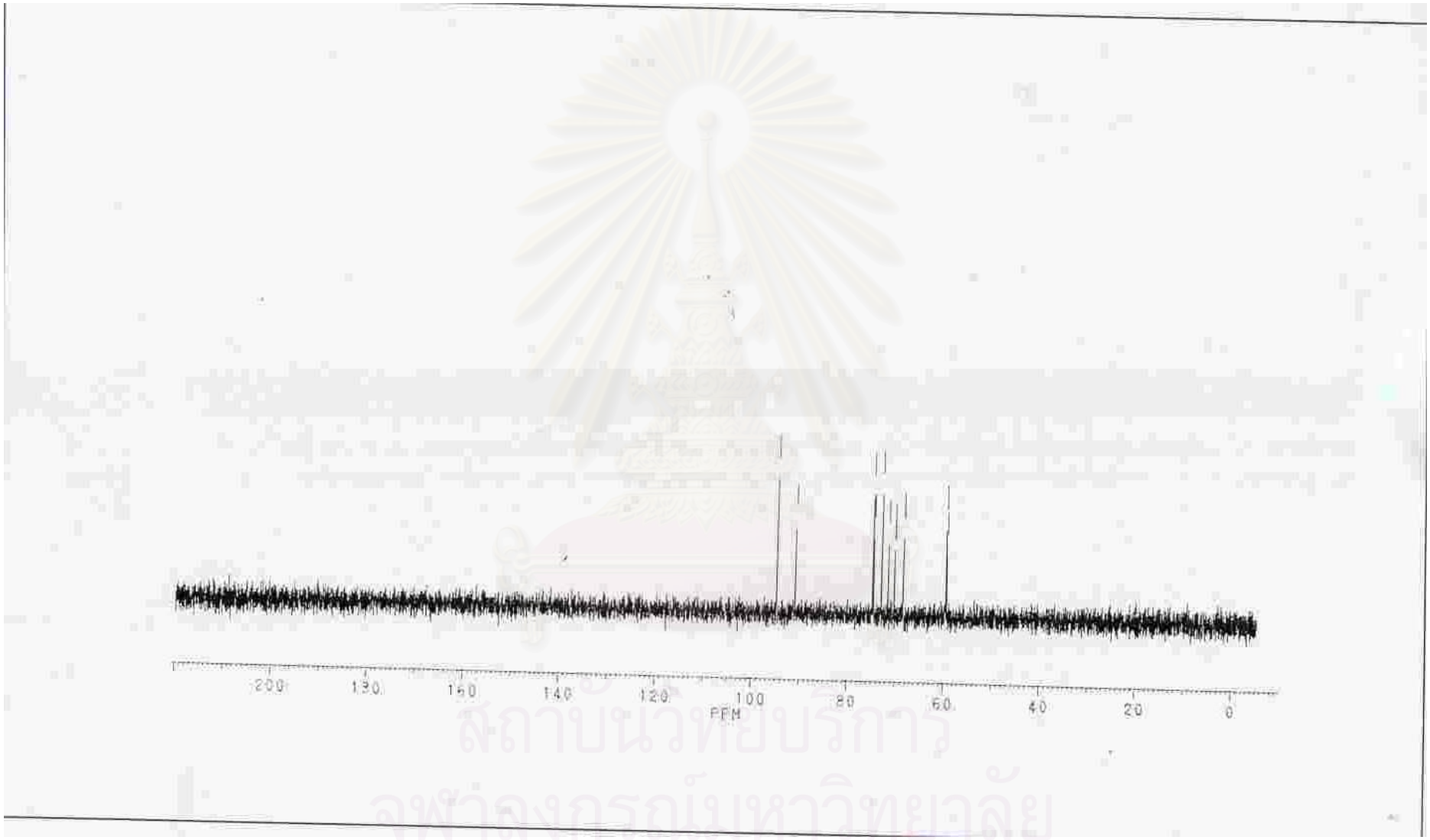

Figure 46. The 13C-NMR spectrum of Compound 3 (D -(+)- glucose)

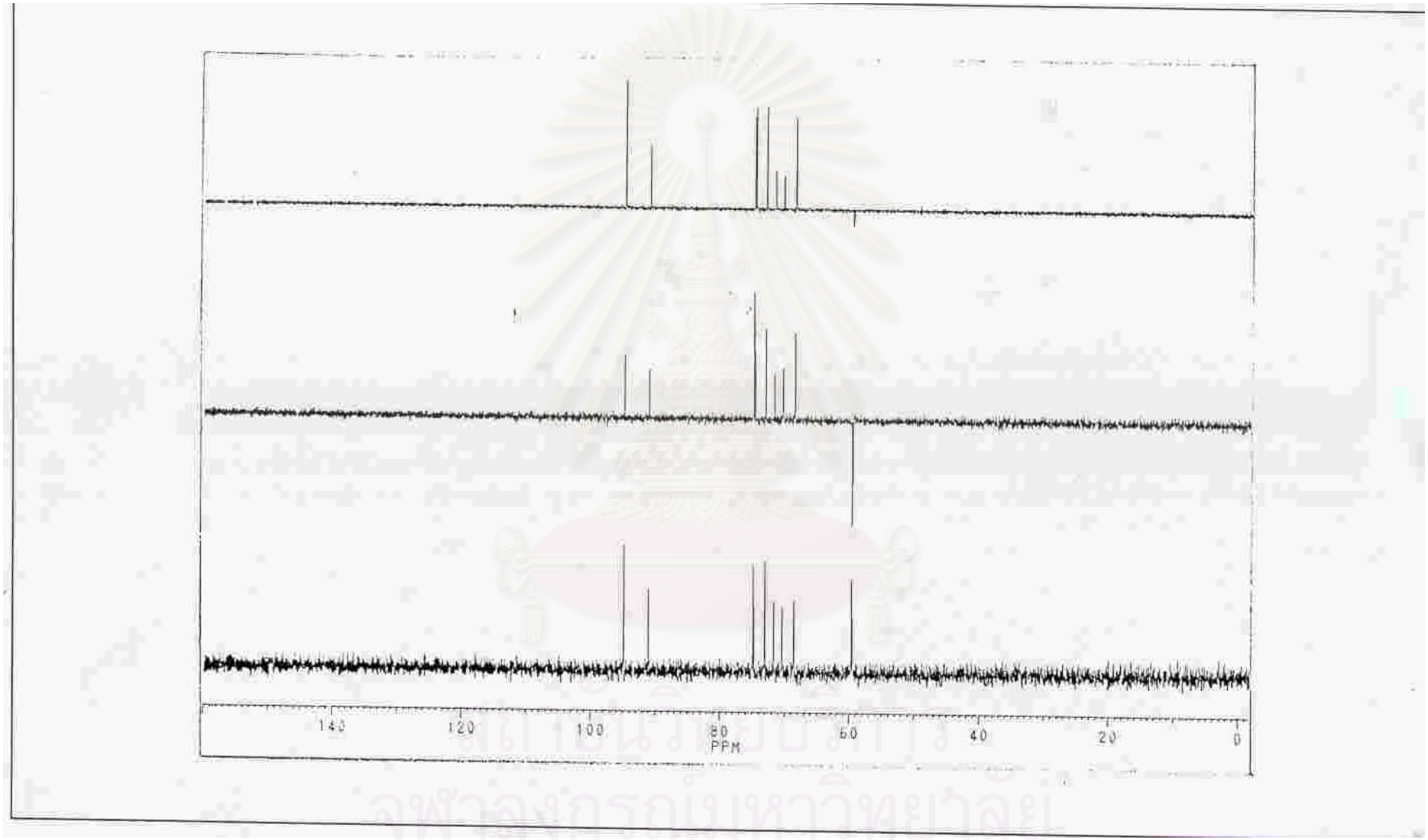

Figure 47. DEPT 90, 135 and 13C-NMR spectrum of Compound 3 (D -(+)- glucose)

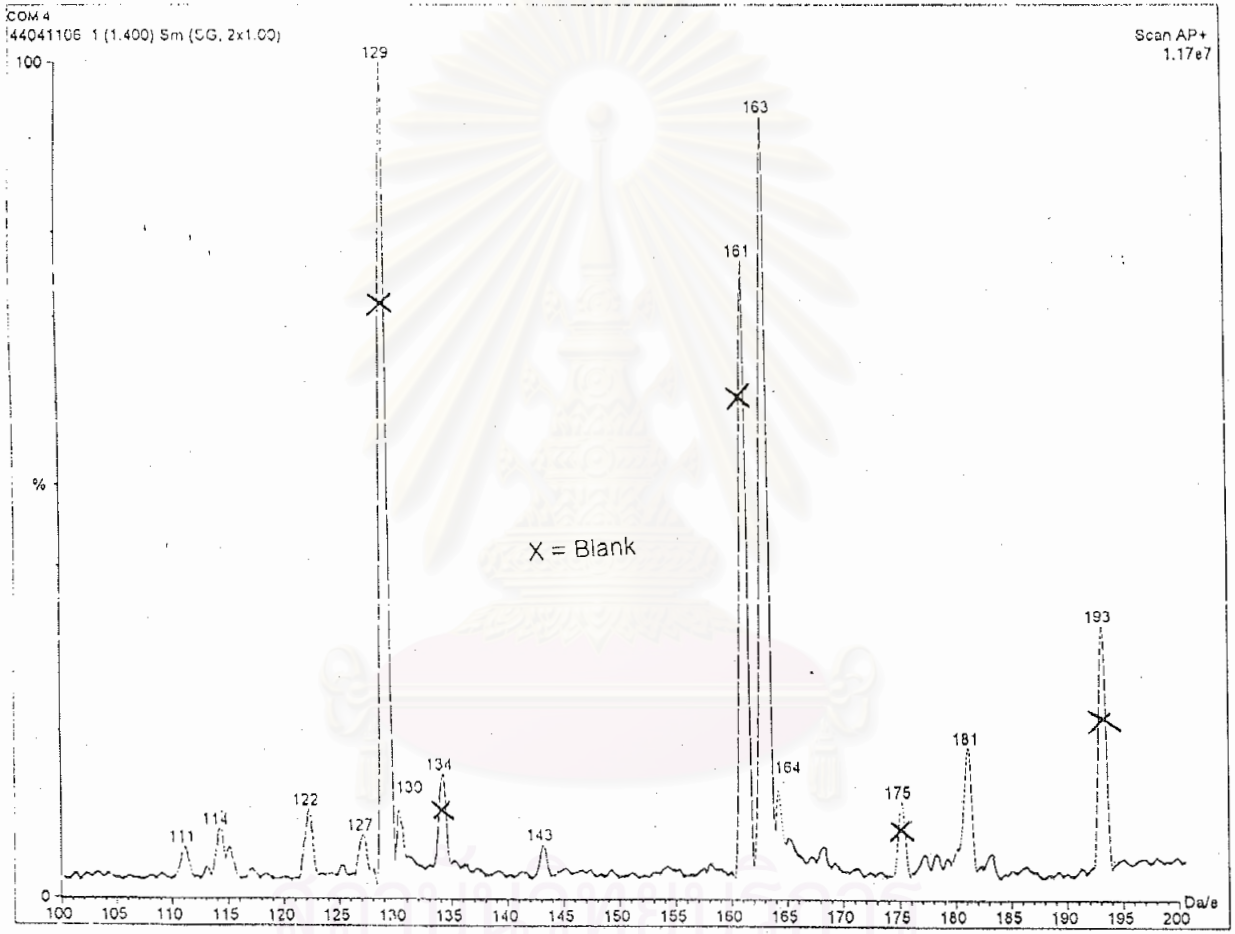

Figure 48. The LC mass spectrum of Compound 3. (D -(+)- glucose)

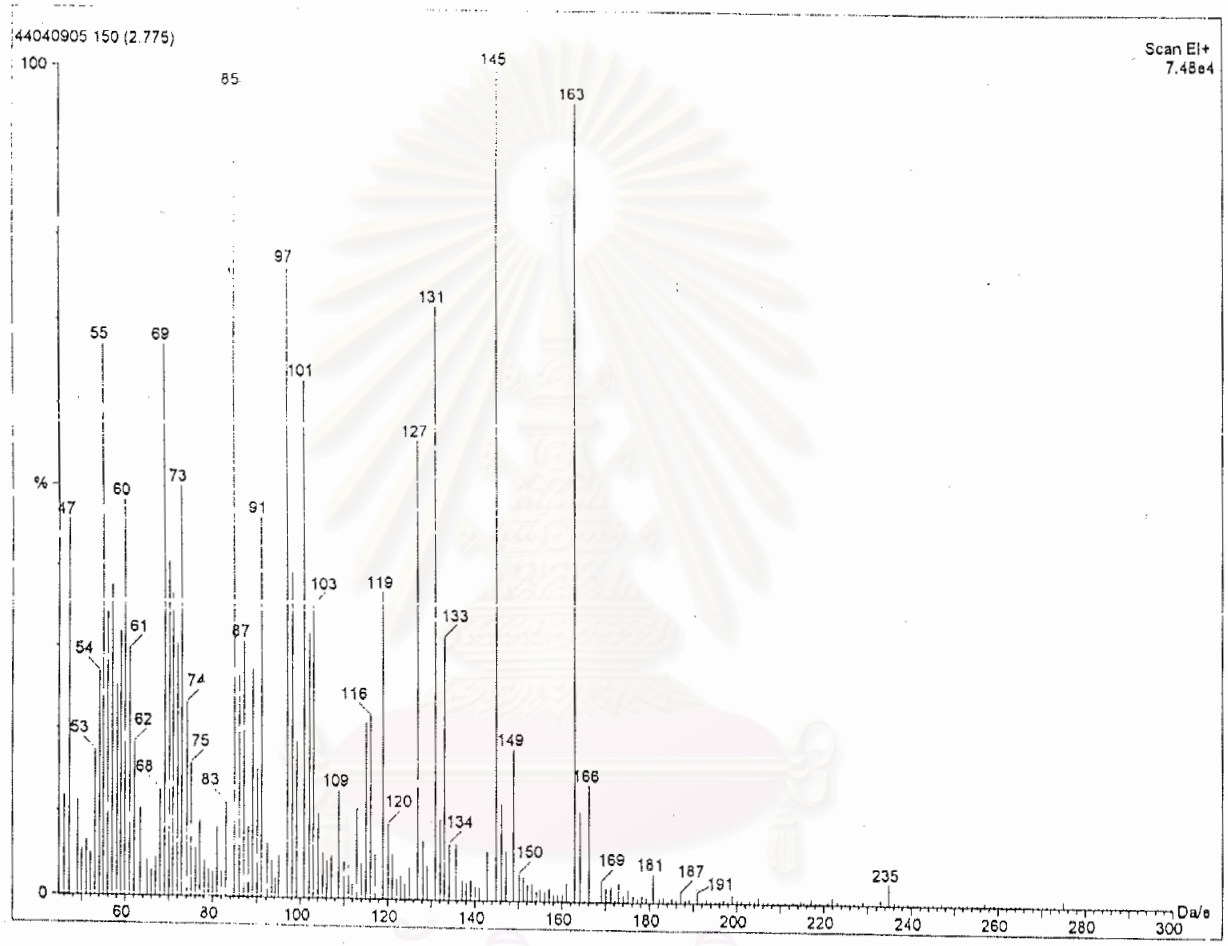

Figure 49. The EI mass spectrum of Compound 3. (D -(+)- glucose)

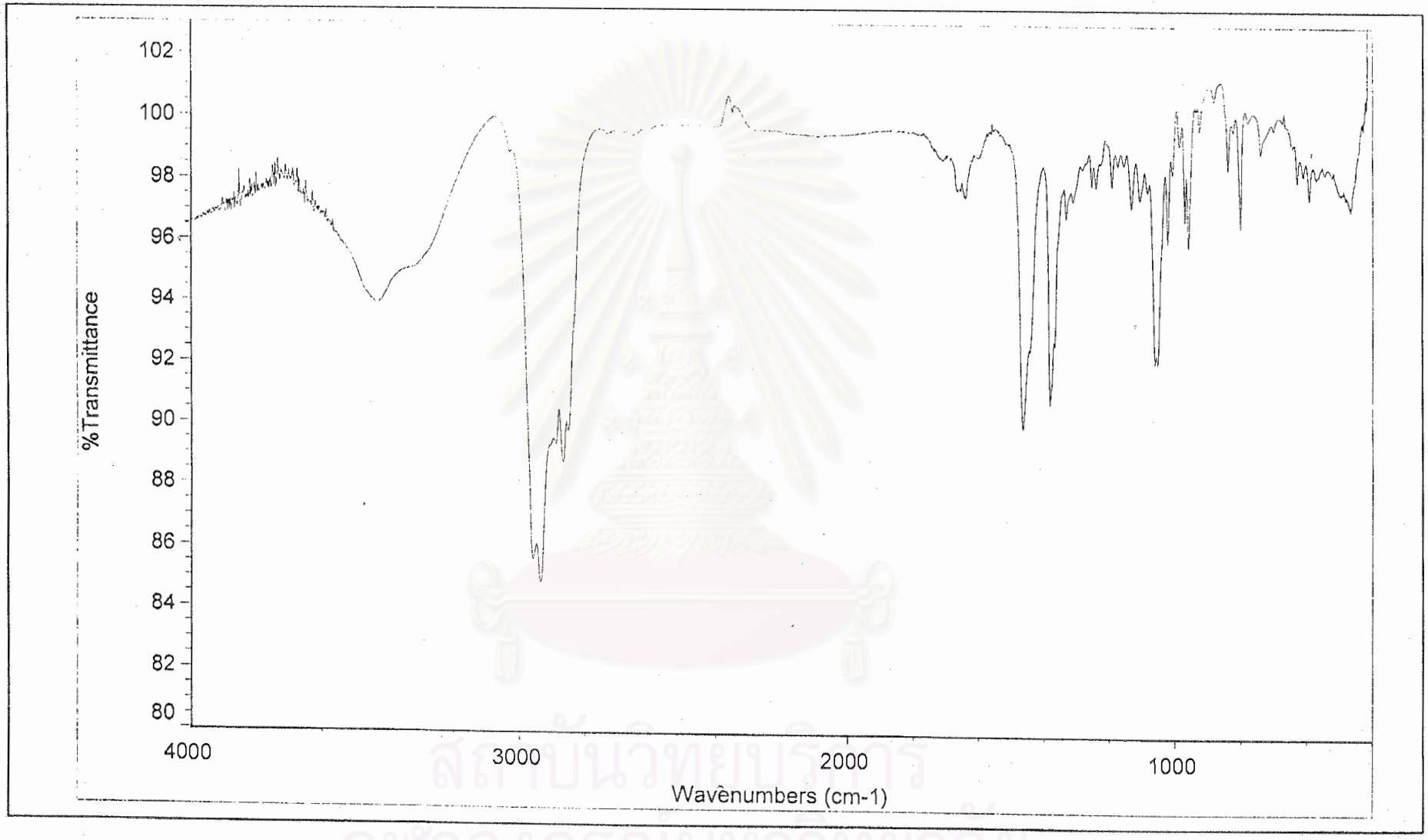

Figure 50. The IR spectrum of Mixture 4. (Mixture of stigmasterol and β-sitosterol)

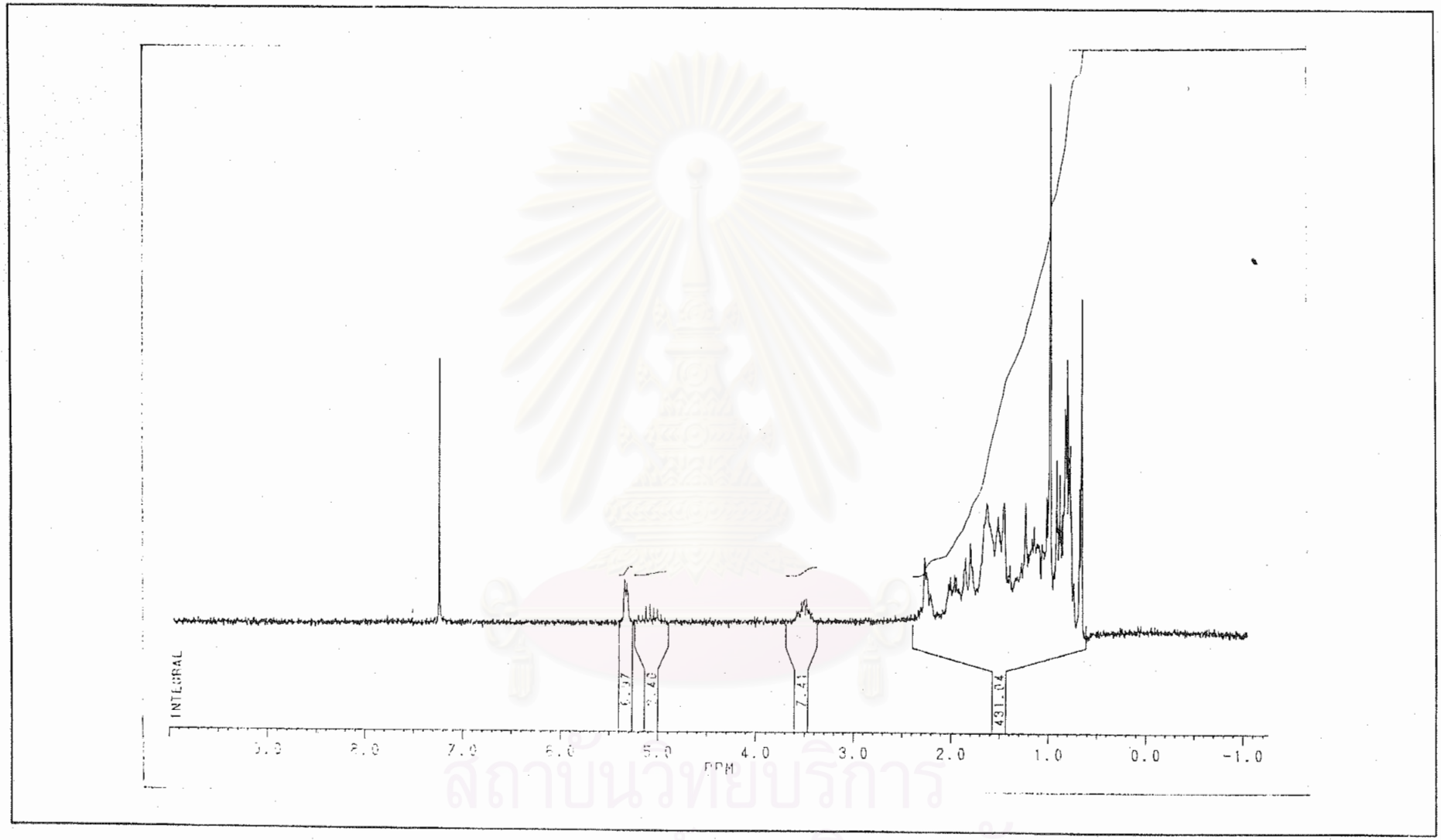

Figure 51. The ^{1}H-NMR spectrum of Mixture 4. (Mixture of stigmasterol and β-sitosterol)

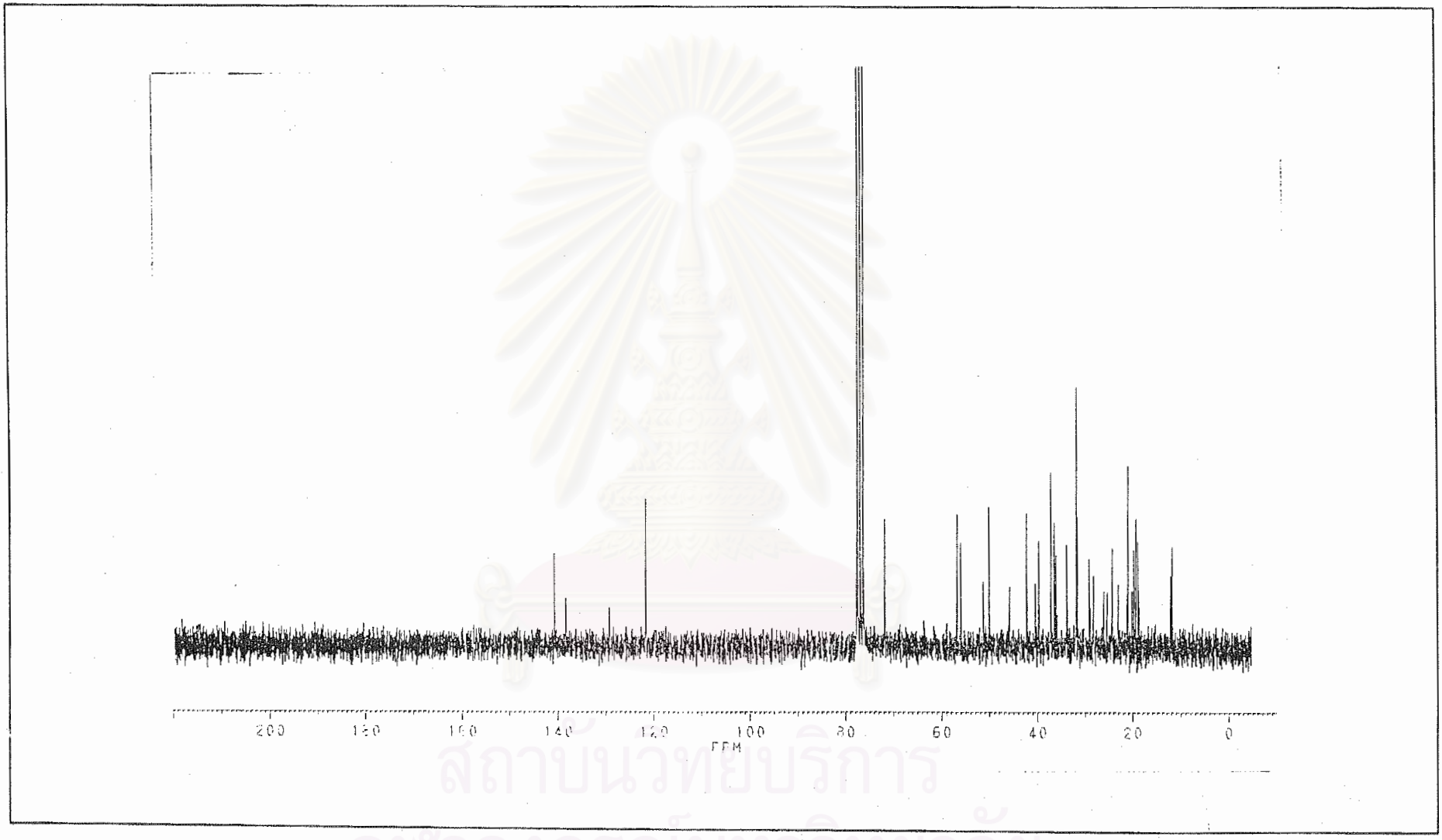

Figure 52. The ^{13}C-NMR spectrum of Mixture 4. (Mixture of stigmasterol and β-sitosterol)

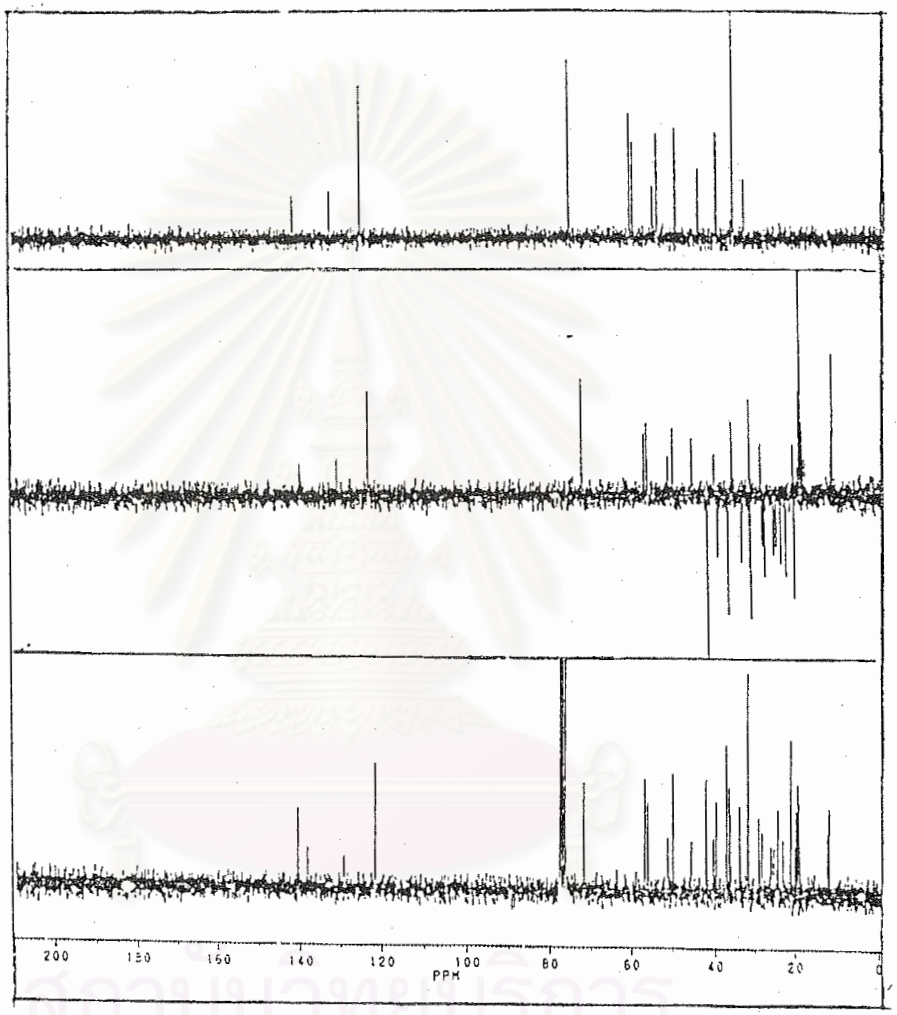

Figure 53. DEPT 90, DEPT 135 and ^{13}C-NMR spectrum of Mixture 4.
(Mixture of stigmasterol and β-sitosterol))

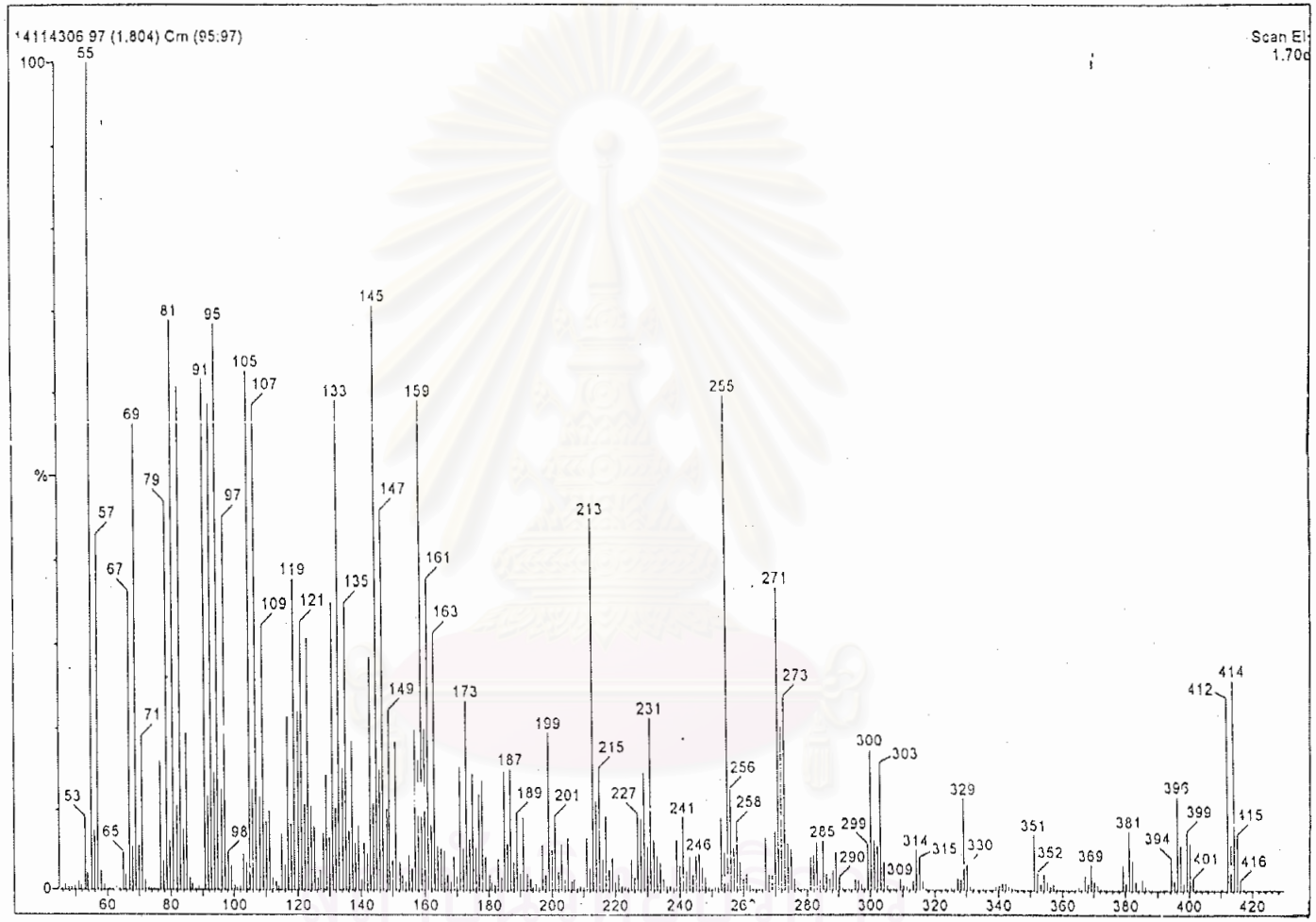

Figure 54. The EI mass spectrum of Mixture 4. (Mixture of stigmasterol and β-sitosterol)

VITA

Miss Somjintana Taveepanich was born on March 2, 1976 in Bangkok, Thailand. She graduated with a Bachelor Degree of Science in Chemistry from Khonkaen University in 1997. In 1998, she was admitted into a Master Degree program in organic chemistry at Chulalongkorn University. During her study toward the Master's degree, she received a teaching assistantship by the Faculty of Science in 1999 and financial support from University Development Commission (UDC) scholarship in 2000.